

# Collider Particle Physics - Chapter 6 -

**LEP: accelerator, detectors  
and experimental methods**

Claudio Luci



SAPIENZA  
UNIVERSITÀ DI ROMA

*last update : 070117*

# Chapter Summary

- The birth of LEP
- Lep collider main features
- Lep detectors
- A closer look at the L3 detector
- First look at the data
- Some experimental methods and tools
- Luminosity measurement

# The birth of LEP

- ❑ A preliminary study started at CERN in 1976 about what should be the next step after ISR and SPS
- ❑ In 1977 ECFA pushed to build an electron-positron collider of at least 100 GeV per beam
- ❑ In July 1978 came into operation at DESY the electron-positron collider PETRA with 19 GeV per beam and soon after at SLAC the Positron-Electron Project (PEP) with similar parameters where one could expect many discoveries, but still the arguments in favour to build LEP were considered valid.
- ❑ The first project (LEP 100) was for a machine 50 km long with 100 GeV beam, but it was too expensive and with some problems unsolved.
- ❑ A second study in 1978 (Blue book) was for a smaller machine of 22 km who could eventually reach 70 GeV per beam. The project was rejected because it could not cross the threshold for a pair of W bosons.
- ❑ In 1979 a third project (Pink book) was presented of a circumference of 30.6 km with an initial energy of 62 GeV that could reach 130 GeV with superconducting RF cavities. However, it was proposed to place it in such a way that about 12 km would be located in the rocks of the Jura, indeed passing under the crest at a depth of 860 m.
- ❑ January 1<sup>st</sup> 1981: Herwing Schopper became the (only) CERN Directory: CERN reunification.
- ❑ In June 1981 there was the last proposal (Green book): the circumference was reduced to 26.7 km, the ring was moved toward the airport and it was inclined by 1.5° in order not to go too deep under the Jura. The PS and SPS became part of the injection chain.

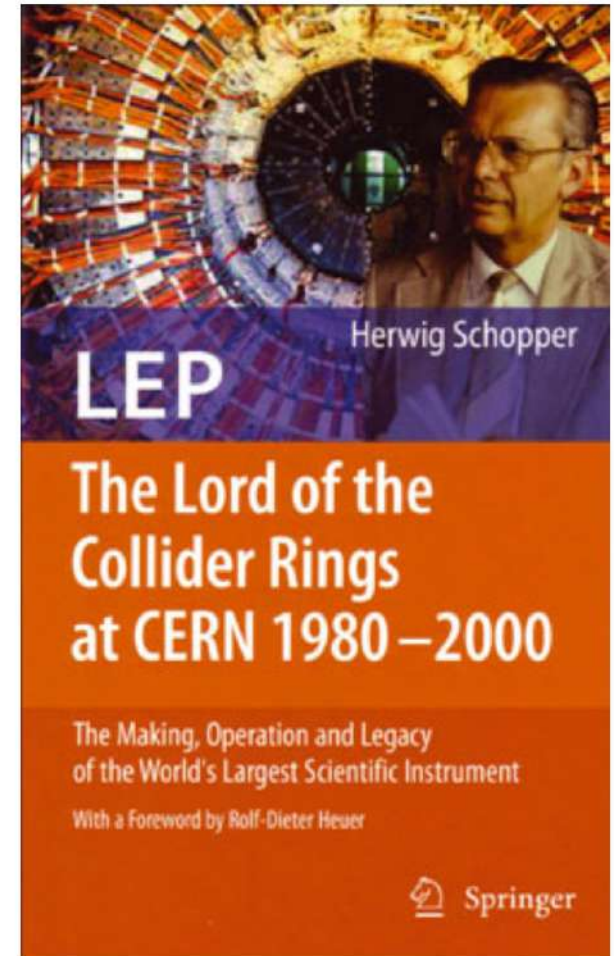
# LEP parameters of the various proposal

- ❑ Beam energies with superconducting RF cavities in a second stage, are given in parentheses

Study	Maximum beam energy (single beam) (GeV)	Circumference (km)	Cost (millions of Swiss francs)	Year
LEP 100	100	50	Too high	1976
Blue Book	70	22	?	1978
Pink Book	86 (120)	30.6	1,300	1979
Green Book	50 (100)	26.7	910	1981

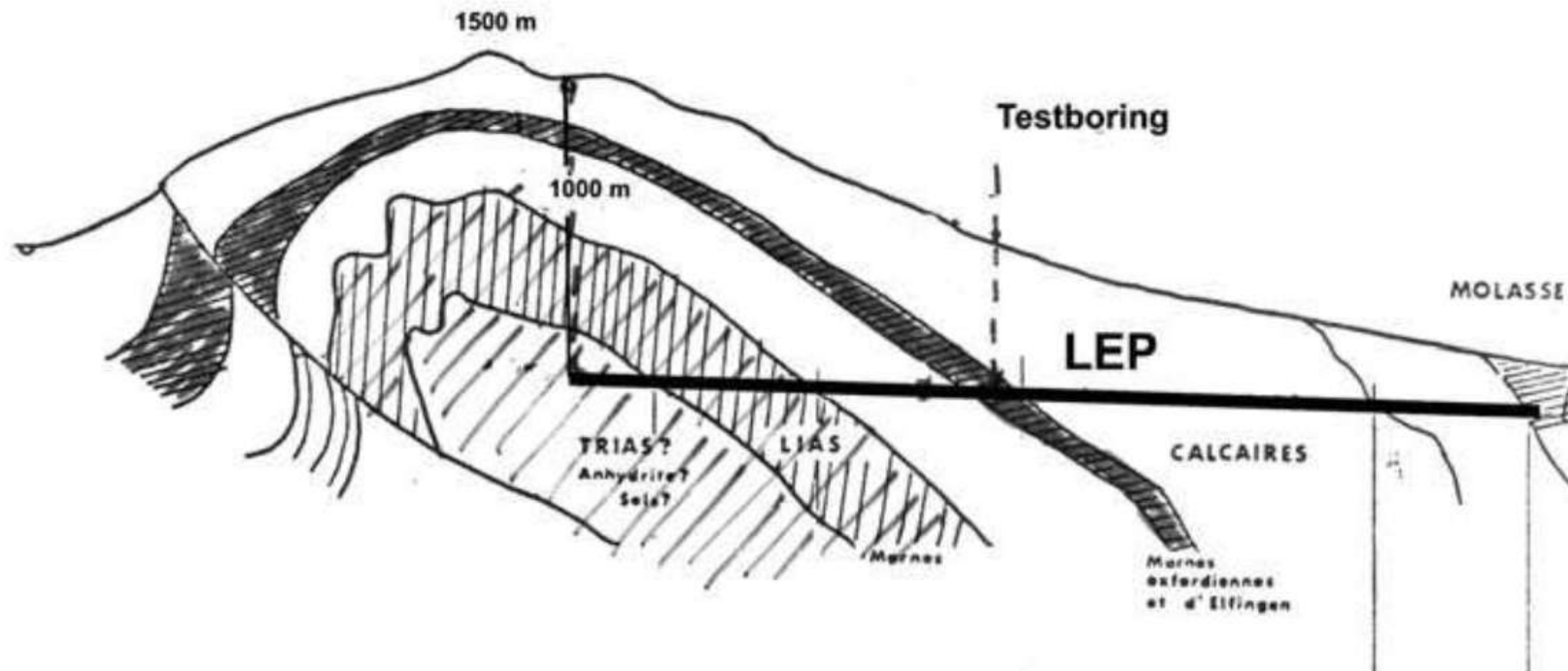
120 GeV would have been the ideal energy for the Higgs ... too bad!

All historical and technical info taken from this book



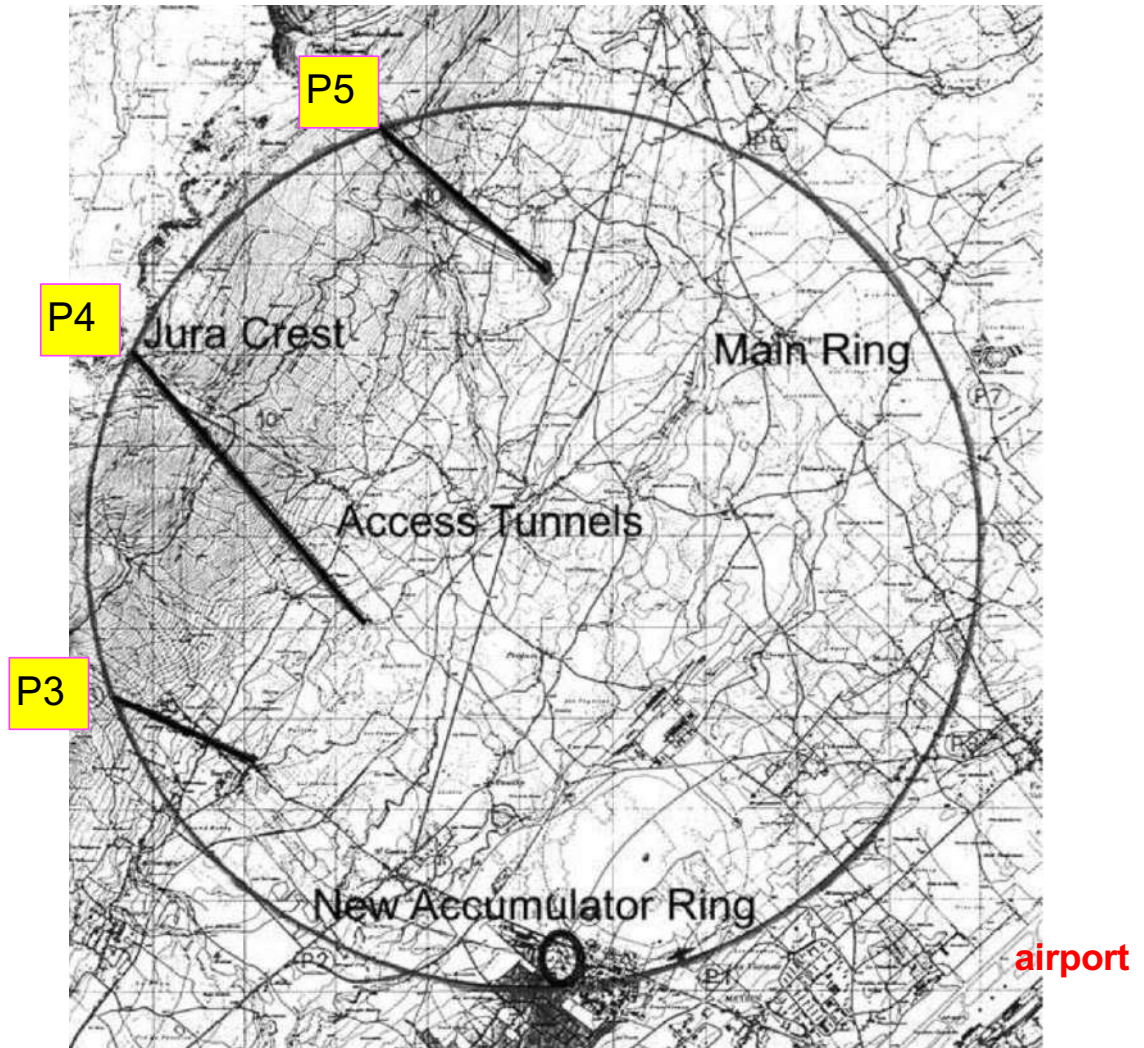
# Pink book proposal

- Geological cross-section showing the position of the LEP tunnel according to the original proposal. A section would be deep under the Jura Mountains in bad rock.



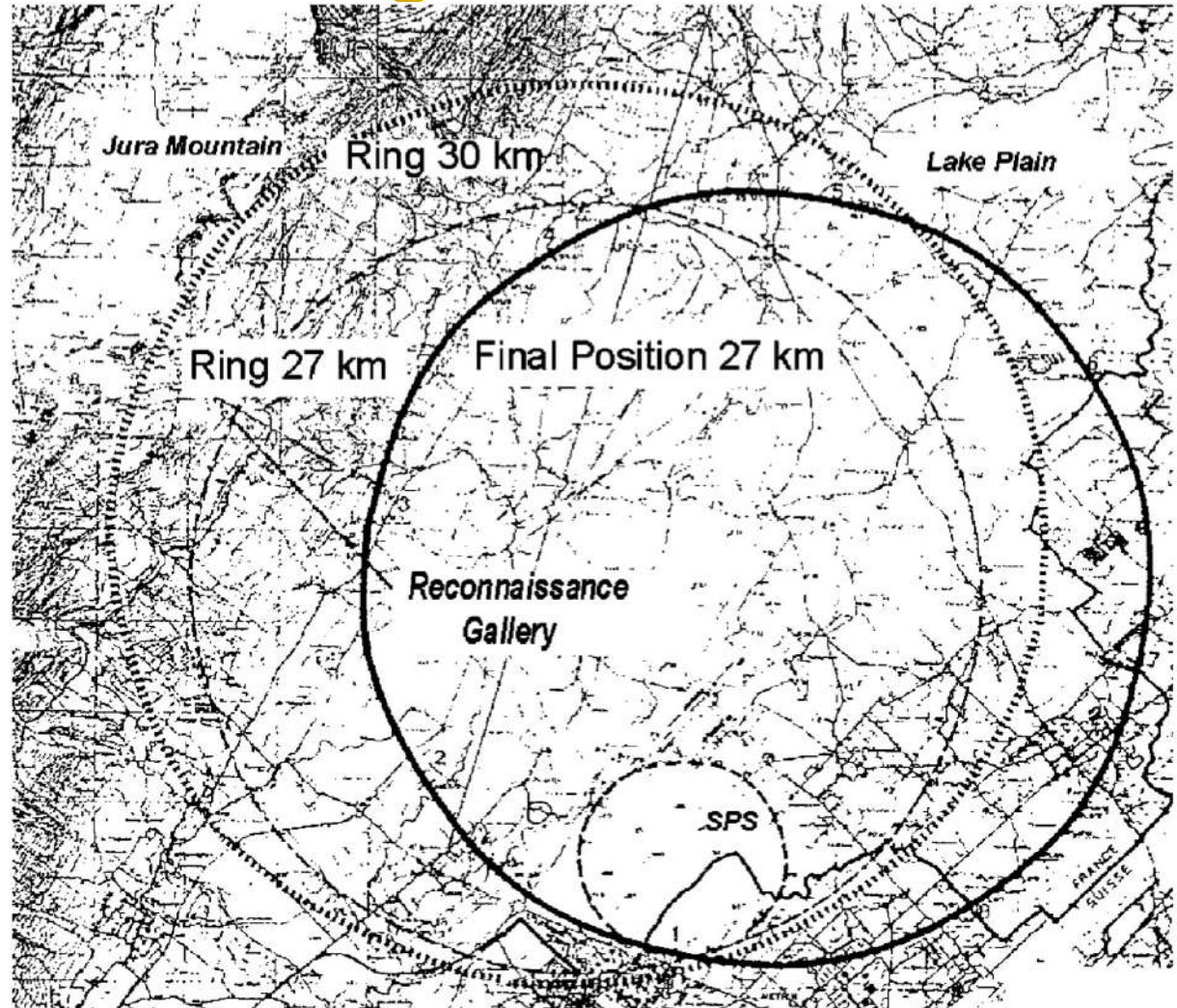
# LEP third proposal (Pink book)

- ❑ **30.6 km proposal.**
- ❑ **One of the reasons why CERN originally was not considered as a good place for LEP was the fact that there was not much room between Lake Geneva and the Jura Mountains to place a tunnel with a circumference of more than 30 km.**
- ❑ **The ring passes under the Jura crest; three long access galleries were necessary to provide access to the underground halls at points P3, P4 and P5.**
- ❑ **A new accumulator ring under the old ISR was also proposed. PS and SPS were NOT part of the LEP injector facility.**

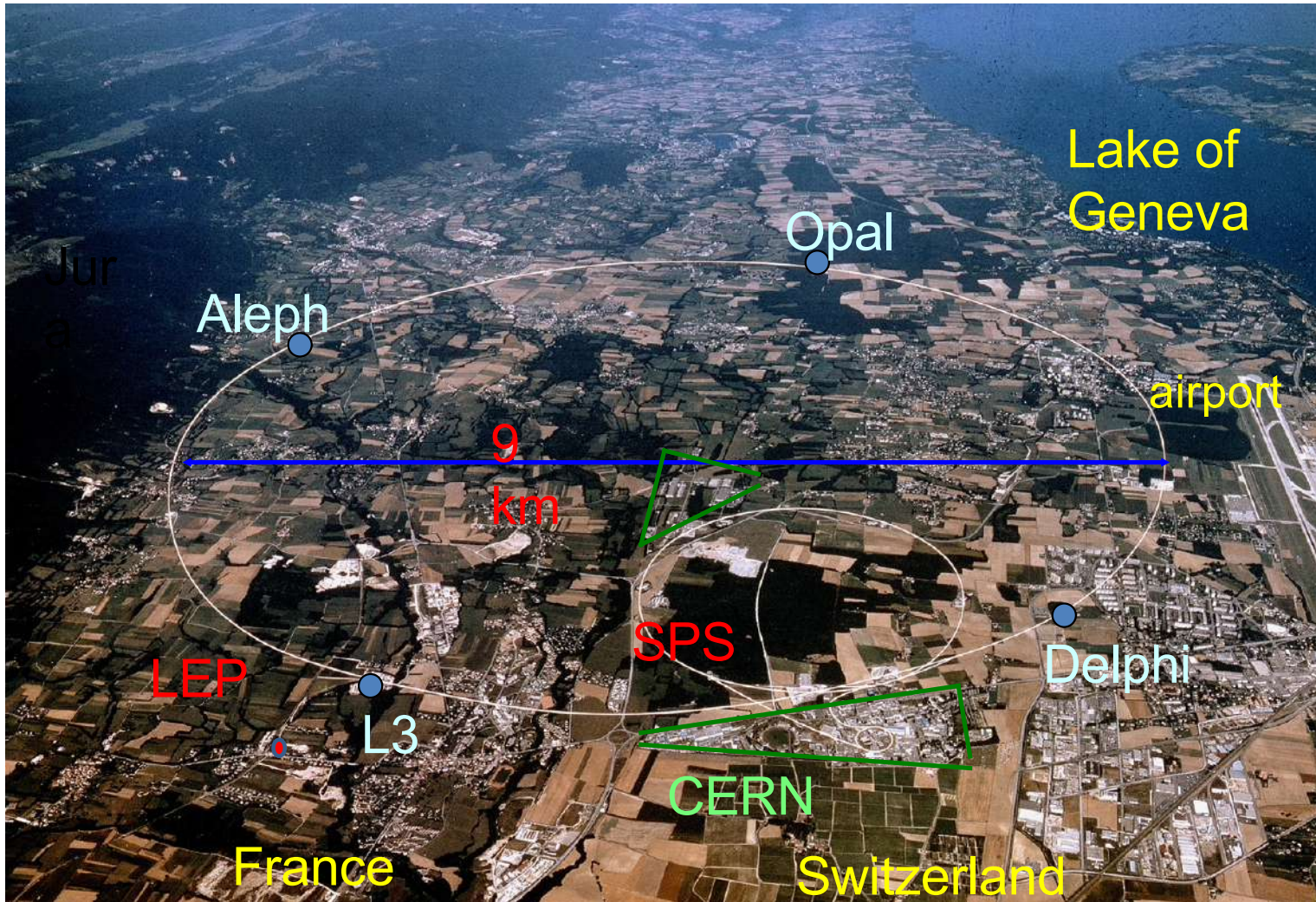


# How the LEP ring moved

- ❑ The three positions of the LEP tunnel: the originally proposed (30 km circumference), the intermediate choice as approved by CERN Council (27 km) and the final position.
- ❑ Reducing the LEP ring was a wise decision given the financial constraints and the high risk to go deep under the Jura, however ... it prevented LEP to discover the Higgs boson, as we will see.
- ❑ In 1983 began the tunnel excavation. The gallery has a diameter of 3.8 m and it is located at about 100 m underground. It has a 1.5° slope toward Geneva.
- ❑ In 1988 the tunnel was completed. At that time it was the longest tunnel in Europe.



# LEP: aerial view



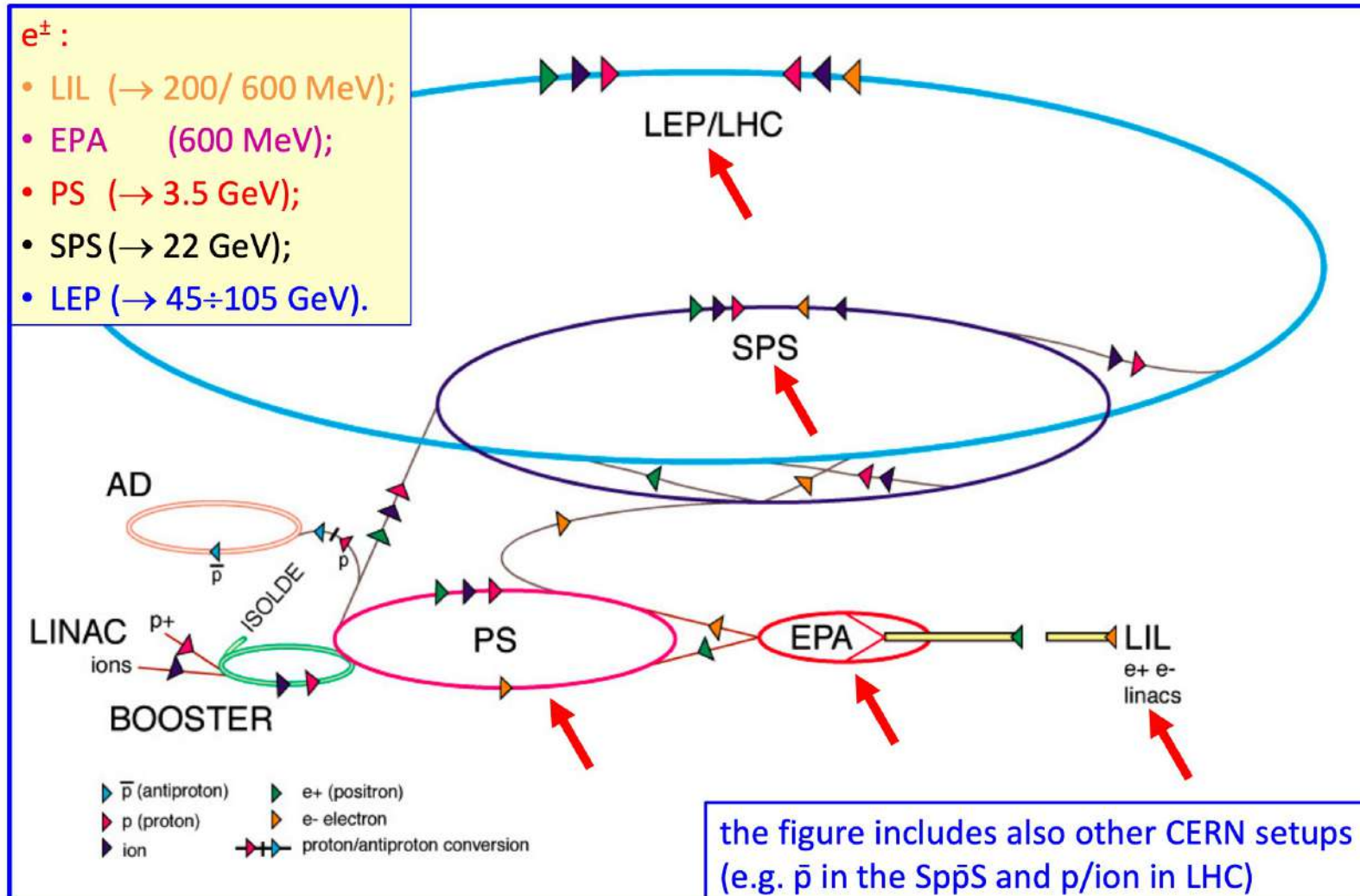
New CERN landscape



Old picture.  
Now there are many more  
buildings everywhere

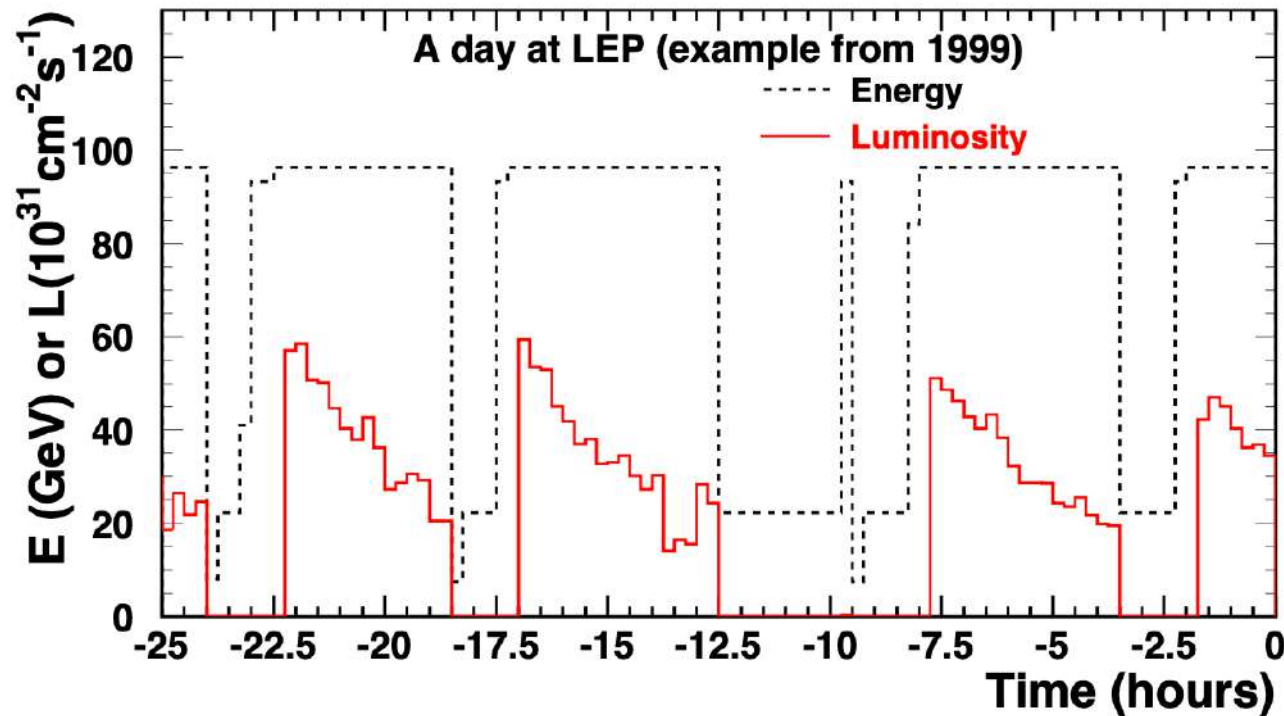
# LEP collider main features

# The LEP injecton chain



# A day at LEP

- A good fill lasts around 10 h (LEP1 at Z) or 3 h (LEP2)



*In order to maximize the integrated luminosity, it is convenient to dump the beam and to start a "fresh" one if the turn around is fast enough.*

- *Considering the complexity, the performances of LEP in terms of reliability were remarkable. As an example, in the year 2000, the total time that LEP did not have beam, for any reason including power cuts, was 383 hours out of 5107 scheduled, a down time of only 7.5%.*

# The LEP collider parameters

	LEP 1	LEP 2
Circumference (Km)	26.66	
$E_{\max}$ / beam (GeV)	50	105
max lumi $\mathcal{L}$ ( $10^{30}$ cm <sup>-2</sup> s <sup>-1</sup> )	~25	~100
time between collisions ( $\mu$ s)	22 (11)	22
bunch length (cm)	1.0	
bunch radius (hori.) ( $\mu$ m)	200÷300	
bunch radius (vert.) ( $\mu$ m)	2.5÷8	
injection energy (GeV)	22	
particles/packet ( $10^{11}$ )	4.5	
packet number	4+4 (8+8)	4+4
years	1989-1995	1996-2000

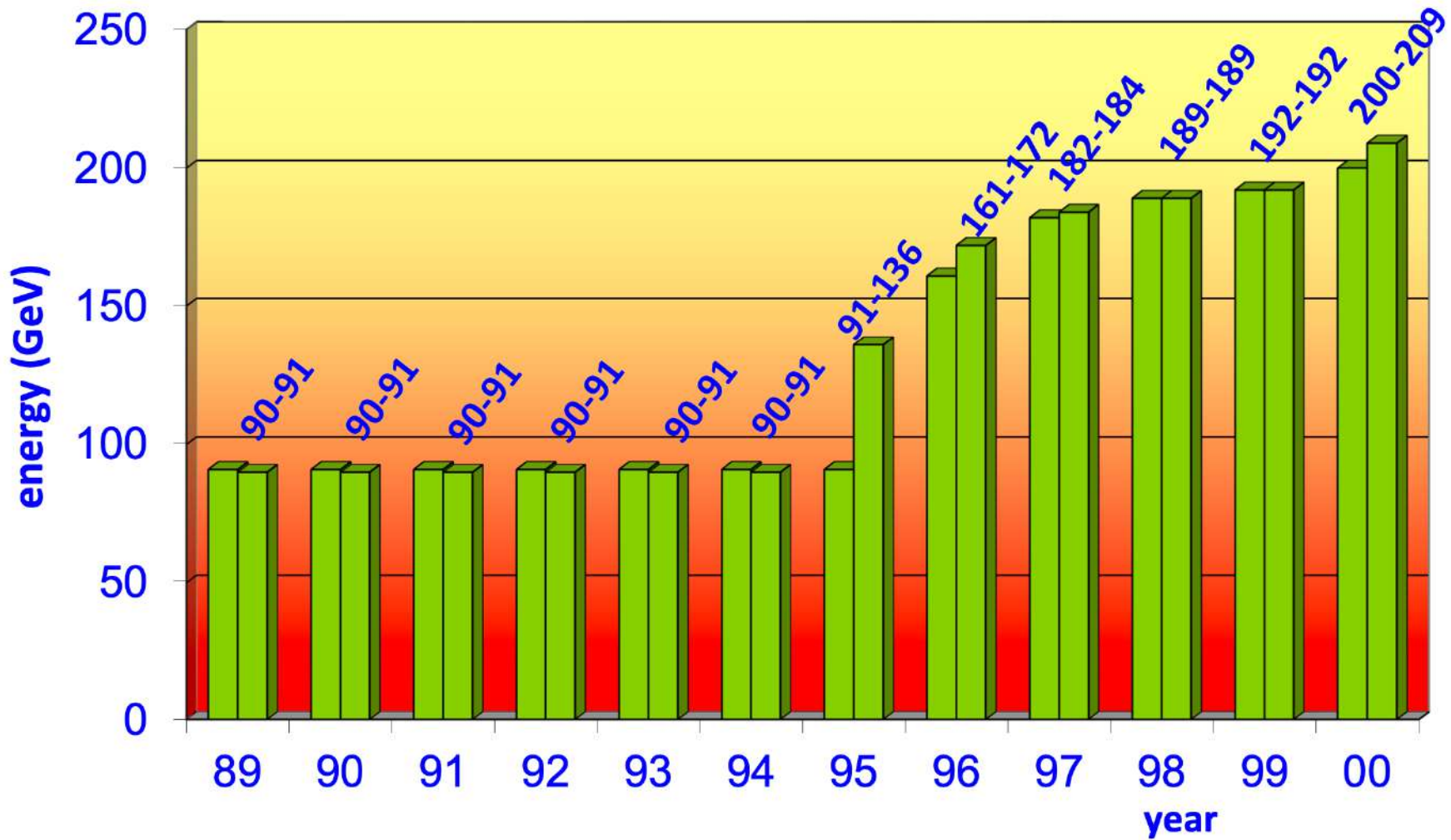
**To increase the number of bunches two methods were used:**

1. The “pretzel” scheme with 8 bunches colliding (from 1992 to 1994).
2. The bunch train scheme, which evidently consists of making trains of bunches, with the spacing between bunches in a train very small compared to distance between the trains. This scheme was used from 1995, initially with four trains of three bunches, then later with four trains of two.

**Actually we had also LEP 1.5  
In late 1995 we took data at ~136 GeV.**

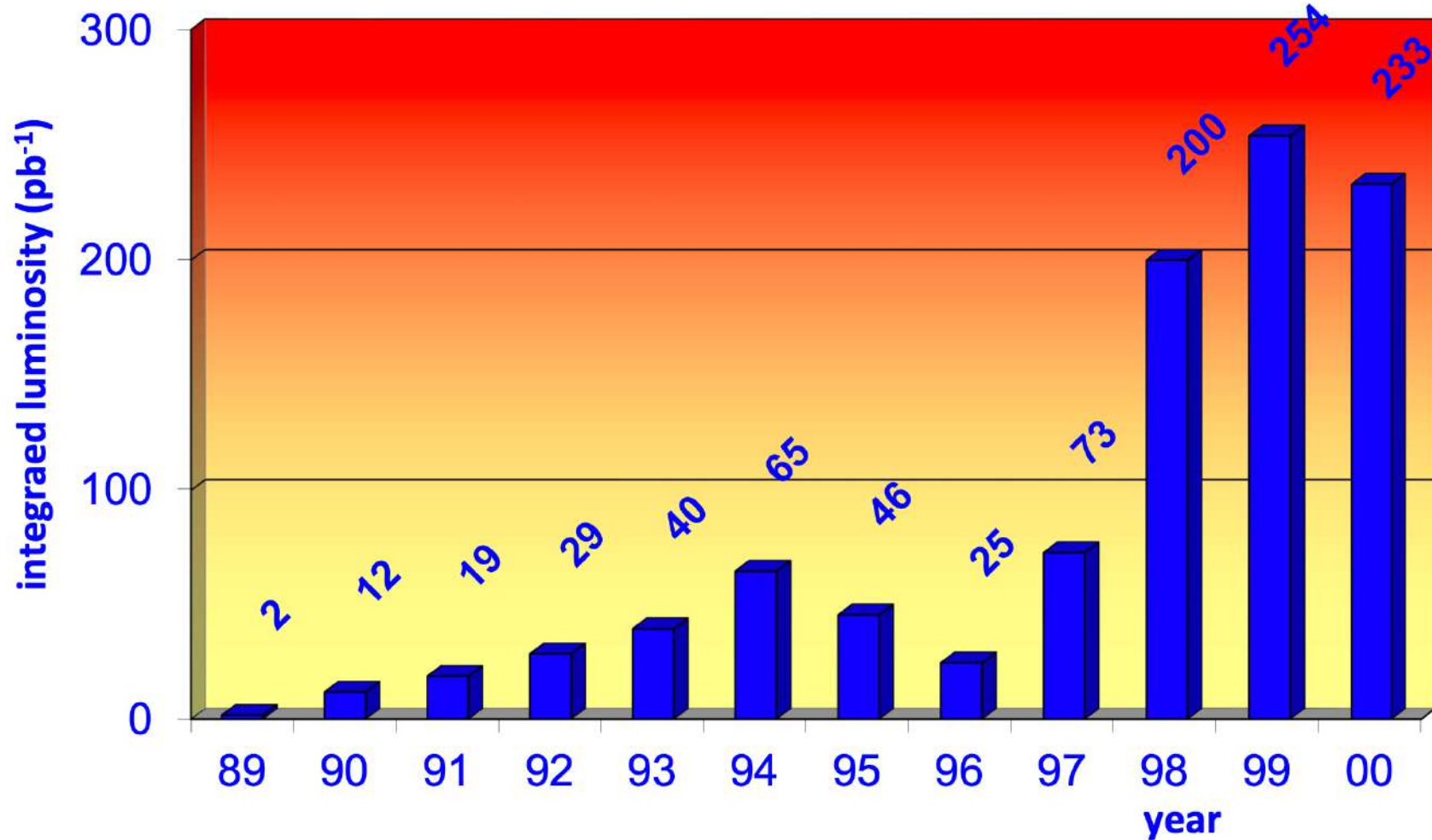
# The LEP collider: $\sqrt{s}$ versus year

Slide from  
P. Bagnaia

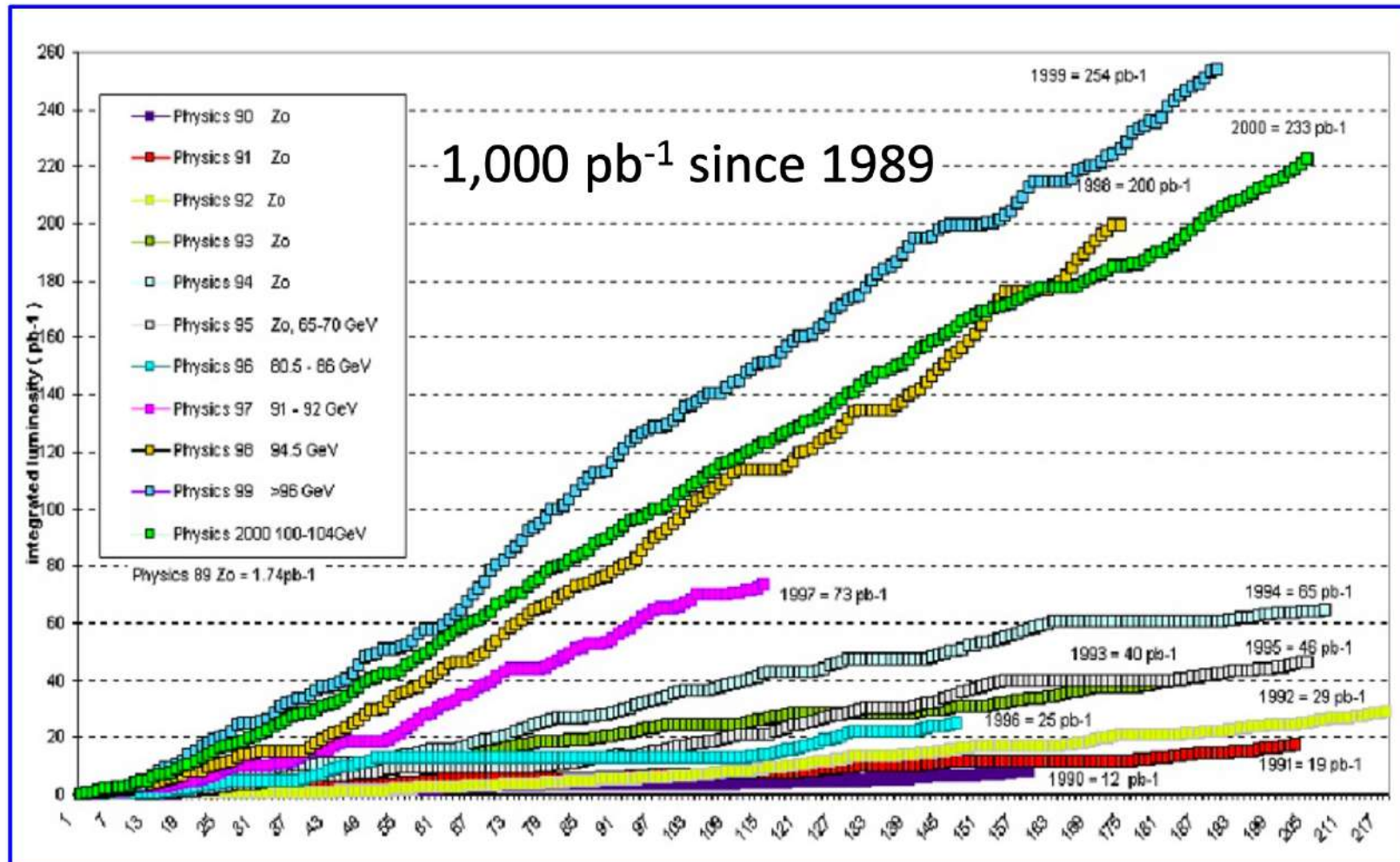


# The LEP collider: integrated luminosity

Slide from  
P. Bagnaia



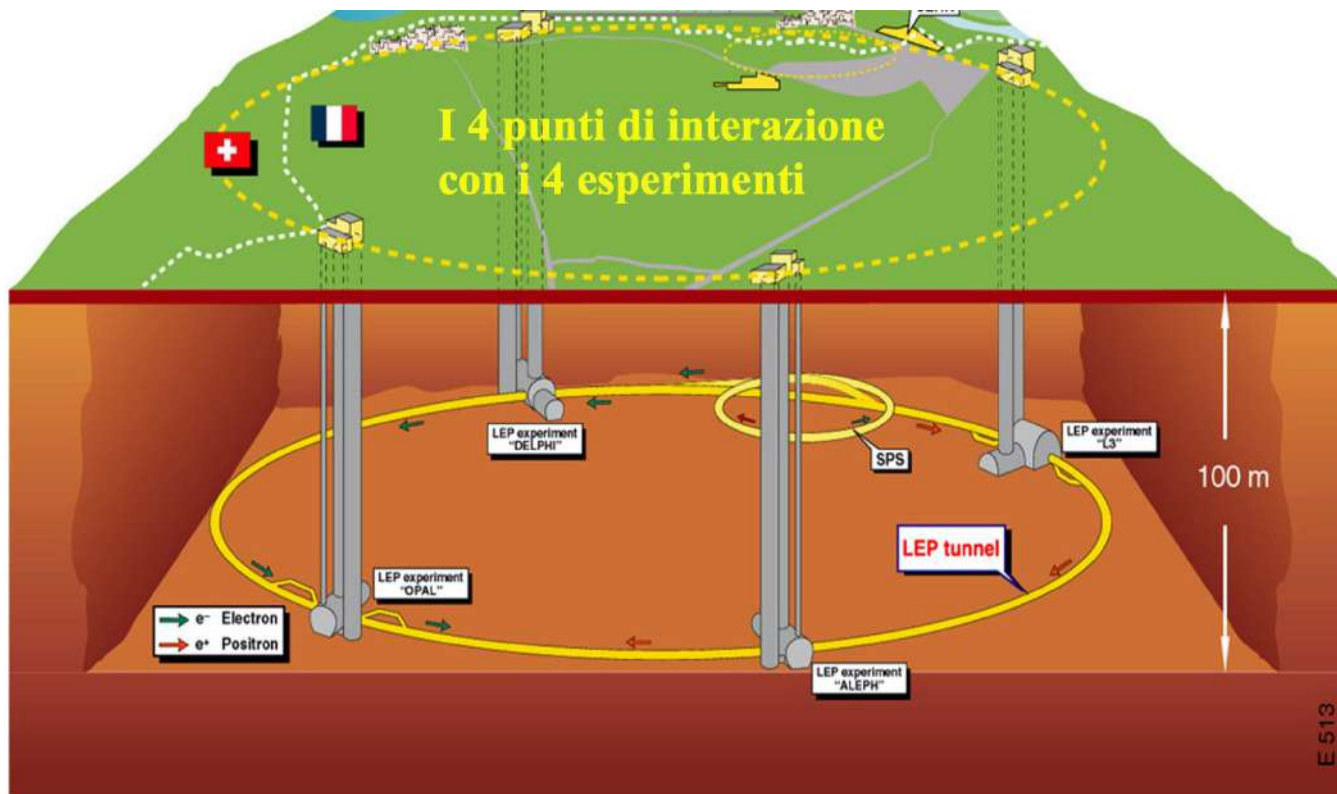
# The LEP collider: integrated lumiosity versus day



# LEP magnet and RF systems

(not part of the exam program)

# LEP magnet parameters



- ❖ Approximately 3400 dipoles,
- ❖ 800 quadrupoles,
- ❖ 500 sextupoles
- ❖ and more than 600 orbit correction dipoles

- The lattice was of type FODO
  - with a periodicity of 79 m,
  - with 31 such cells per octant.
- The angle of deviation per cell was 22.62 mrad.

**At LEP the critical factor determining the circumference was the problem of synchrotron radiation**

- ❑ The 3.8 m diameter tunnel is all underground, at a depth which varies from 50 to 175 m.
- ❑ The ring of 26.67 km circumference is composed of eight 2.9 km long arcs and
- ❑ eight straight sections extending 210 m on either side of the eight possible collision points.

# LEP magnet system

- To make 100 GeV electrons circulate in a ring as large as LEP is easy since a field of only 0.1 T is required. This allowed some innovation on the design of the core, filling with cement the 4 mm spaces between the 1.5 mm steel laminations. Compared to a classic scheme, this technique brought an economy of around 40%.



*Dismounting of the last LEP dipole*



The alignment of the components of the collider was realised with a relative precision of better than 0.1 mm. The first precise measurement made with beam showed that the circumference of LEP was in fact twice as good as predicted: **better than 1 cm in 26.67 km.**

# How to measure the beam energy

- Do you remember?

$$\alpha = \int \frac{dl}{\rho} = \int \frac{Bdl}{B\rho} = 2\pi \quad \frac{\int B dl \approx N l B}{\frac{p}{e} = B\rho} \rightarrow$$

$$B = 2\pi p / (qNl)$$

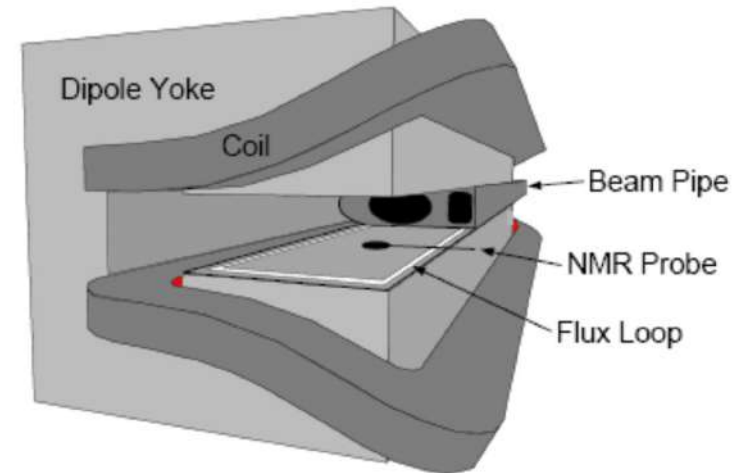
$N$ : number of magnets  
 $l$ : length of a magnet

$N$  (LEP) = 3200

- From this formula we get the relation:

$$E = \frac{e}{2\pi c} \oint_{LEP} B dl$$

- To measure the beam energy we have to know with the highest possible precision the B-field and the radius.
- To measure  $B$ , at the beginning of LEP-1, it was used a reference dipole powered in series with the main dipoles. It was equipped a NMR probe to monitor continuously the field and a flux loop to measure  $B$  in dedicated runs where the magnets were cycled.
- This method aimed to a precision in the beam energy of about 25 MeV, however LEP people found a much better way to measure the energy: the Resonant Depolarization with an ultimate precision of about 1 MeV.
- In LEP-2 RD could not be used because depolarising effects increase sharply with the energy. Therefore 16 NMR probes were placed in some of the 3200 main dipoles along with flux loops.
- The relationship between the fields measured by the probes and the beam energy was calibrated against precise measurements of the average beam energy between 41 and 55 GeV made using the resonant depolarisation technique. It was reached a precision on the beam energy of 10-15 MeV.



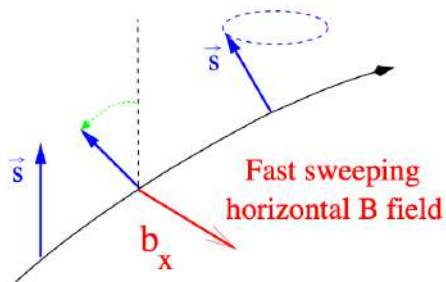
# Beam energy - Resonant Depolarisation

□ During the synchrotron radiation emission a very small probability exists for an electron to experience a spin flip. When this is the case however, the preference for a final spin state anti-parallel to the magnetic field is very large and the electron beam becomes slowly polarised.

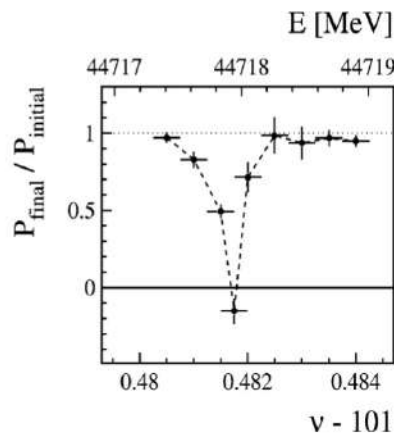
□ Spins precess in B field. Number of precessions per turn of LEP:

$$\nu_s = \frac{g_e - 2}{2} \frac{e}{2\pi m_e} \oint B \cdot dl = \frac{g_e - 2}{2} \frac{E_{\text{beam}}}{m_e c^2}$$

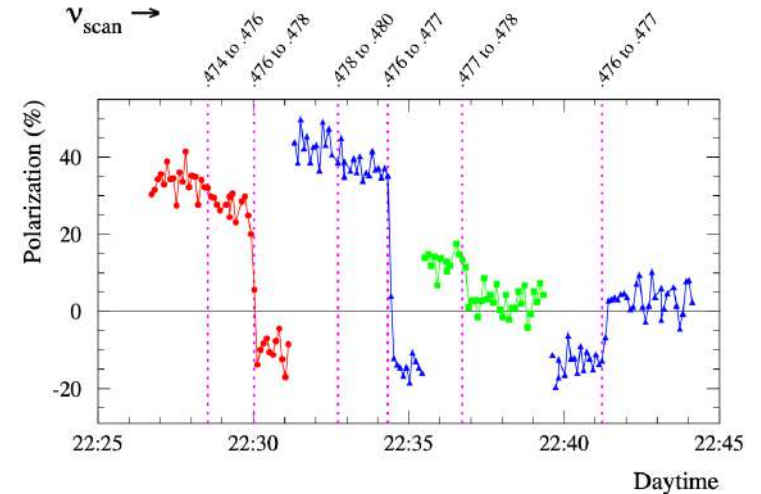
$$\nu_s \approx 101.5, 103.5, 105.5 \text{ at } \sqrt{s} = \text{peak}-2, \text{ peak}, \text{ peak}+2$$



Apply oscillating horizontal B field,  $\nu$ , at one place. Scan  $\nu$ .  
If  $\nu = \nu_s$ , polarisation is destroyed.



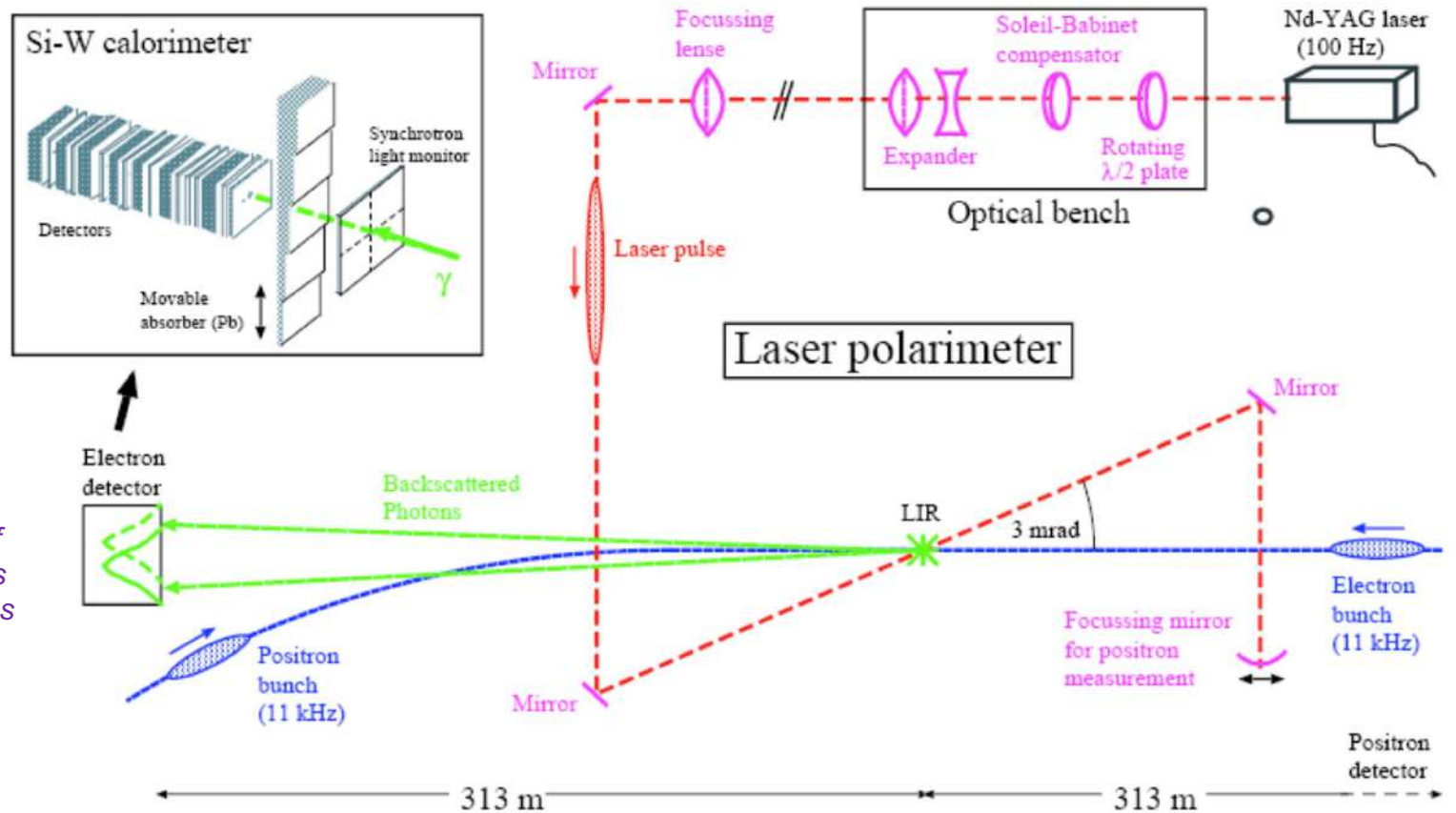
Width of a depolarising resonance



Energy calibration showing multiple spin flips

# LEP Laser Polarimeter

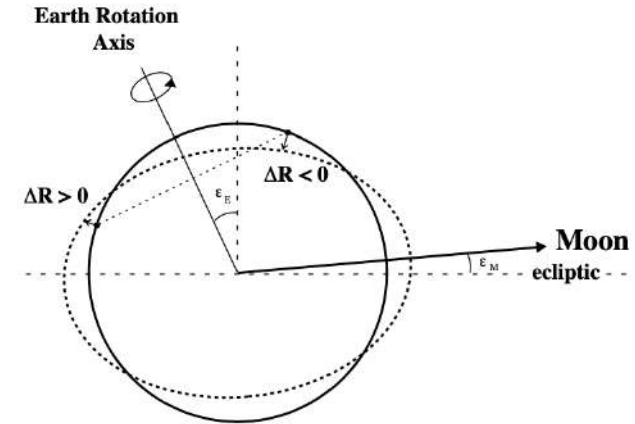
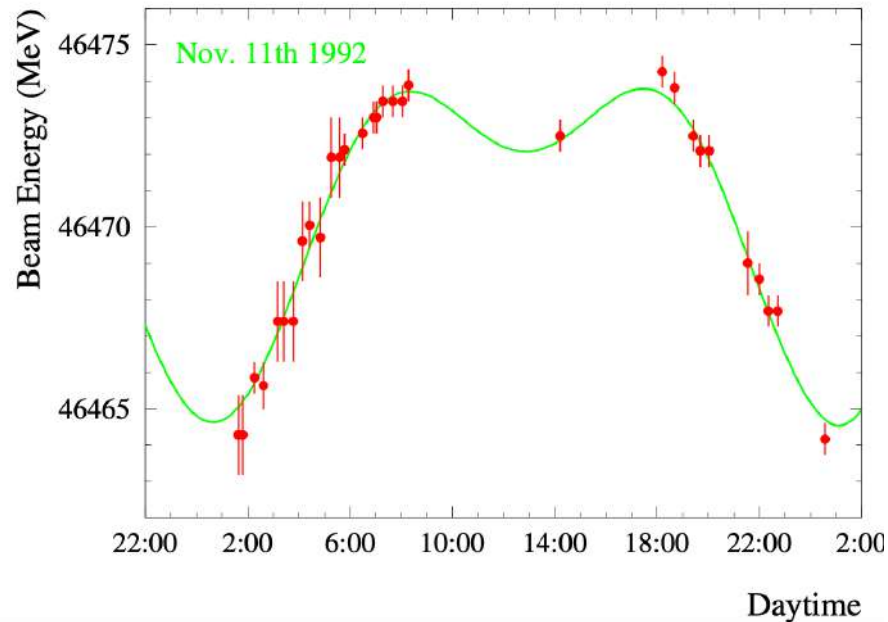
- ❑ The fast LEP polarimeter was based on spin-dependent Compton scattering of *circularly* polarised photons from *transversely* polarised electrons and positrons.



The observable was a shift  $\Delta Y$  in the mean of the vertical distributions of the scattered photons

# Tide effect on the beam energy

- ❑ In 1991 were observed daily fluctuation of the order of 10 MeV.



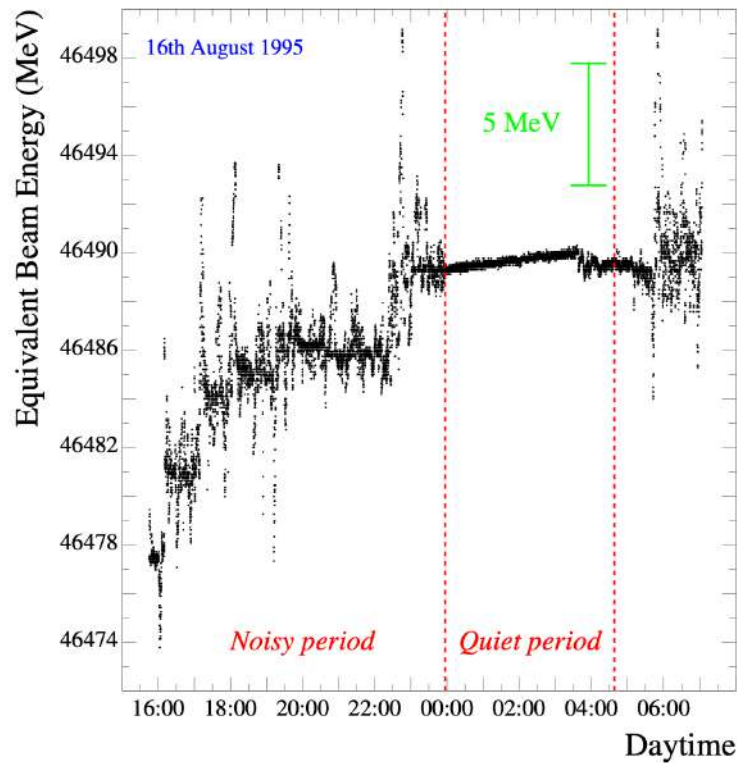
*It was later understood they were due to Earth tides driven by Sun and Moon*

- ❑ Length of orbit fixed by RF system, but magnets move with ground. Beam no longer goes through centre of quadrupoles. Sensitive to 1mm change in 27 km, typical 10 MeV peak-to-peak.
- ❑ Also seen ground distortion due to lake level, heavy rain...
- ❑ Of course this effect was taken into account to measure the beam energy.

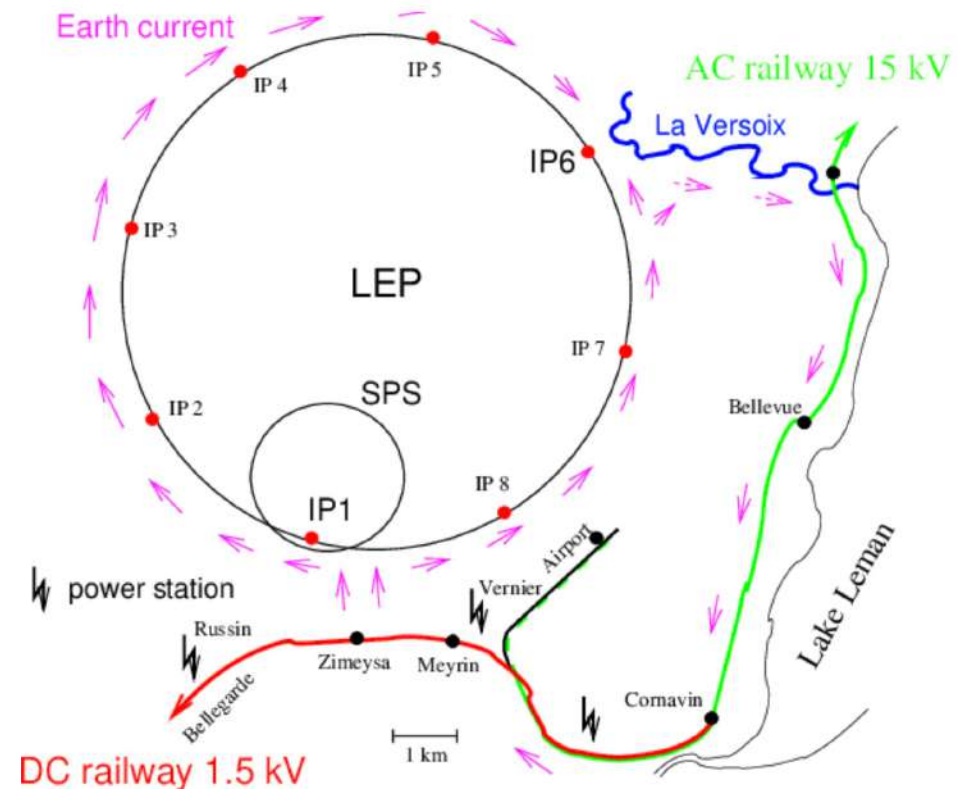
# TGV effect on beam energy

- In 1993 were observed other strange fluctuation in the beam energy related to night versus day or holidays versus working days.

*Long investigation revealed cause - Vagabond electric currents from nearby trains that causing fluctuations in the dipole current.*



Human activity increasing dipole fields during fill:  
BIAS  $\approx$  5 MeV



# Synchrotron Radiation (*Bremsstrahlung*)

$$W_{\text{Larmor}} = \frac{e^2 a^2}{6\pi\epsilon_0 c^3}; \quad [\text{non-rel.}]$$

$$= \frac{e^2 \gamma^6}{6\pi\epsilon_0 c^3} \left[ a^2 - \left( \frac{\vec{v} \times \vec{a}}{c} \right)^2 \right]; \quad [\text{rel.}]$$

circle:  $|\vec{a}| = \frac{v^2}{R}$ ;  $|\vec{v} \times \vec{a}| = \frac{v^3}{R}$ ;  $[\dots] = \frac{v^4}{R^2} \left( 1 - \frac{v^2}{c^2} \right) \approx \frac{c^4}{\gamma^2 R^2}$

$$W_{\text{Larmor}} = \frac{1}{6\pi\epsilon_0} \frac{e^2 c \gamma^4}{R^2};$$

$$T_{\text{orbit}} = \frac{2\pi R}{v} \approx \frac{2\pi R}{c};$$

$$\Delta E_{\text{orbit}} = W_{\text{Larmor}} T_{\text{orbit}} = \frac{1}{3\epsilon_0} \frac{e^2 \gamma^4}{R} = \frac{1}{3\epsilon_0} \frac{e^2 E^4}{R M^4};$$

$$\Delta E_{\text{electron orbit}} = 8.85 \times 10^{-5} \left( \frac{E_e}{1\text{GeV}} \right)^4 / \left( \frac{R}{1\text{Km}} \right) \text{MeV};$$

$$\Delta E_{\text{proton orbit}} = 7.8 \times 10^{-3} \left( \frac{E_p}{1\text{TeV}} \right)^4 / \left( \frac{R}{1\text{Km}} \right) \text{KeV}.$$

$(m_p/m_e)^4 \approx 1.1 \times 10^{13}$

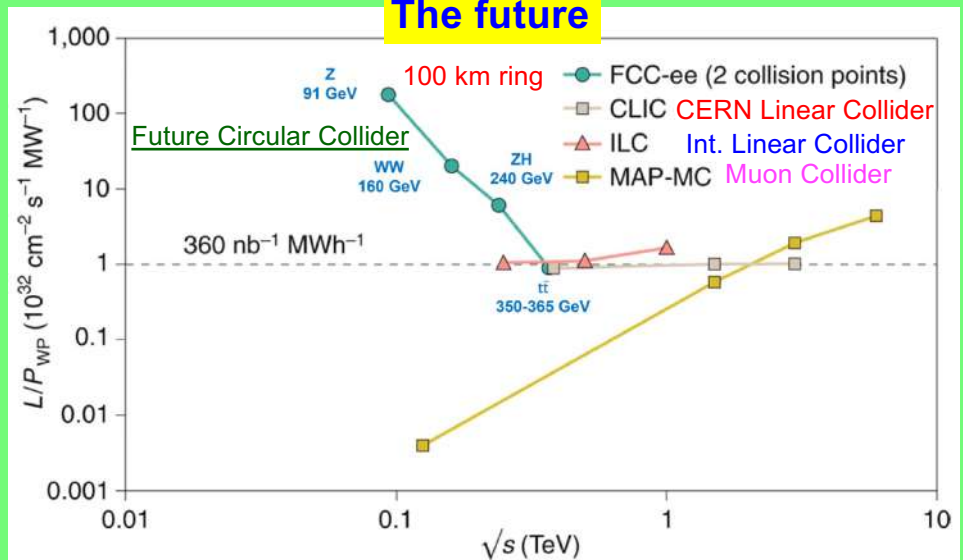
	$\Delta E \propto M^{-4}$	$\sqrt{s}$ (GeV)	$\Delta E$
LEP 1	$e^+e^-$	90	121 MeV
LEP 2	$e^+e^-$	200	2,500 MeV
LHC	pp	14,000	6.9 KeV

$$\text{Synch. Rad.} \propto \frac{E^4}{R}$$

This is the energy lost by one particle in one turn. Then you have to multiply by the number of particles in the collider

LEP is the last  $e^+e^-$  collider (but never say never again).

The future



# RF system

## □ LEP-1: RF copper cavities



128 five-cell copper cavities, powered by 16 klystrons of 1 MW (maximum value, mean value delivered was 0.6 MW).

E-field  $\sim 1.5$  MV/m; peak accelerating voltage 400 MV per revolution.

The operating frequency of the cavities is 352.209 188 MHz, which corresponds to 31 320 times the revolution frequency in LEP

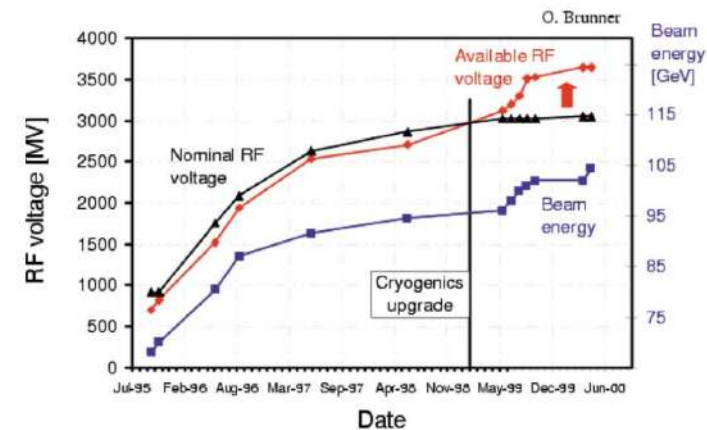
To operate LEP at 103 GeV with classical cavities would require 1280 of them, with 160 MW of RF power, which makes no sense for many reasons.

## □ LEP-2: Superconducting RF cavities



A superconducting cavity, cut in two. One can see the inner layer of sputtered niobium.

□ From 1995 copper cavities were gradually replaced with SC cavities up to a maximum of 288, each with an average field of 7.5 MV/m ( design was 6.0 MV/m)

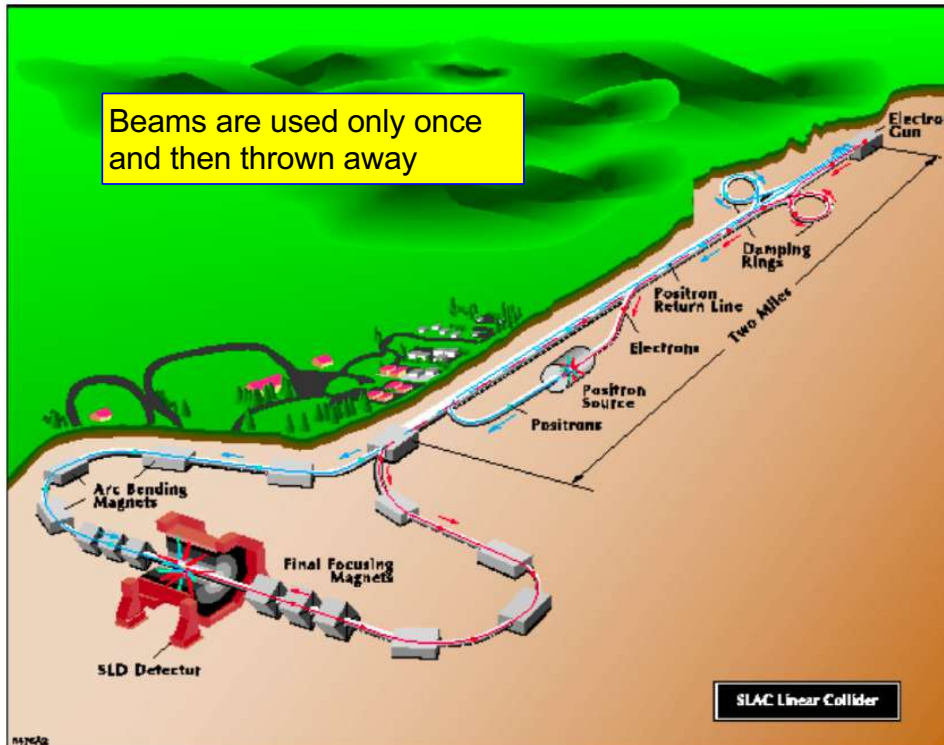


Evolution of the accelerating voltage at LEP-2

□ The only regret was to have lost the possibility to attain a centre of mass energy  $\sim 7\%$  higher, because a further 80 to 100 cavities could have been accommodated in the accelerating sections without prohibitive civil engineering work.

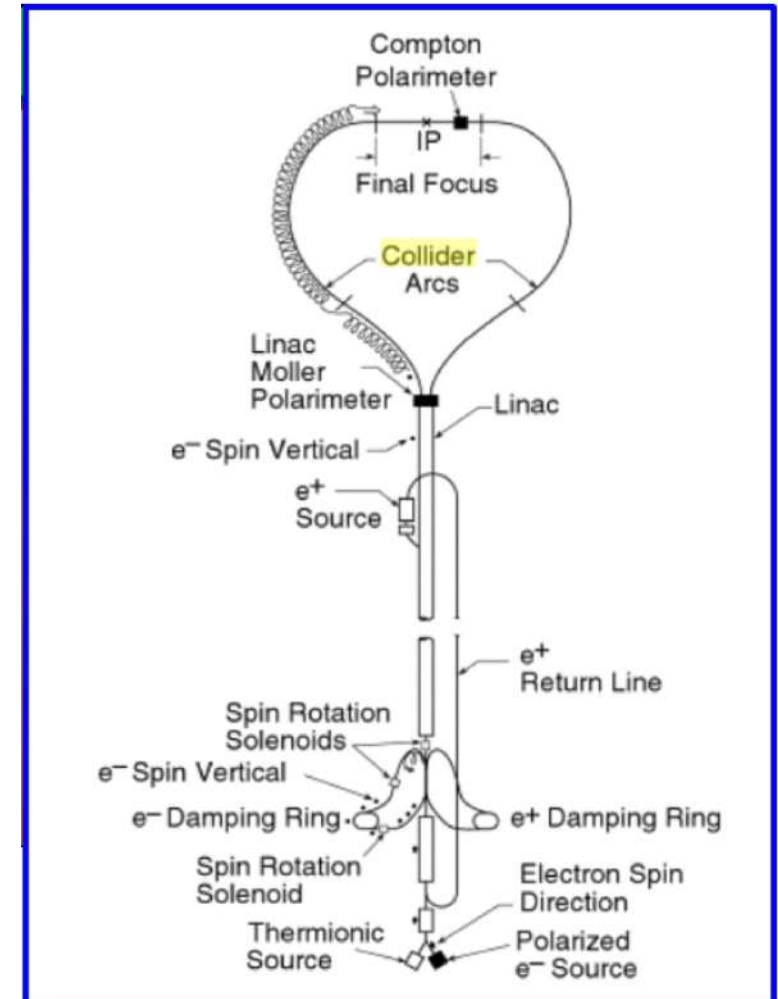
# The competitor: SLC

# Stanford Linear Collider

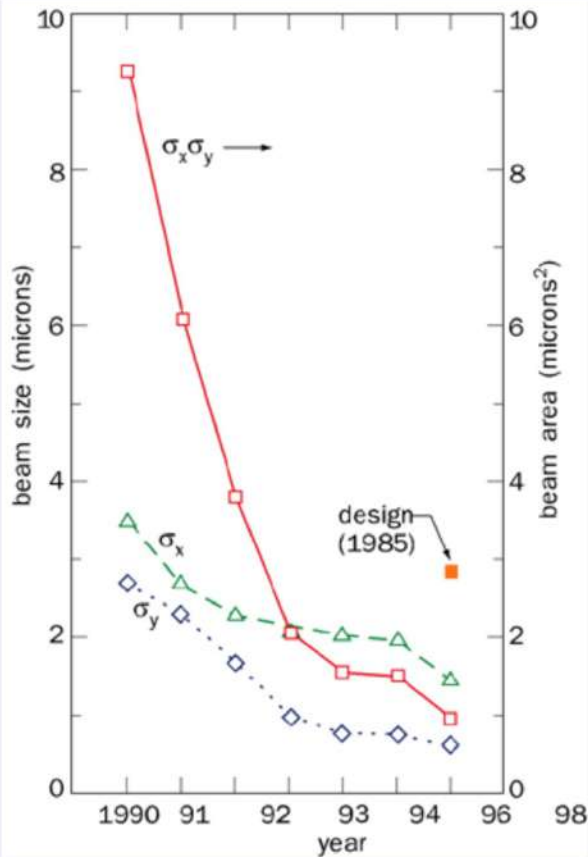


SLC : Stanford Linear Collider (1989-98):

- the first example of linear  $e^+e^-$  collider;
- lower energy (only Z pole) and less intense;
- polarized beams; (since 1992)

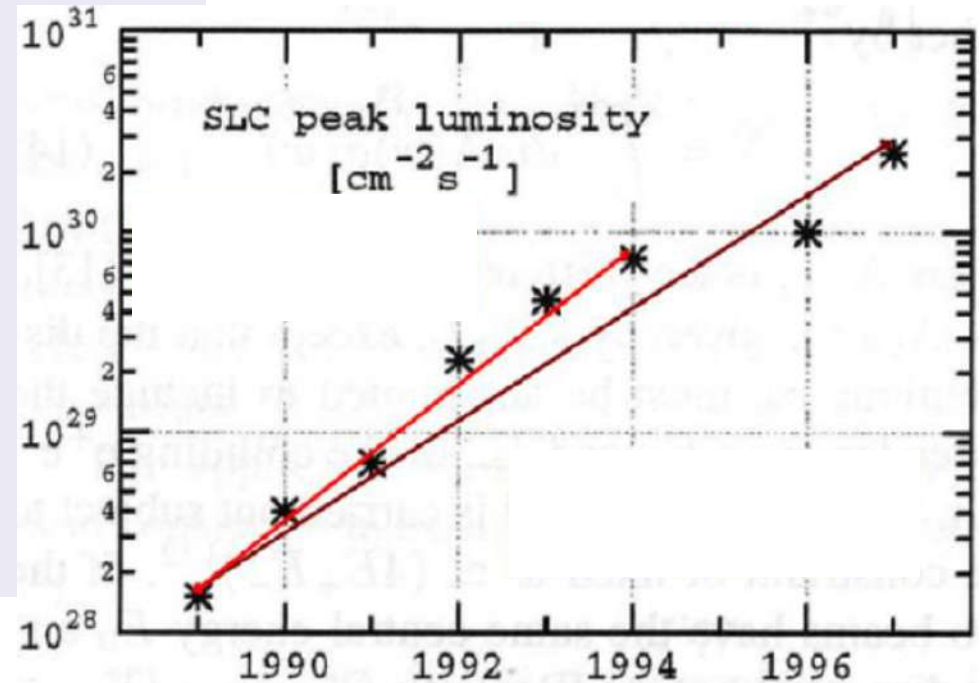


# SLC: beam size and luminosity

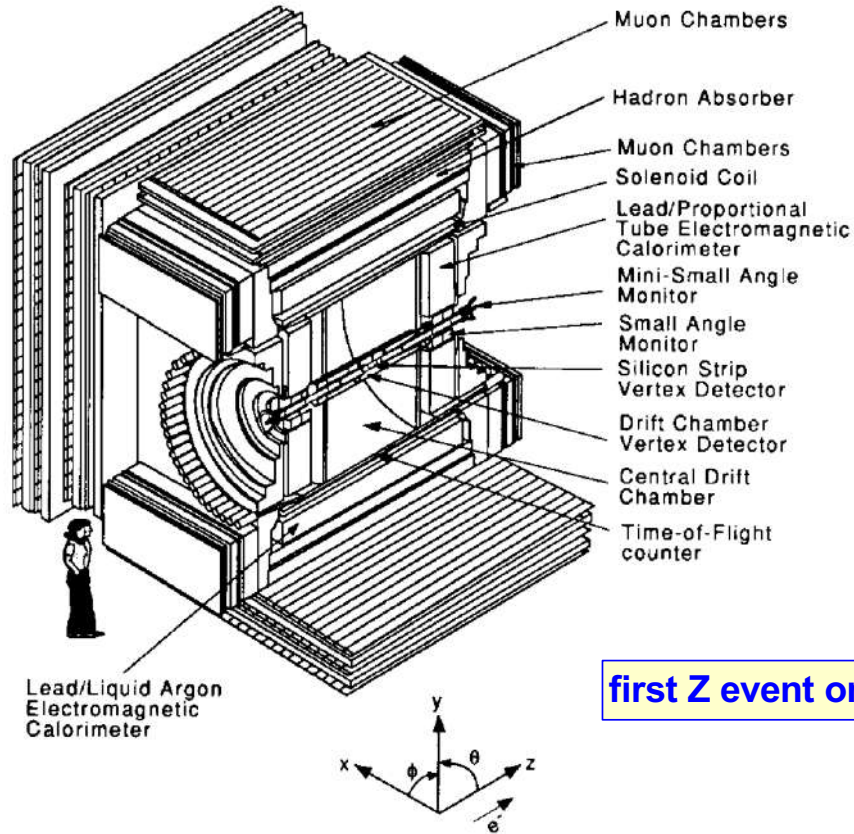


By compressing the size of the electron and positron beams at the interaction point (IP), the SLC has substantially increased its luminosity, a measure of the electronpositron collision rate.  $s_x$  and  $s_y$  are the rms beam half width and height, respectively; their product is a measure of the cross sectional area of the beam at the interaction point.

In a circular collider you can not "squeeze" the beams "too much", otherwise they become unstable and you loose the control. But here is not an issue, since you are "throwing away" the beam in any case.

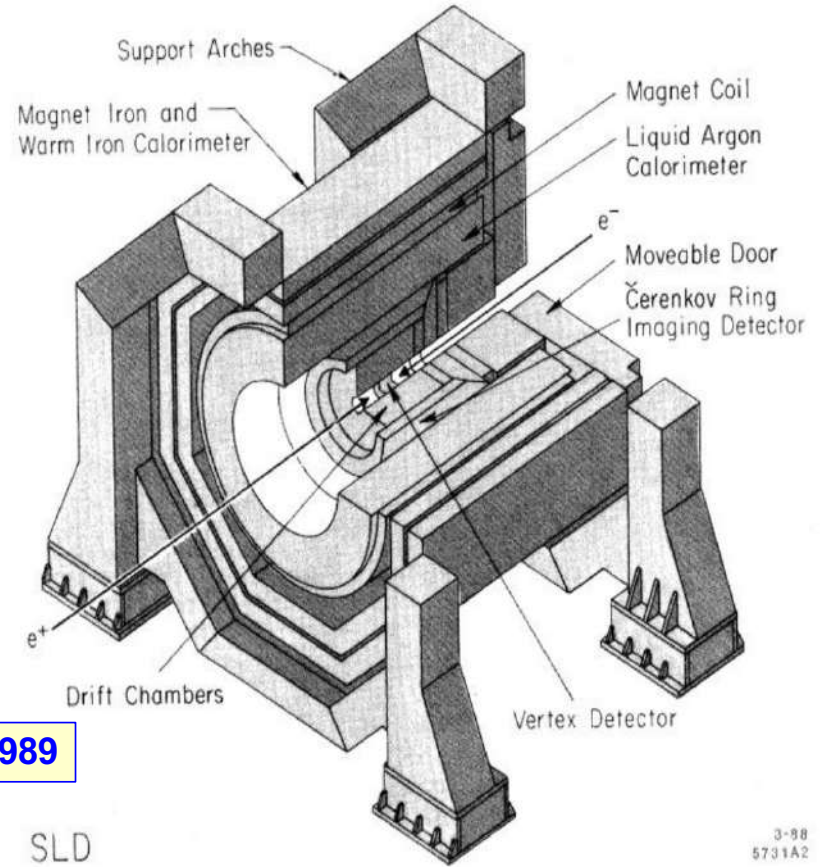


# SLC Detectors



first Z event on 12 April 1989

MARK-II Detector: 1989-1990



SLD

3-88  
5731A2

Cut-away view of the SLD with one endcap removed.

SLD Detector: 1991 - 1998

# First MARK-II paper on Z properties

VOLUME 63, NUMBER 7

PHYSICAL REVIEW LETTERS

14 AUGUST 1989

## Initial Measurements of Z-Boson Resonance Parameters in $e^+e^-$ Annihilation

$\langle E \rangle$ (GeV)	$\langle \sigma_E \rangle$ (GeV)	SAM $e^+e^-$	Z decays			$\sigma_Z$ (nb)
			Had.	Lep.	Tot.	
89.24	0.22	24	3	0	3	$5.5^{+6.1}_{-3.1}$
89.98	0.25	37	8	2	10	$11.8^{+6.9}_{-4.1}$
90.70	0.28	44	27	3	30	$30.4^{+2.1}_{-2.1}$
91.50	0.29	53	32	6	38	$31.9^{+8.4}_{-6.4}$
92.16	0.28	33	11	0	11	$14.2^{+7.8}_{-4.8}$
92.96	0.23	43	13	1	14	$13.5^{+5.6}_{-4.6}$
Totals		234	94	12	106	

TABLE II. Z resonance parameters. The three fits are described in the text.

Fit	$m_Z$ (GeV/ $c^2$ )	$N_\nu$	$\Gamma$ (GeV/ $c^2$ )	$\chi^2/N_{DF}$
1	$91.11 \pm 0.23$	...	...	4.1/5
2	$91.11 \pm 0.23$	$3.8 \pm 1.4$	...	3.7/4
3	$91.06 \pm 0.17$	$3.2^{+1.3}_{-1.1}$	$1.61^{+0.60}_{-0.43}$	1.5/3

Remember: the first Z produced at LEP was on 15 August 1989

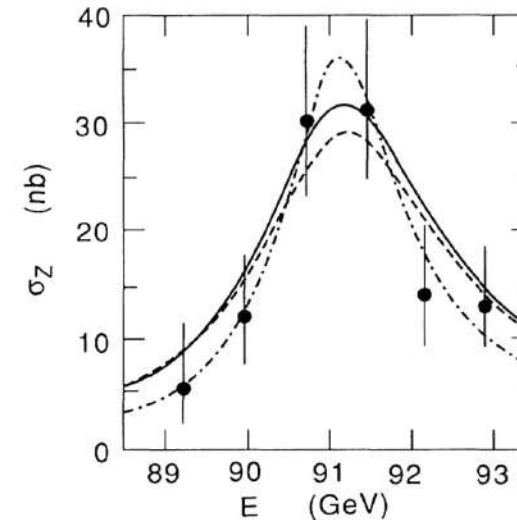


FIG. 2.  $e^+e^-$  annihilation cross sections to all hadronic events plus  $\mu$  and  $\tau$  pairs with  $|\cos\theta| < 0.65$ . The curves represent the result of different fits: solid,  $m_Z$  free; dashed,  $m_Z$  and  $N_\nu$  free; and dot-dashed,  $m_Z$ ,  $N_\nu$ , and  $\Gamma$  free. The peak  $\sigma_Z$  occurs approximately 100 MeV higher than  $m_Z$  due to radiative corrections.

$\sigma(M_Z)$  about 340 MeV from UA2+CDF in 1989

# Second MARK-II paper on Z properties

VOLUME 63, NUMBER 20

PHYSICAL REVIEW LETTERS

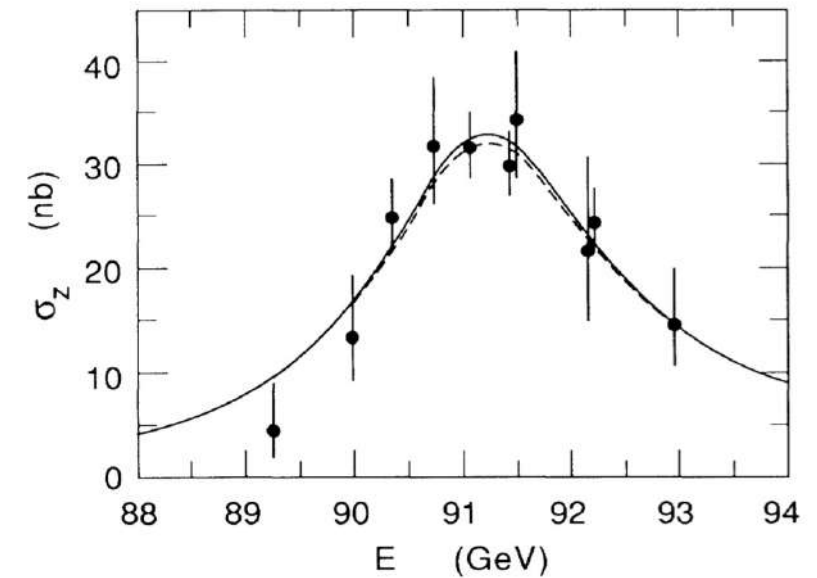
13 NOVEMBER 1989

## Measurements of Z-Boson Resonance Parameters in $e^+e^-$ Annihilation

Scan point	$\langle E \rangle$ (GeV)	$N_S$	$N_M$	$\epsilon_M$	$\mathcal{L}$ (nb $^{-1}$ )	Had.	Z decays Lep.	Tot.	$\sigma_Z$ (nb)
3	89.24	24	166	0.99	$0.68 \pm 0.05$	3	0	3	$4.5^{+4.3}_{-2.3}$
5	89.98	36	174	0.99	$0.76 \pm 0.05$	8	2	10	$18.5^{+4.9}_{-4.9}$
10	90.35	116	617	1.00	$2.61 \pm 0.10$	60	2	62	$24.8^{+3.8}_{-3.8}$
2	90.74	54	266	0.96	$1.21 \pm 0.07$	33	3	36	$31.7^{+3.8}_{-3.8}$
7	91.06	170	923	0.99	$4.08 \pm 0.12$	114	6	120	$31.6^{+3.1}_{-3.1}$
8	91.43	164	879	0.91	$4.12 \pm 0.13$	108	6	114	$29.8^{+2.9}_{-2.9}$
4	91.50	53	275	0.99	$1.23 \pm 0.07$	33	6	39	$34.3^{+3.9}_{-3.9}$
1	92.16	31	105	0.97	$0.54 \pm 0.05$	11	0	11	$21.5^{+2.8}_{-2.8}$
9	92.22	128	680	0.98	$3.05 \pm 0.11$	67	4	71	$24.3^{+3.4}_{-3.4}$
6	92.96	39	214	0.98	$1.00 \pm 0.07$	13	1	14	$14.6^{+4.0}_{-4.0}$
Totals		815	4299		$19.3 \pm 0.9$	450	30	480	

TABLE II. Z resonance parameters. The three fits are described in the text.

Fit	$m_Z$ (GeV/ $c^2$ )	$N_\nu$	$\Gamma$ (GeV)	$\sigma_0$ (nb)
1	$91.14 \pm 0.12$	...	...	...
2	$91.14 \pm 0.12$	$2.8 \pm 0.6$	...	...
3	$91.14 \pm 0.12$	...	$2.42^{+0.45}_{-0.35}$	$45 \pm 4$



$N_\nu$  is getting close to 3

# First L3 paper on Z properties

Volume 231, number 4

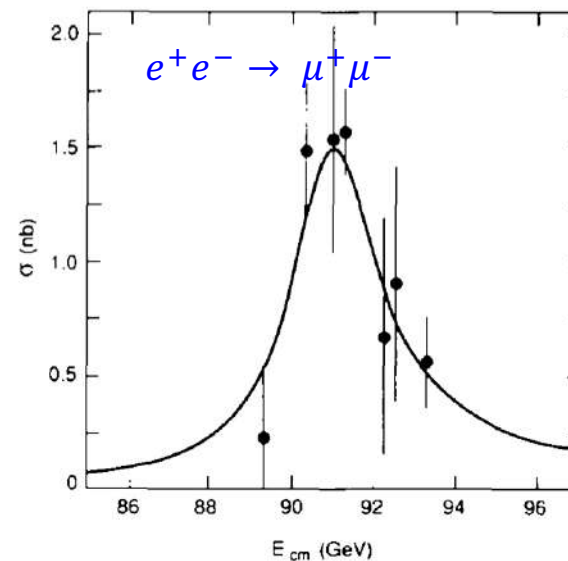
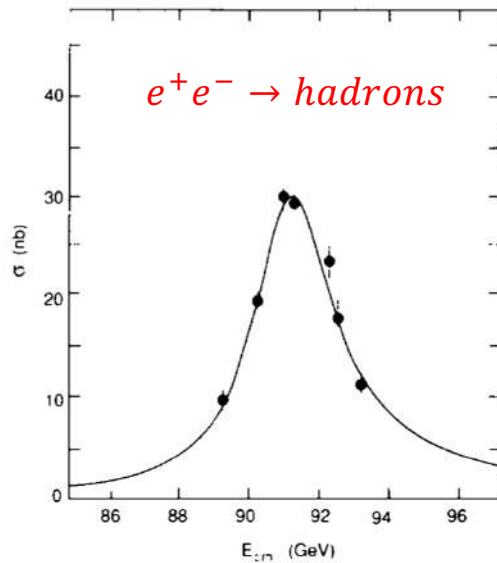
PHYSICS LETTERS B

16 November 1989

## A DETERMINATION OF THE PROPERTIES OF THE NEUTRAL INTERMEDIATE VECTOR BOSON $Z^0$

Received 12 October 1989

Fit	$Z^0$ mass (GeV)	Total width (GeV)	Invisible width (GeV)	$\chi^2/DF$
1	$91.135 \pm 0.057$			4.7/5
2	$91.132 \pm 0.057$	$2.588 \pm 0.137$		3.8/4
3	$91.133 \pm 0.056$		$0.567 \pm 0.080$	4.0/4



Thanks to the excellent performance of LEP, we have analysed 2538 hadron events, 95 electron pairs and 97 muon pairs near the  $Z^0$  mass region. With a conservative estimate of our overall normalization uncertainty of 6%, we have measured: the mass of the  $Z^0$  to be

$$M_{Z^0} = 91.132 \pm 0.057 \text{ GeV}$$

(not including the 46 MeV machine energy uncertainty).

the width of the  $Z^0$  to be:

$$\Gamma_{Z^0} = 2.588 \pm 0.137 \text{ GeV},$$

the invisible width:

$$\Gamma_{\text{invisible}} = 0.567 \pm 0.080 \text{ GeV},$$

which gives for the number of neutrinos:

$$3.42 \pm 0.48.$$

We also determined independently

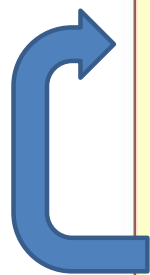
$$\Gamma_{\mu\mu} = 92 \pm \text{MeV}, \text{ and } \Gamma_{ee} = 88 \pm 9 \pm 7 \text{ MeV}.$$

# LEP Detectors

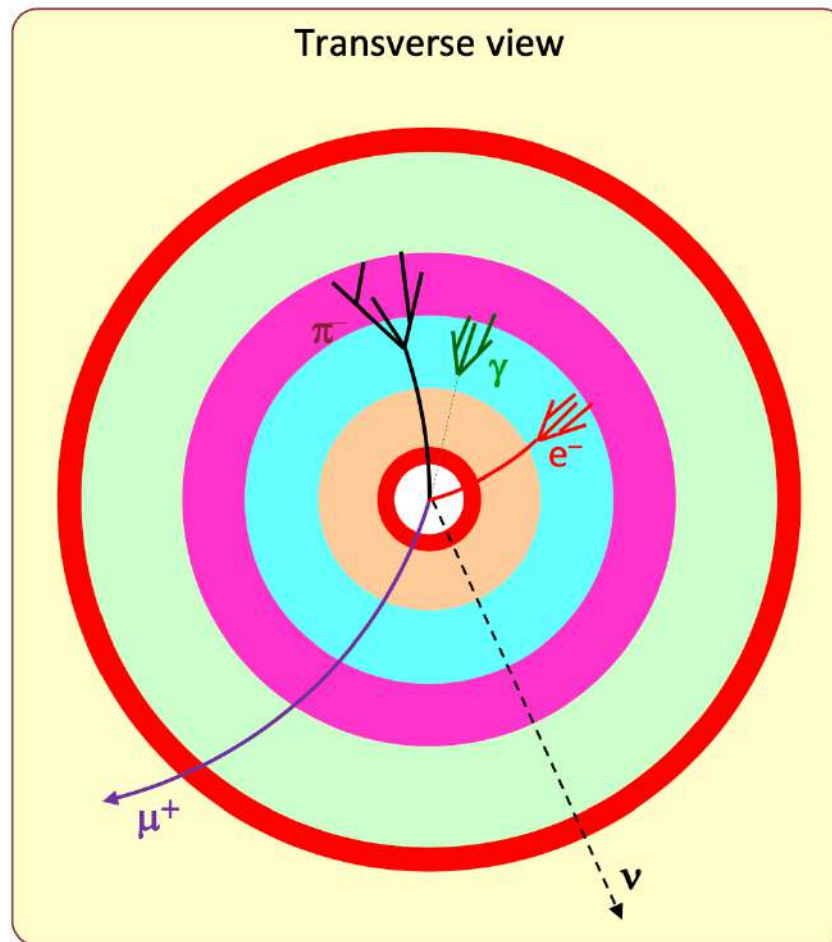
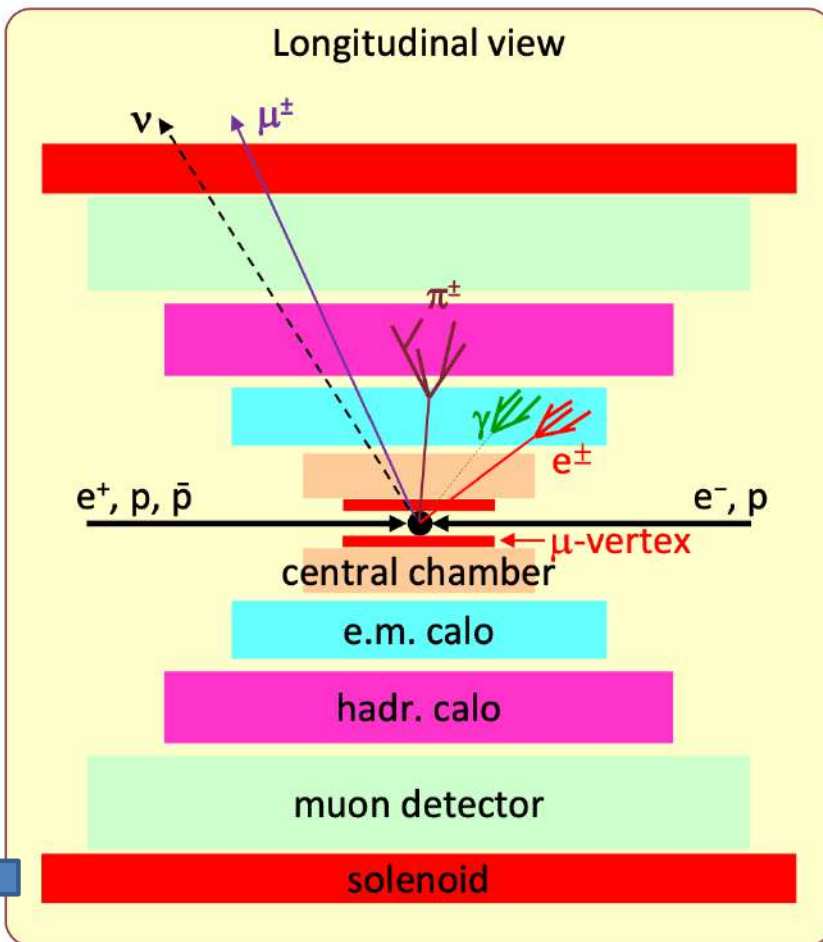
# Detector basic principles

Typical detector of an electron/hadron collider

Usually the solenoid is between ecal and hcal calorimeters.



L3 was an exception in this respect

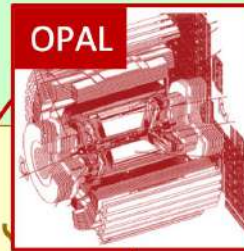
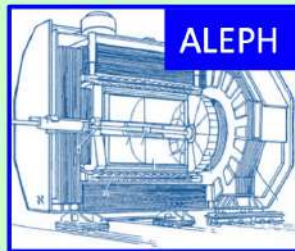


Also ATLAS is an exception with the toroidal field in the muon spectrometer

# Detectors Main Features

## Jack Steinberger

*ALEPH had reasonably new technologies, homogeneous detector, granularity more than energy resolution. The heart of the detector is a large TPC and a high granularity (200 000 channels) ecal in a large superconducting magnet. The technologies are the same for barrel and end-cap detectors, giving only 5 types of detectors.*

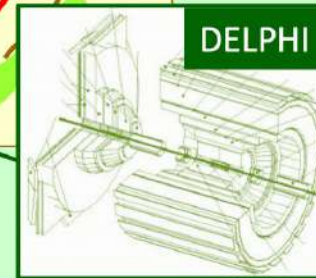
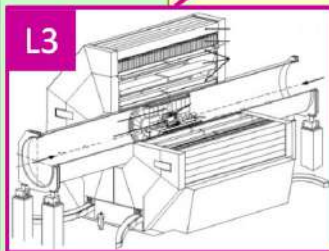


## Alberto Michelini

*OPAL was designed to use only proven and reliable technologies, to be sure at least one of these huge detectors would be ready in time. A classical magnet, 11 700 lead glass blocks and drift wire chambers for the tracking are the main components.*

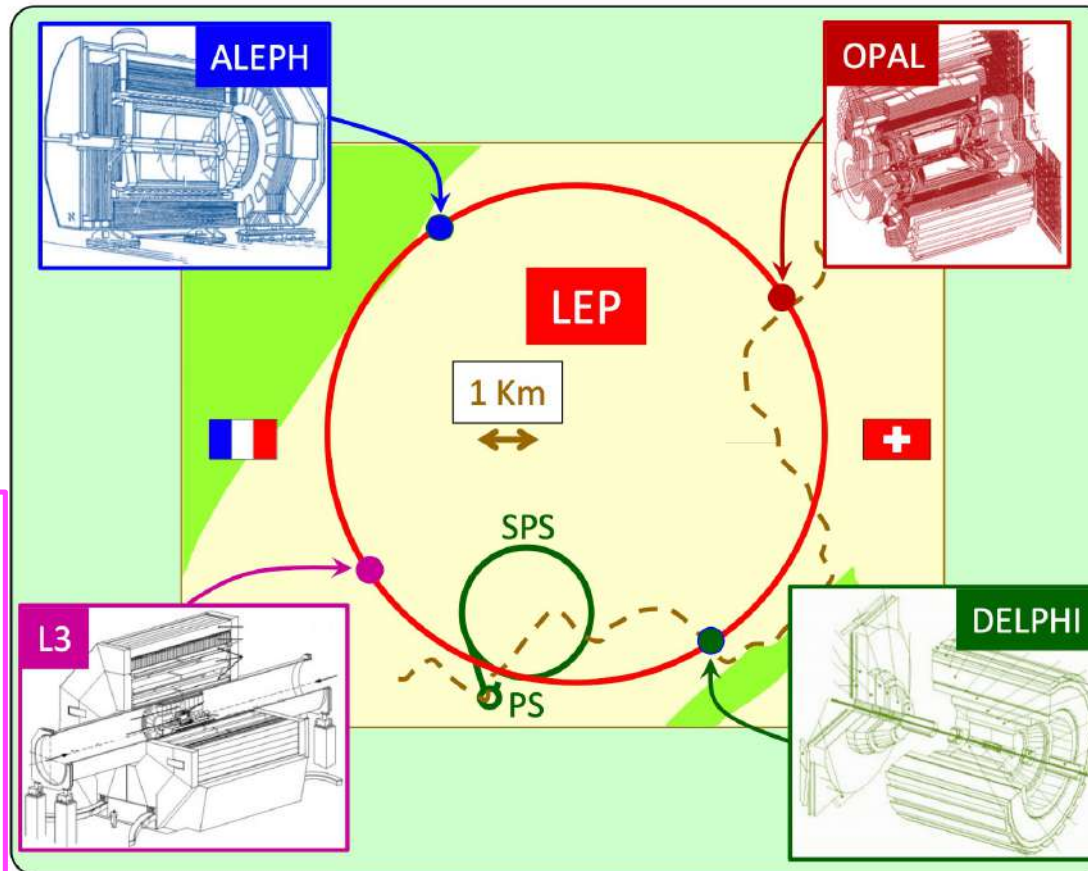
## Samuel Ting

*L3 was quite different from the 3 others. The emphasis was put on measuring leptons (and photons) with high resolution. The tracking system is very small, and is surrounded by a very high resolution calorimeter with 10 700 BGO crystals. The muon system has many large chambers, and the whole detector is inside a huge warm magnet, having around 10 m internal aperture.*



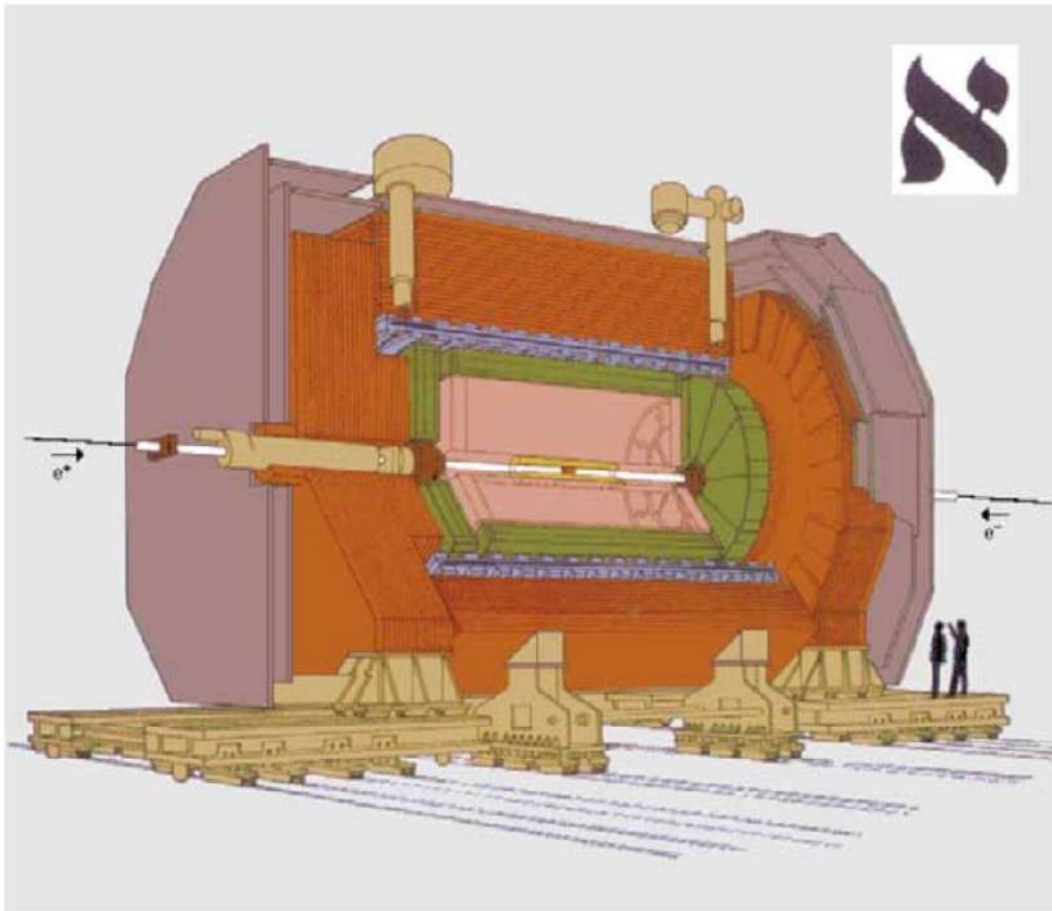
## Ugo Amaldi

*DELPHI had many detectors. Here, the choice was more on very new technologies, and a larger variety of techniques. The main components are a TPC, a Ring Imaging Cherenkov (RICH) to identify charged particles, and a very fine grained calorimeter. The superconducting solenoid was the largest ever built.*



# ALEPH Detector

## Apparatus for LEP PHysics



**Vertex Detector**

For each track, the vertex detector measured two pairs of coordinates, 6.3 cm and 11 cm away from the beam axis over a length of 40 cm along the beam line

**Inner Tracking Chamber**

an axial-wire drift chamber with inner and outer diameters of 13 cm and 29 cm and a length of 2 m. It provided 8 track coordinates and a trigger signal for charged particles

**Time Projection Chamber**

4.4 m long and 3.6 m in diameter. It provided a 3D measurement of each track segment. In addition, it provided up to 330 ionisation measurements for a track.

**Electromagnetic Calorimeter**

It consisted of alternating layers of lead and proportional tubes read out in 73,728 projective towers, each subdivided into three depth zones.

**Superconducting Magnet Coil**

**1.5 T ; 6.4 m long and 5.3 diameter**

**Hadron Calorimeter**

The iron was 1.2 m thick equipped with streamer tubes to act also as hadron calorimeter. It was read out in 4608 projective towers.

**Muon Chambers**

Outside the iron, there were two double layers of streamer tube chambers to record the position and angle of muons.

**Luminosity Monitors**

highly segmented luminosity calorimeter, composed of twelve-layer tungsten/silicon sandwiches.

# TPC

❑ Unlike Multiwire Proportional Chambers (MWPC) or Drift Chambers (DC), TPCs measure directly points on the charged tracks trajectories in 3 dimensions.

The principle the following: a large vessel contains an ionisable gas (mixture of Argon and methane) in which charged particles produce ionisation electrons.

An electric field lets these electrons drift in the vessel towards a MWPC located at the end of the drift volume.

This MWPC is equipped with readout electronics on its wires and rows of pads are designed on the cathode to allow a two-dimensional measurement of the avalanche position. An interpolation method between the pads hit by an avalanche give a precision of about 250  $\mu\text{m}$ .

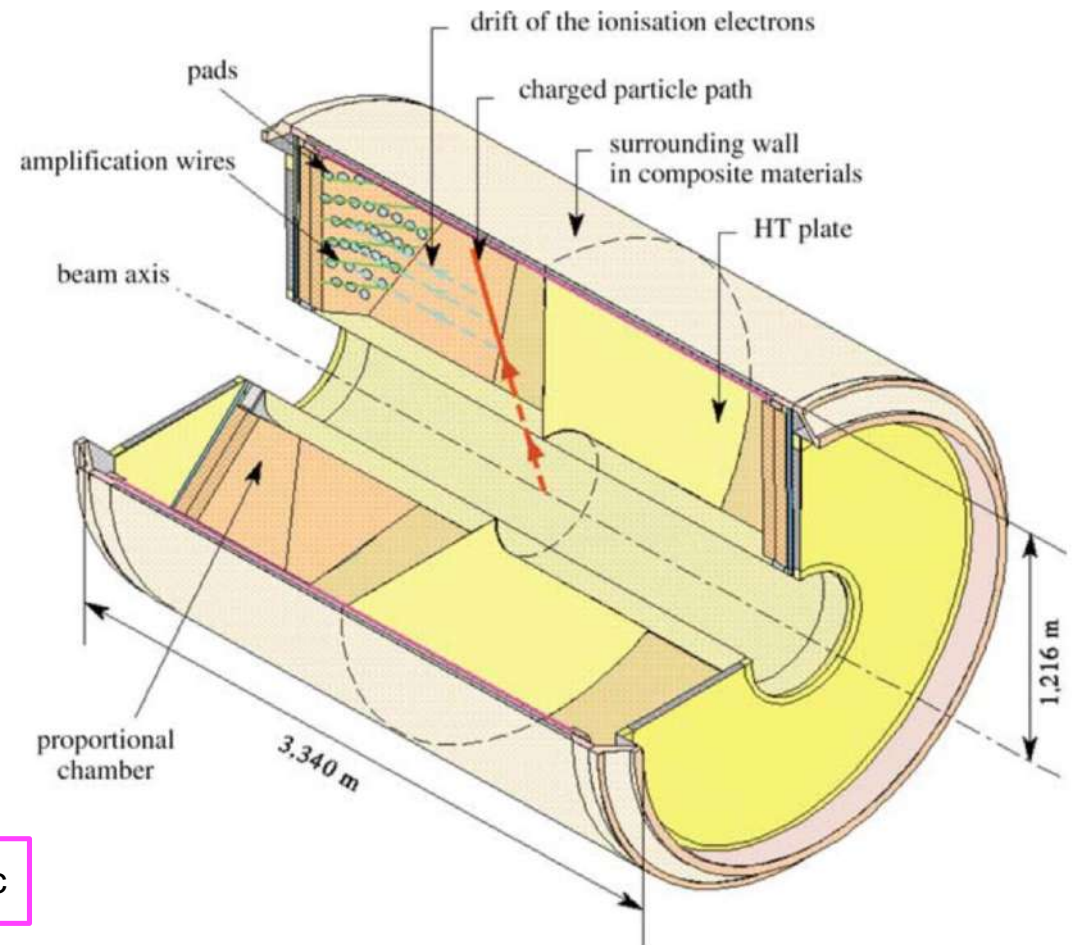
The third dimension (the distance between the track and the MWPC) is obtained by measuring the drift time of the electrons. A precision of the order of 0.5 mm can be obtained on each measured point for this third dimension.

Drifting electrons over long distances (1–2 m) however poses problems such as dispersion of the electrons due to their interaction with the gas.

This effect is much reduced by the fact that the drifting vessel is contained in a magnetic field. The B-field has a focussing effect on the electrons which tend to follow it rather than the electric field.

It is thus very important that both fields are quite parallel, to better than  $10^{-4}$ .

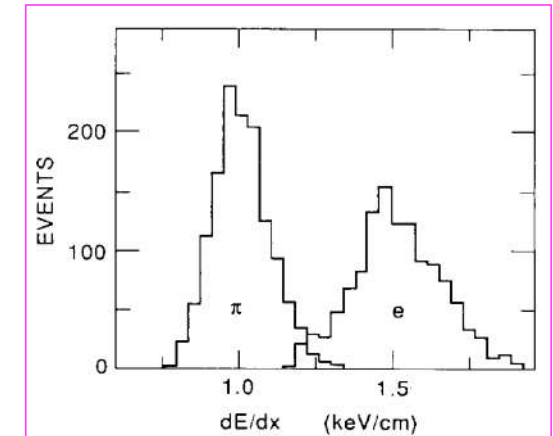
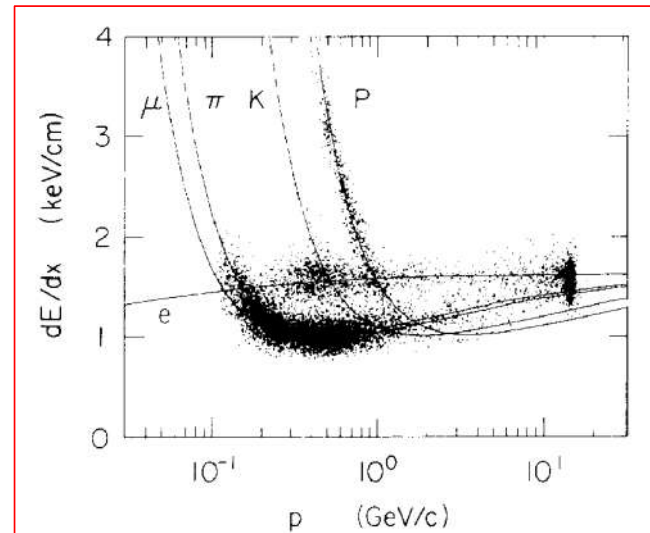
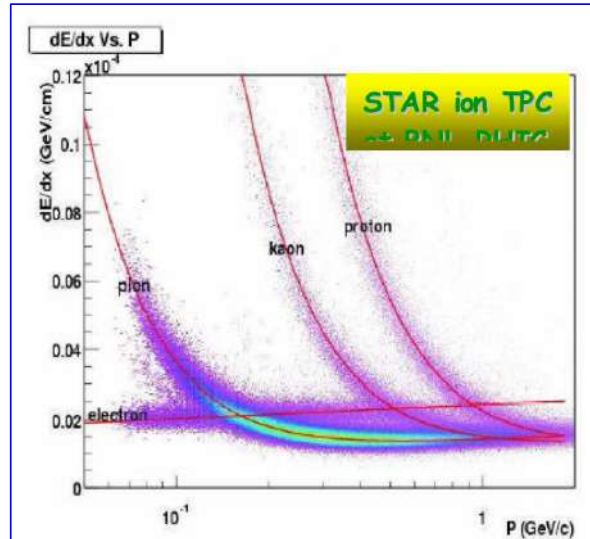
$$\text{Aleph TPC: } \frac{\Delta p}{p^2} = 1.2 \times 10^{-3} (\text{GeV}/c)^{-1} \rightarrow \sim 5\% \text{ at } 45 \text{ GeV}/c$$



# Particle Identification through dE/dx

- If the inner tracker device is able to measure the energy loss during the ionisation process, this information can be used to identify the particle, i.e. to measure the mass.

Two examples of a TPC chamber.



Example: pion/electron separation

A simplified form of the Bethe-Bloch equation describing the average ionisation energy loss by charged particles is :

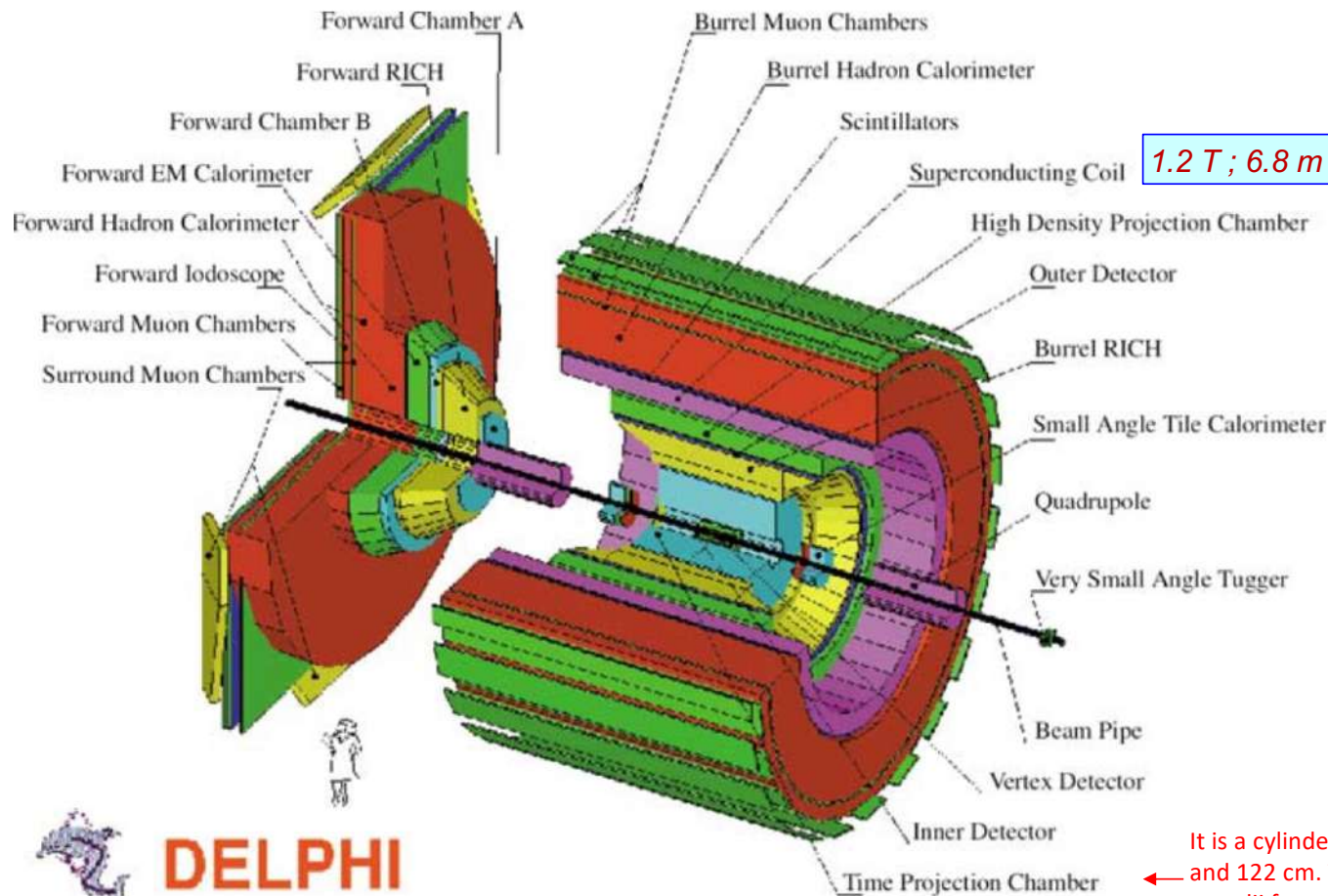
$$-\frac{dE}{dx} \propto \frac{1}{\beta^2} \left[ \ln \left( \frac{2m_e c^2 \beta^2 \gamma^2}{I} \right) - \beta^2 \right],$$

where  $m_e$  is the mass of the electron and  $I$  is the ionization potential of the material.  $\beta = v/c$  and  $\gamma = 1/\sqrt{1 - \beta^2}$  have their usual relativistic definitions.

- The energy loss depends on the velocity of the particle
- Combining the momentum measurement with the dE/dx, one can guess the particle mass
- For a given event, you can not tell what particle it is; you can only give the probability that the particle belongs to a given category or to another.

# DELPHI Detector

## DEtector with Lepton, Photon and Hadron Identification



1.2 T ; 6.8 m long and 5.5 diameter

The RICH technique is based on the detection of Cherenkov light emitted by the particle. The DELPHI RICH contains two radiators of different refractive indices. The liquid radiator is used for particle identification in the momentum range from 0.7 to 9 GeV/c. The gas radiator is used from 2.5 to 25 GeV/c. The full solid angle coverage is provided by two independent detectors, one in the endcap regions (Forward RICH), and one in the the barrel regions (Barrel RICH).

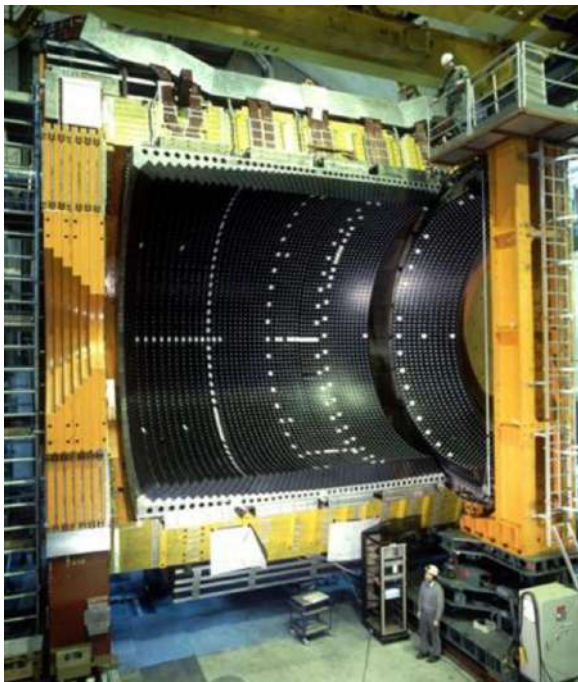
The Barrel RICH is a 350 cm long cylinder with inner radius 123 cm and outer 197 cm,

It is a cylinder of 2x130 cm situated between the radii 29 cm and 122 cm. The detector provides points per particle trajectory at radii from 40 to 110 cm between polar angles from 39 to 141 degrees.

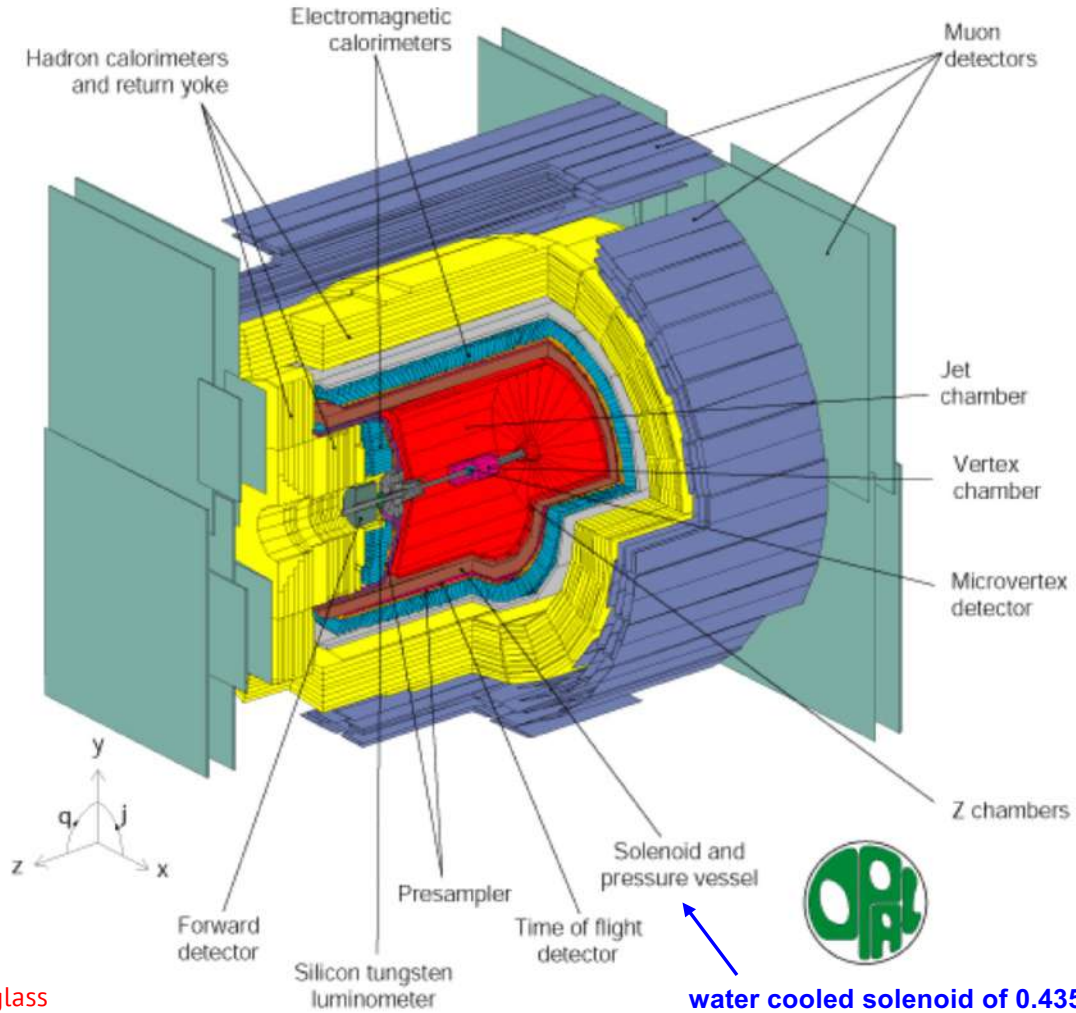
# OPAL Detector

## Omni-Purpose Apparatus for Lep

The OPAL was about 12 m long, 12 m high and 12 m wide



Half of the ECAL. This calorimeter consists of 4720 blocks of lead glass

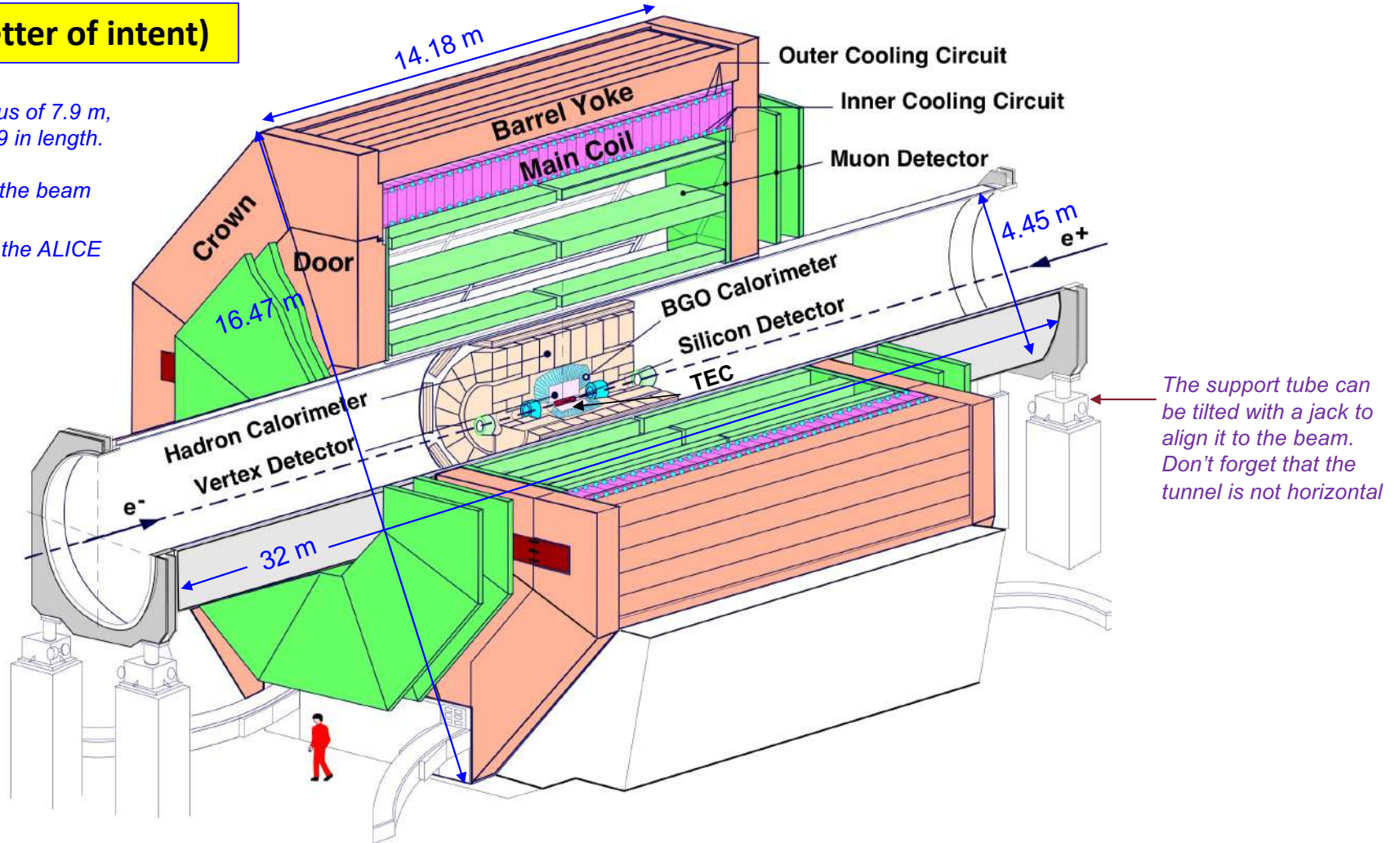


# A deeper look to the L3 Detector

# L3 Detector

## Letter 3 (the third letter of intent)

The magnet has an outside radius of 7.9 m, inside radius of 5.9 m and is 11.9 m in length. The total weight is 7800 tons. It provides 0.5 T field parallel to the beam axis. Currently this magnet is used in the ALICE detector.



# Inner part of L3 Detector

Scintillators were used to give the "T<sub>0</sub>" to the muon chambers, to reject cosmic muons and to provide a very simple L1 trigger for hadronic Z decays

Time resolution = 1.9 ns

Endcap scintillator

SLUM

Hadron calorimeter endcaps HC1

HC3

HC2

BGO

Z-chamber

TEC

BGO

FTC

SMD

Luminosity Monitor

Active lead rings

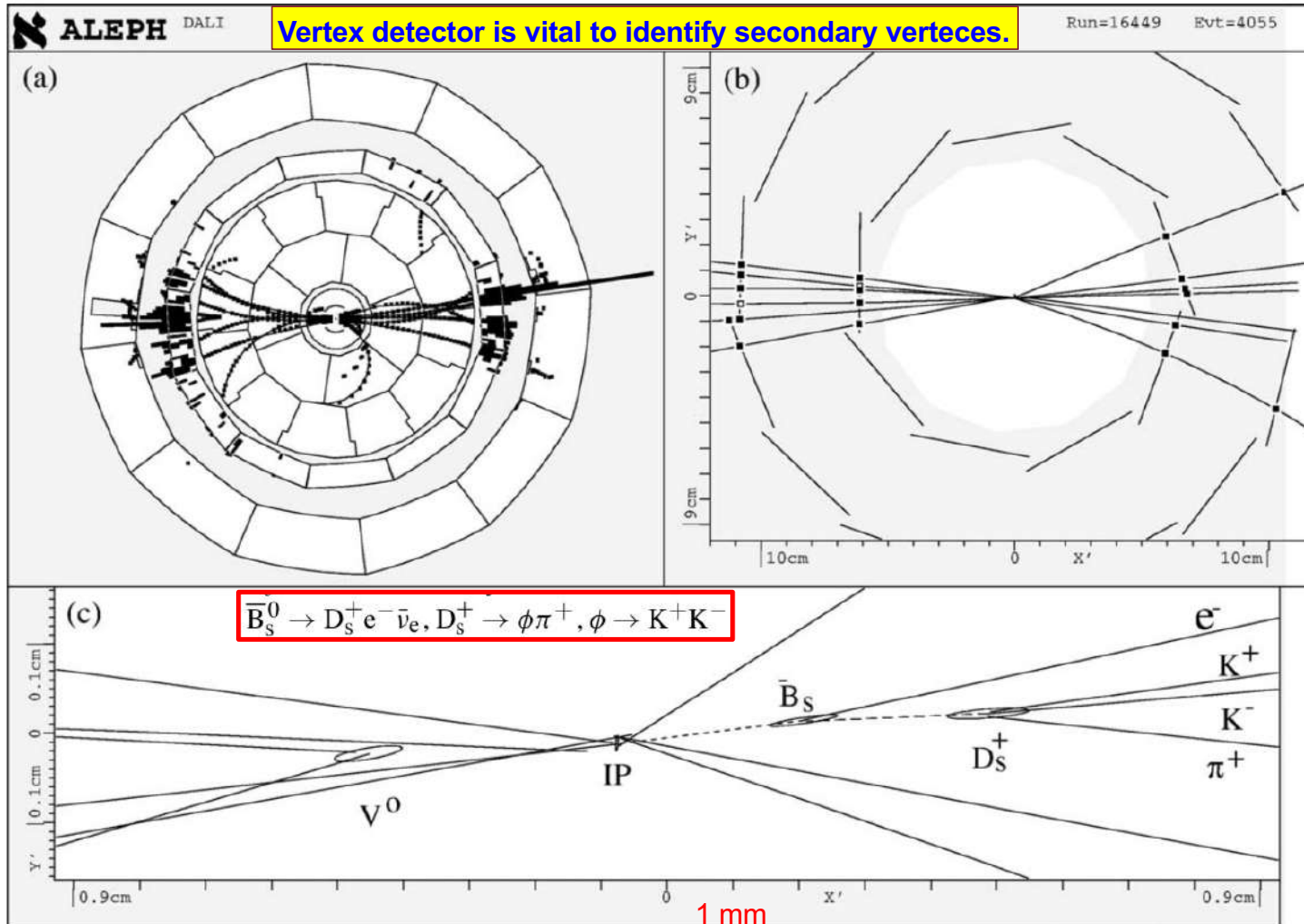
Barrel scintillator (Time resolution = 0.8 ns)

SPACAL

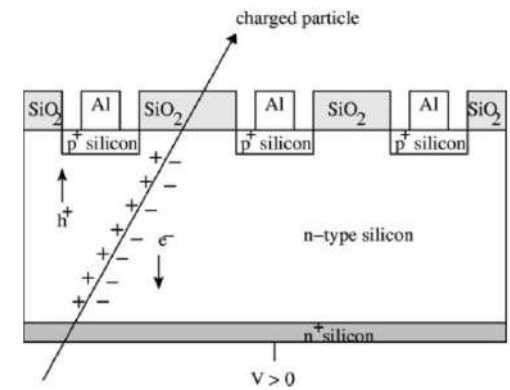
Moveable detector. It was inserted close to the beam only when stable beam was reached.

They were added later to improve the hermeticity of the detector (for instance for the single photon measurement).

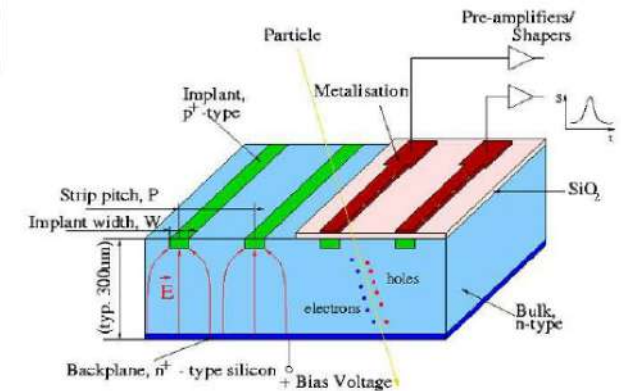
# Vertex Detector



Principle of operation

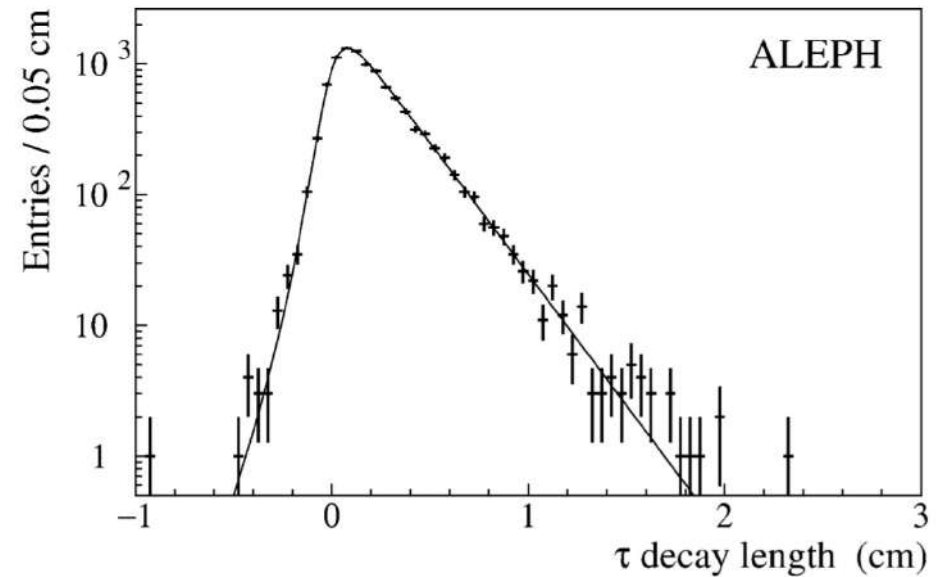
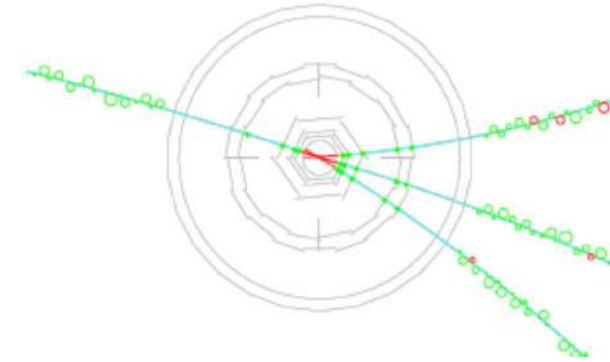
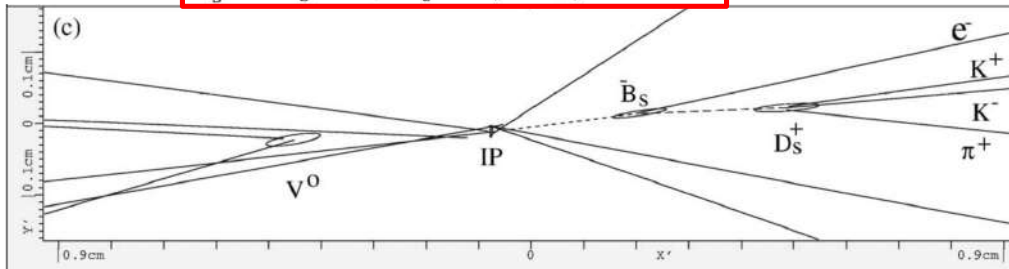
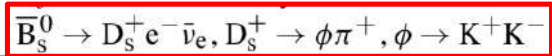
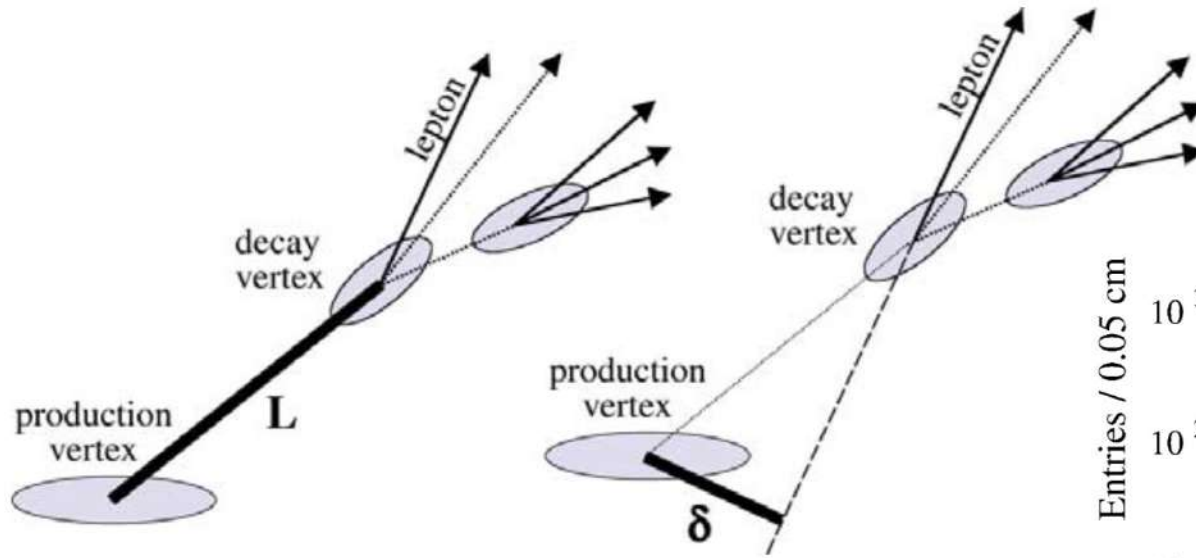


Principles of operation



# Decay Length L and Impact Parameter $\delta$ (or DCA)

□ Impact Parameter is also called Distance of Closest Approach (DCA)

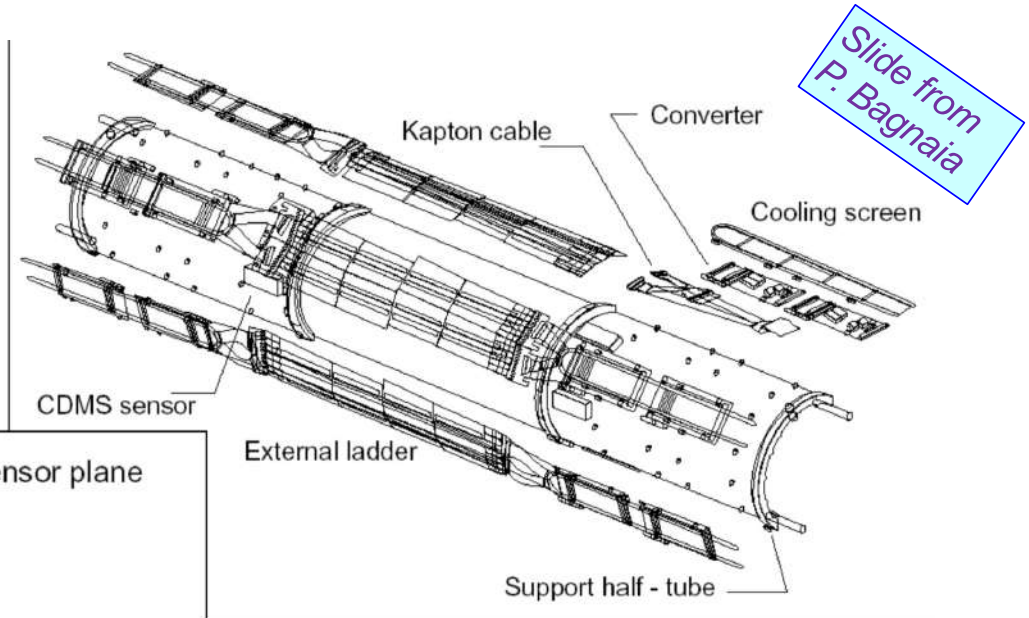
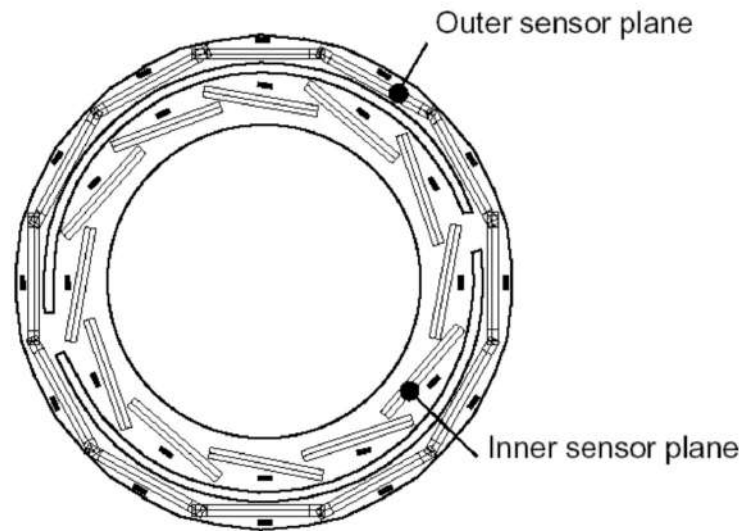


Decay Length distribution for a three-prong tau decay in ALEPH

# The L3 Detector: SMD

The ALEPH and DELPHI collaborations decided very early on (the 1982 letters of intent) to adopt the then novel silicon vertex detectors in the baseline design of their experiments. In contrast, the OPAL and L3 collaborations decided much later to incorporate such detectors, benefiting from the space liberated by the reduction in the beam-pipe radius in 1991.

- 96 silicon wafers
- 70 mm × 40 mm × 300 μm
- two layers:
  - ∅ inner layer : 120 mm
  - ∅ outer layer : 150 mm
  - zenith coverage :  $|\cos\theta| < 0.93$ .



2 read outs :

- 50 μm in  $\phi$ ;
- 150÷200 μm in z

# LEP Vertex Detectors performance

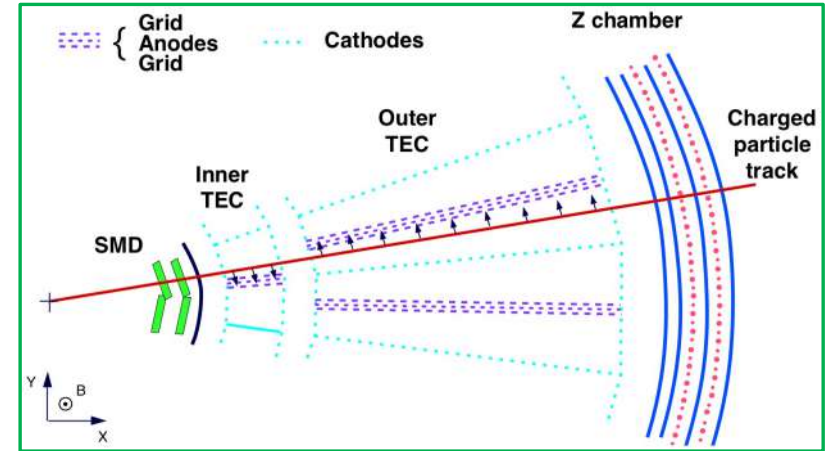
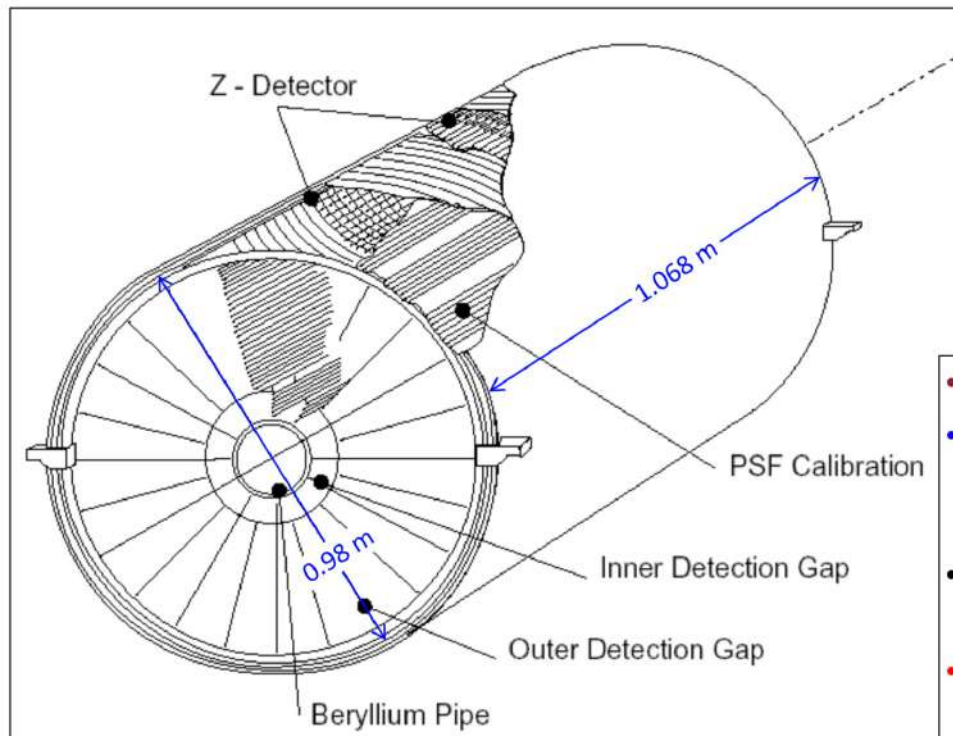
□ The four detectors had similar performance

	ALEPH	DELPHI	L3	OPAL
Signal-to-noise ( $r\phi$ )	31	10–28	18	24/29
Signal-to-noise ( $z$ )	18	10–28	18	20/24
Point resolution ( $r\phi$ ) [ $\mu\text{m}$ ]	8	8	8	8–10
Point resolution at $90^\circ$ ( $z$ ) [ $\mu\text{m}$ ]	12	11	20	10–12
i.p. resolution ( $r\phi$ ) [ $\mu\text{m}$ ]	$34^a$	25	30	18
i.p. resolution ( $z$ ) [ $\mu\text{m}$ ]	$34^a$	34	130	24
Multiple scattering term <sup>b</sup> [ $\mu\text{m GeV}/c$ ]	70	70	80	100

i.p. = impact parameter

# L3 Detector: Time Expansion Chamber (TEC)

L3 design was to have a calorimeter system as compact as possible, so very little space was left for a tracking chamber.



- ext. – int. radius = 317 mm;
- two separate concentric regions : inner 8 wires + outer 54 wires;
- 80% CO<sub>2</sub>, 20% iC<sub>4</sub>H<sub>10</sub>, 1.2 bar (abs);
- $v_{\text{drift}} = 6 \mu\text{m} / \text{ns}$  ("TEC" = Time Expansion Chamber);
- $\alpha_{\text{Lorentz}} = 2.3^\circ$ ;
- z-detector ( $\sigma = 320 \mu\text{m}$ ).

## Two drift regions

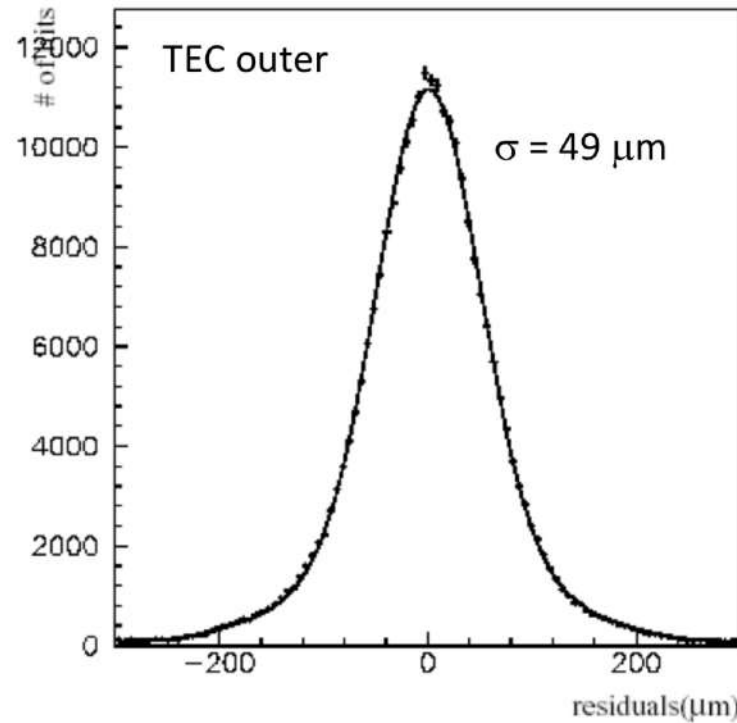
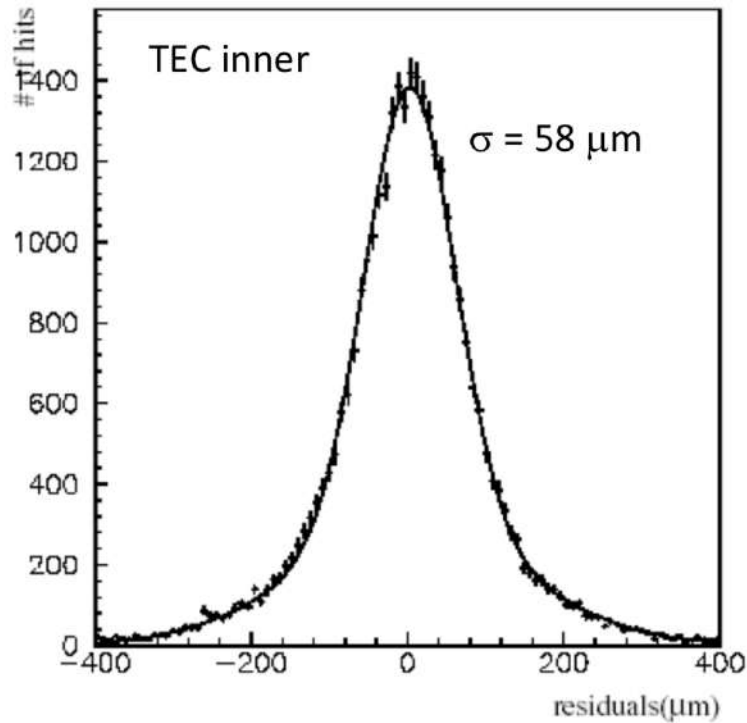
- Low-field region:  $v_{\text{drift}} = 6 \mu\text{m}/\text{ns}$
- Amplification region:  $v_{\text{drift}} = 50 \mu\text{m}/\text{ns}$

Typically hits separated by 500  $\mu\text{m}$  were reconstructed separately

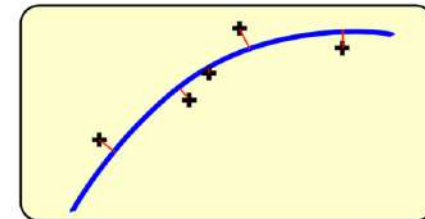
*Very little lever arm and low B-field. TEC did an excellent job but there is no competition with a TPC.*

# The L3 Detector: TEC results

Slide from  
P. Bagnaia



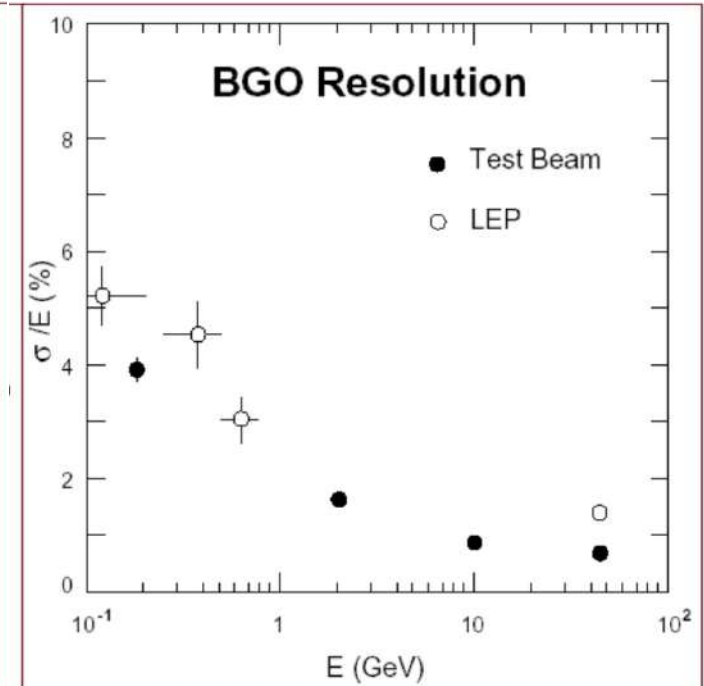
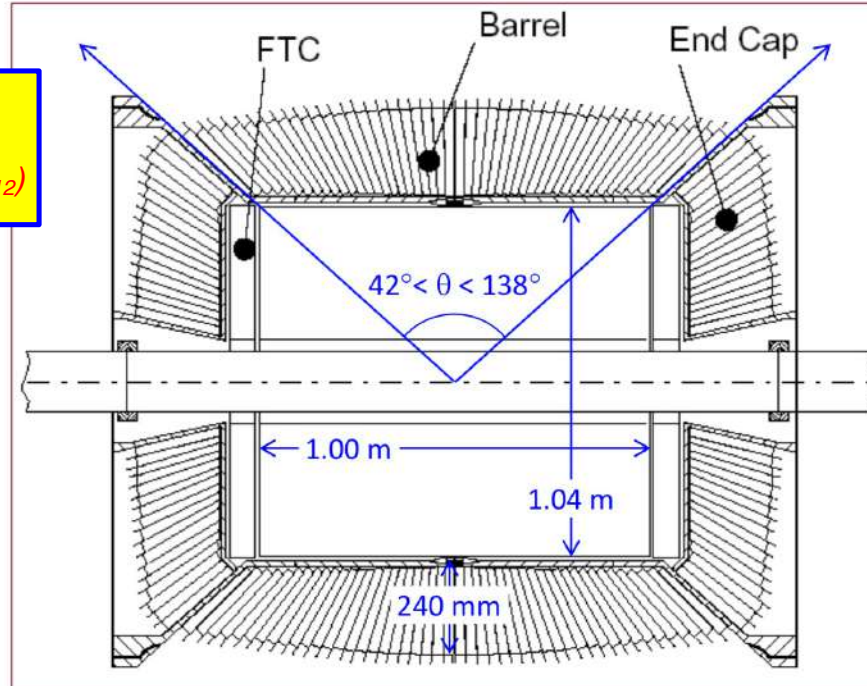
The *residuals* are the distances (with sign) between the measurements and the fitted trajectory. Assuming "many" measurements with the same resolution, their distribution is expected to be gaussian with mean=0 and RMS=resolution.



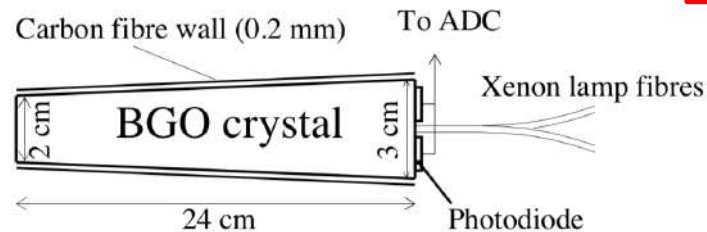
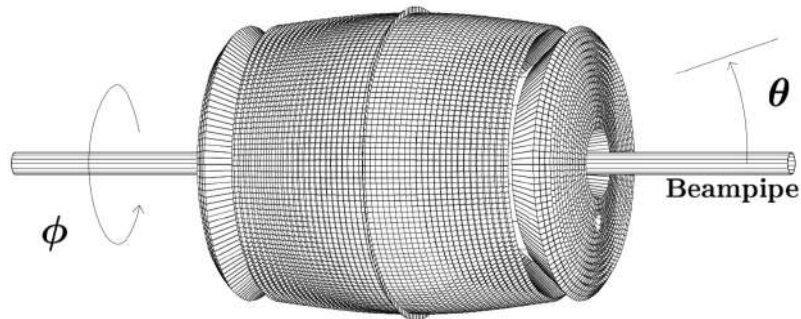
# The L3 Detector: BGO

10734 (3840+3840+1527+1527)  
scintillating crystals of BGO  
(Bismuth germanium oxide  $\text{Bi}_4\text{Ge}_3\text{O}_{12}$ )

The electronic noise in a single crystal was about 2 MeV.  
It could measure photons as low as 30-40 MeV



$$\sigma(E)/E = 3.2\%/\sqrt{E} \oplus 0.9\% \quad (E \text{ in GeV})$$



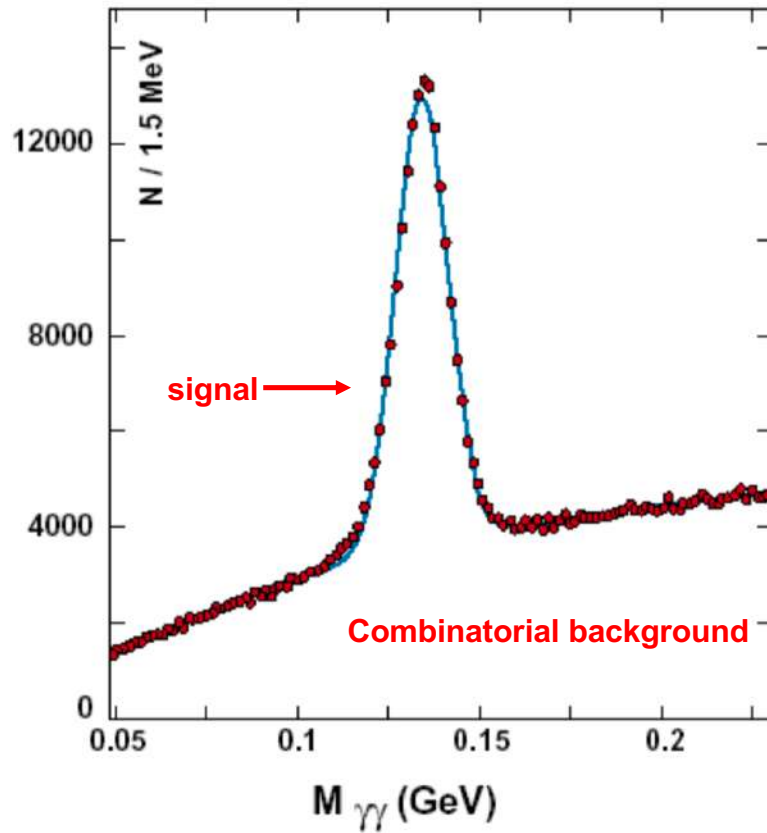
- pyramids  $20 \times 20 \rightarrow 30 \times 30 \text{ mm}^2$ , length 240 mm;
- $X_0 = 11.3 \text{ mm} \rightarrow 21 X_0$ .

# The L3 Detector: BGO results

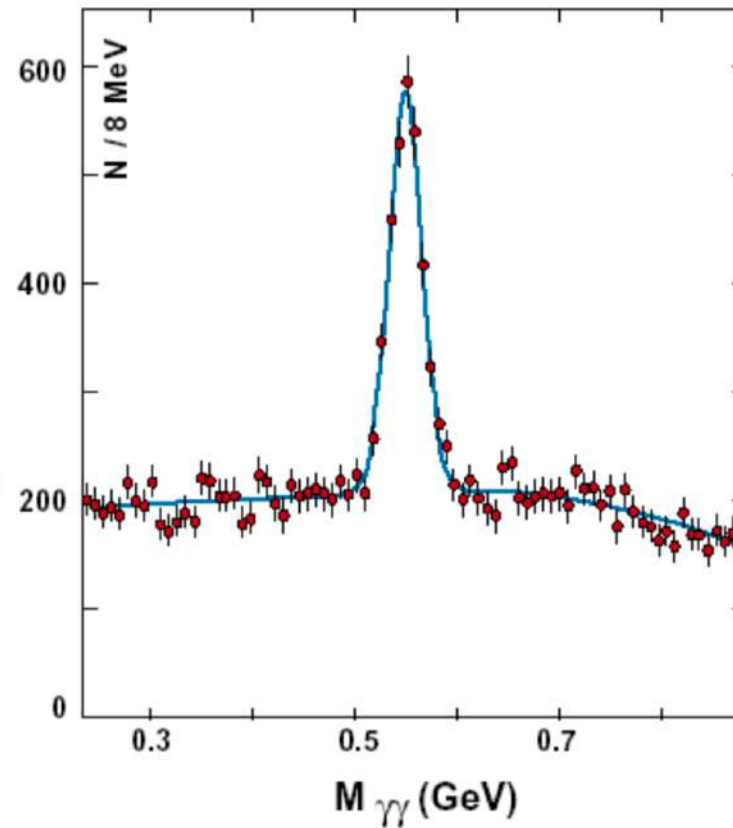
Slide from  
P. Bagnaia

Two photons  
invariant mass

$\pi^0, \sigma = 7 \text{ MeV}$



$\eta, \sigma = 16 \text{ MeV}$

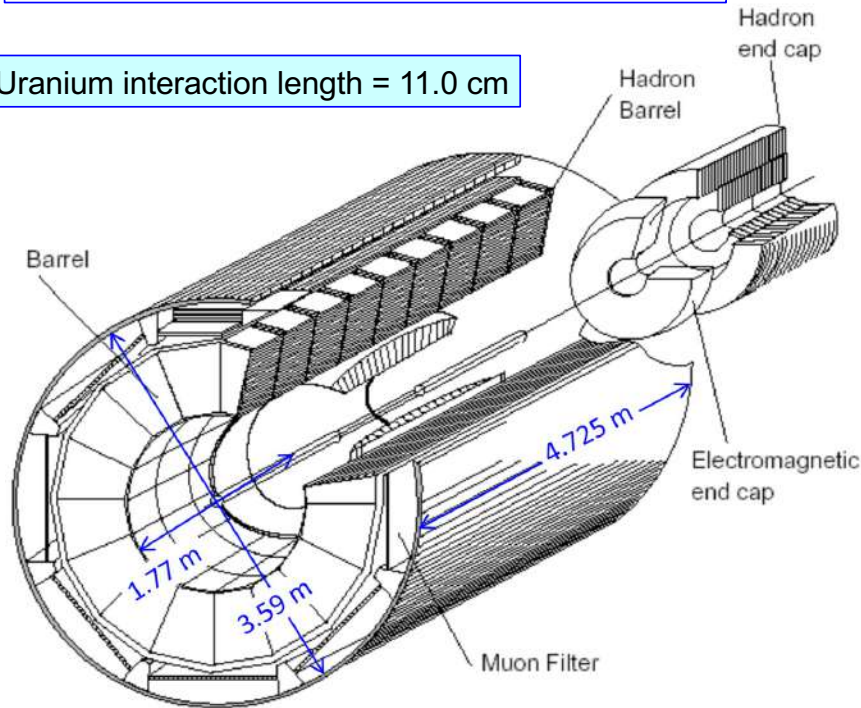


the mass resolution for particles decaying into  $\gamma$ 's is the traditional figure of merit of the e.m. calo (also for  $H \rightarrow \gamma\gamma$  at LHC !!!).

# The L3 Detector: Hadron Calorimeter

plates of depleted U ( $U_{238}$ ) + proportional wire chambers (370,000 wires);  
brass  $\mu$ -filter (65%Cu, 35% Zn) + prop. tubes;

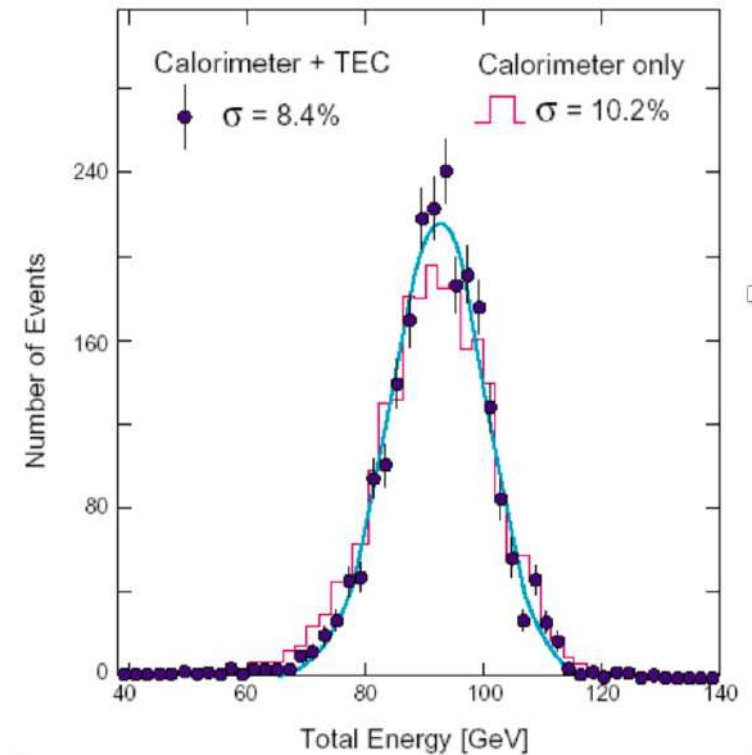
Uranium interaction length = 11.0 cm



- Hcal interaction length varied between  $3.5 - 5.5 \lambda_0$
- Muon filter added another interaction length

$$Z \rightarrow q\bar{q} \text{ at } \sqrt{s} = M_Z$$

Total energy is known and is used to calibrate the calorimeter



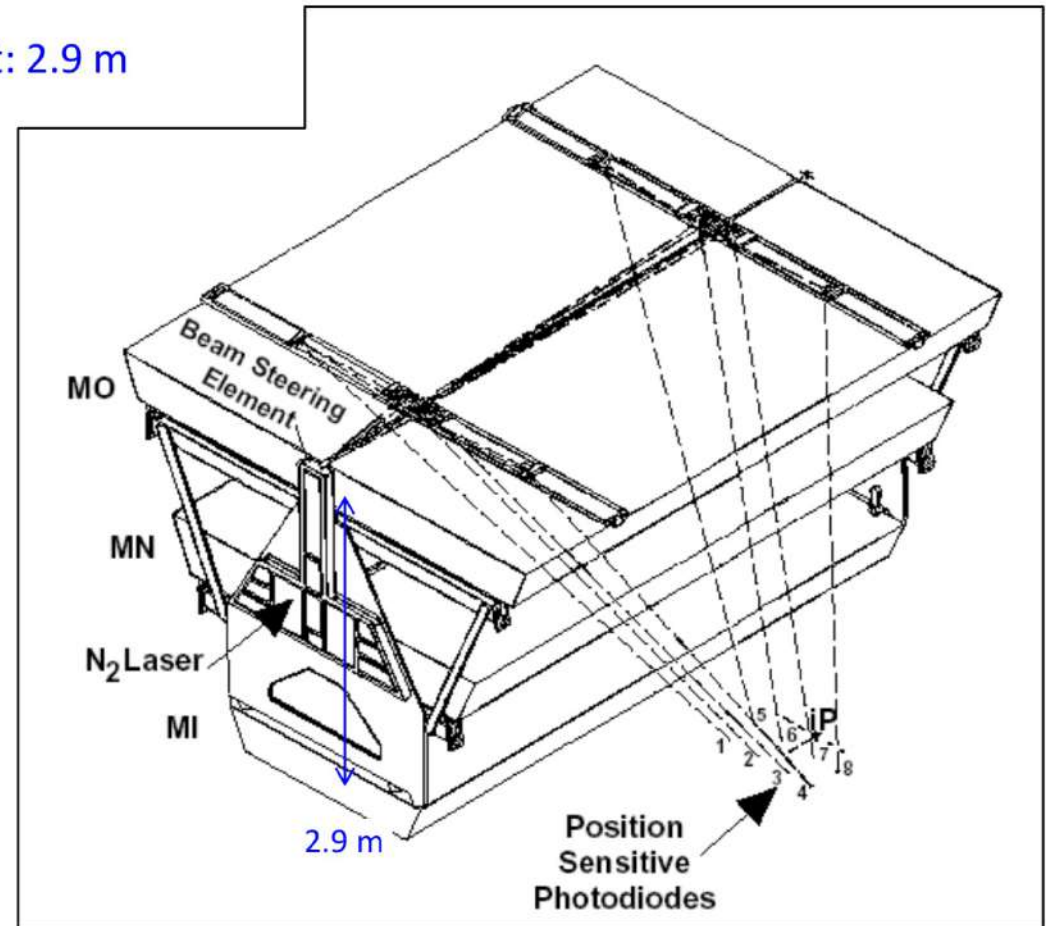
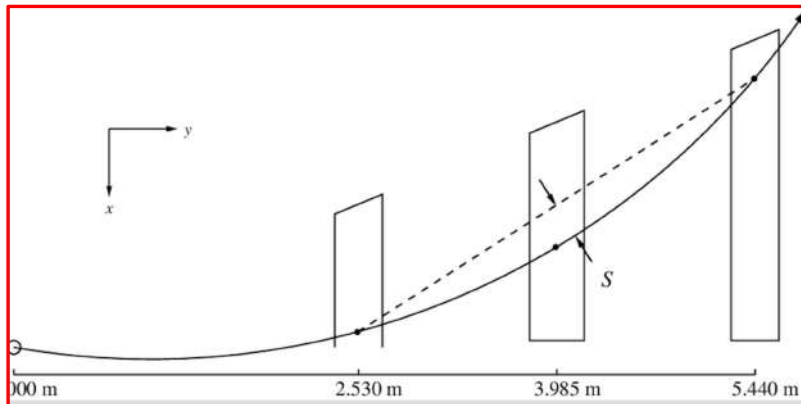
Track information (TEC) can be used to improve the jet energy measurement [energy flow]

# The L3 Detector: muon chambers

Slide from  
P. Bagnaia

- octants, each with three chamber types : MO + MN + MI (16 + 24 + 16 wires);
- effective length of measurement: 2.9 m
- mechanical accuracy:  $\sim 10\mu\text{m}$ ;
- alignment with optical sensors.

The measured quantity is the sagitta.



# Momentum resolution

❑ A charged track spectrometer measure the sagitta, that is proportional to the invers of the momentum

❑ Let's do the example of a muon spectrometer that samples the muon track in three points:  $P_1$ ,  $P_2$  and  $P_3$ .

$L$ : distance between  $P_1$  and  $P_3$ , it is fixed.

$R$ : radius of the trajectory of the muon track, it is proportional to the muon momentum

$s$ : it is the distance from  $P_2$  to the segment between  $P_1$  and  $P_3$ , it is the measured quantity

$$s = R(1 - \cos\frac{\theta}{2})$$

Usually  $s$  is small, then theta is small and we can do a MacLaurin expansion, and we can also approximate the arc with the cord to get theta

$$s = R \frac{\theta^2}{8}; \quad \theta \cong \frac{L}{R} \quad \Rightarrow \quad s = \frac{L^2}{8R}$$

For a particle with charge  $e$ , like the muon, we have:  $R = \frac{p}{B}$

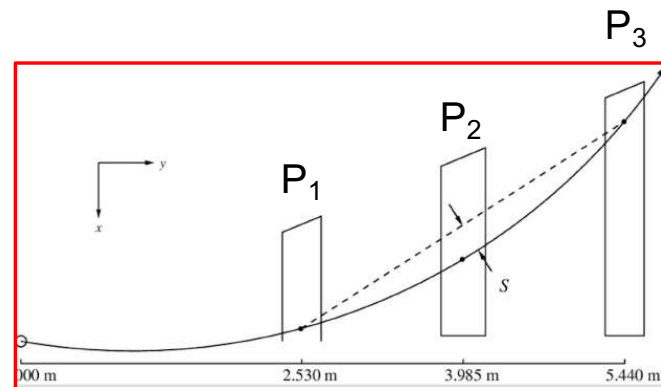
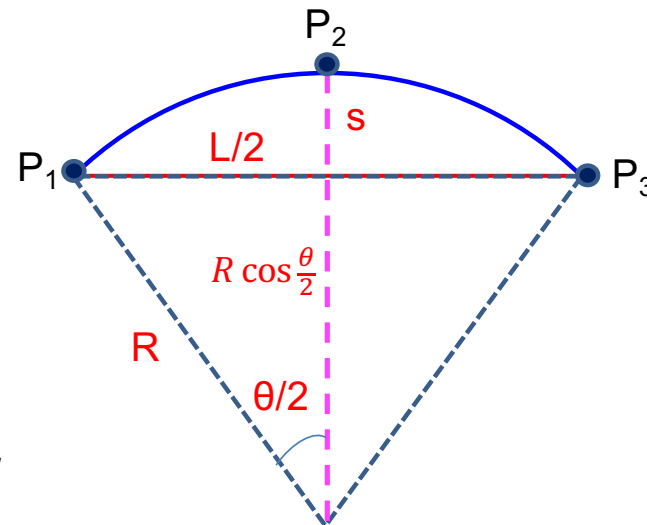
$$\Rightarrow s = \frac{1}{p} \frac{BL^2}{8};$$



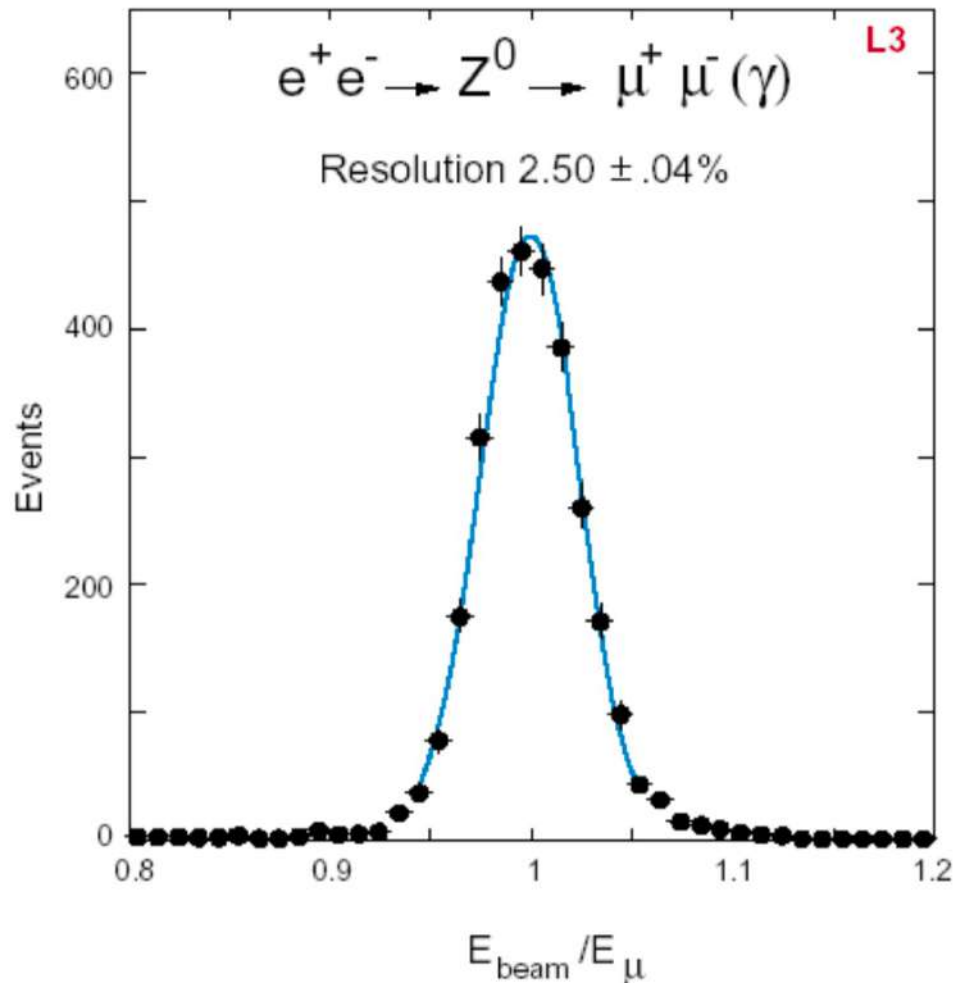
$$\frac{1}{p} = s \frac{8}{BL^2}$$



$$\frac{\Delta p}{p} = p \cdot \Delta s \cdot \frac{8}{BL^2}$$



# The L3 Detector: muon chambers results



- the sagitta ( $\propto 1/p$ ) is the measured parameter;
- therefore  $1/p$  ( $\approx 1/E_{\mu}$ ) expected gaussian, while  $p$  is asymmetric in the tails;
- the beam energy is known with an error of a few MeV, therefore the distribution width is dominated by the muon momentum resolution.



$$\sigma\left(\frac{1}{p_{\mu}}\right) = 2.50\%$$

*This was a great achievement of the L3 detector and it would have been a key feature to discover the Higgs boson.*

# Needs for an online event selection: trigger.

- ❑ Let's compute the time needed for an electron to make a full turn of the accelerator

$$T = \frac{L}{c} = \frac{26657}{3 \cdot 10^8} \cong 88.8 \mu\text{s} \quad \Rightarrow \quad f = \frac{c}{L} = 11.25 \text{ kHz}$$

- ❑ If we have only one bunch of positrons and one bunch of electrons, they collide each 88.8  $\mu\text{s}$ , therefore the collision frequency is 11.25 kHz
- ❑ **If we have N bunches, the collision frequency is multiplied by N. With 4 bunches we have 45 kHz.**
- ❑ *The same is true for LHC, since the tunnel is the same. The number of bunches are about 3600, such to give a collision frequency of 40 MHz and the time between two collisions of 25 ns.*
- ❑ **Let's compute how many Z decays into hadrons we have each second for a given luminosity**

$$\sigma = 30 \text{ nb}; \quad \mathcal{L} = 10^{31} \text{ cm}^{-2} \text{ s}^{-1} \Rightarrow \mathcal{R} = \mathbf{0.3 \text{ Hz}}$$

- ❑ **If we consider the leptonic Z decays (1/7 of the hadron decays) and the luminosity events, we have about 1 Hz of interesting events (we have also the 2 photons physics that could contribute to the physics rate).**
- ❑ **So we need a real time selection (online selection) able to reduce the bunch crossing frequency of 45 kHz to a few Hz of physics events.**
- ❑ **The decision must be taken between two bunch crossing (with 4 bunches, 22.2  $\mu\text{s}$ ) by a system called trigger. With only one trigger level it was not possible, so we used three level of triggers, with increasing complexity.**

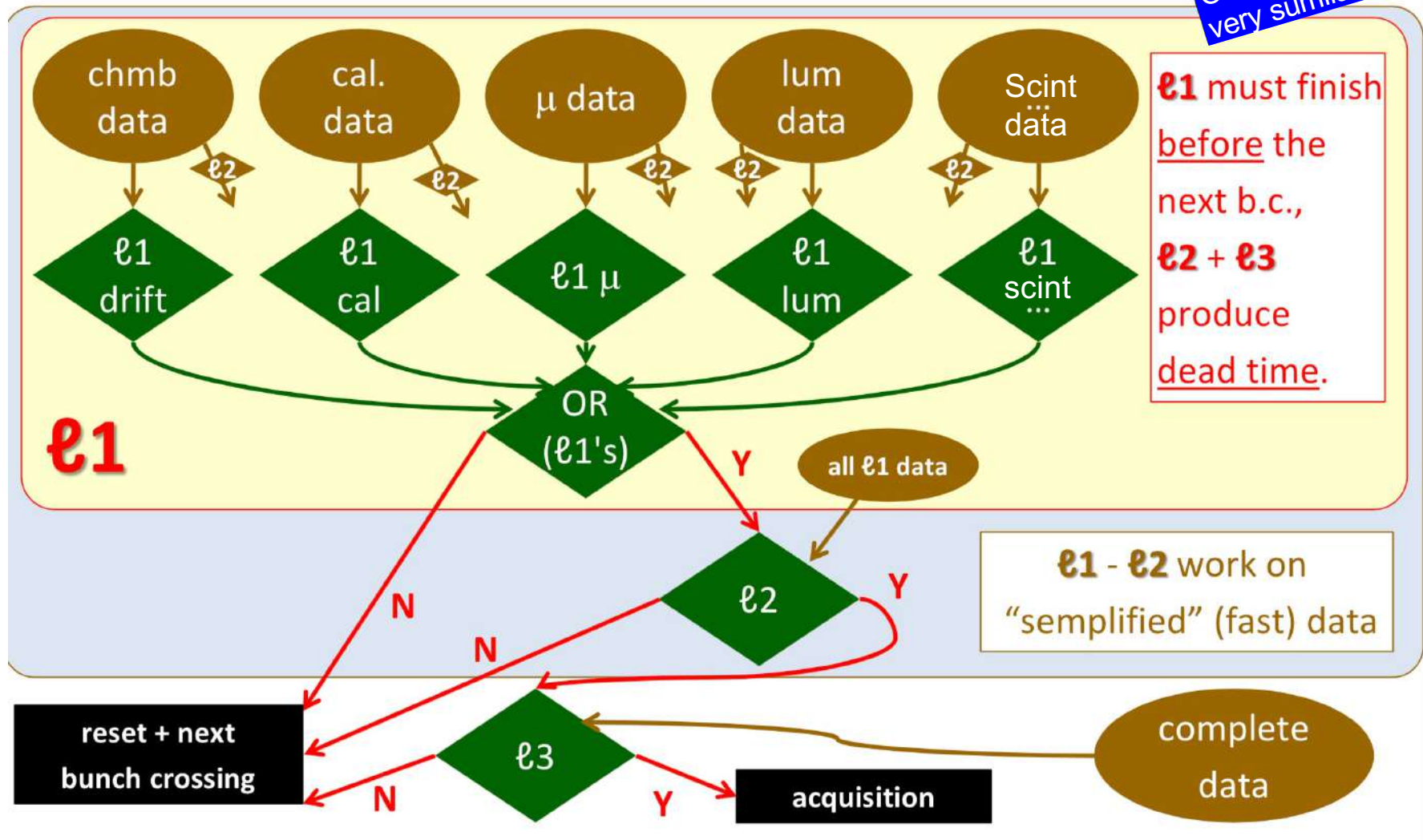
# The L3 Detector: Trigger and DAQ

Other exp. very similar

Slide from P. Bagnaia

Design rates  
 L1: 100-500 Hz  
 L2: 10-50 Hz  
 L3: ~ 1-2 Hz

In reality:  
 L1 ~ 5 Hz



# L3: First Level Trigger

## ❑ Charged track trigger (based on a subsample of TEC hits)

- two tracks back to back ( $Z \rightarrow e^+e^-, \mu^+\mu^-$ )
- at least n (5?) tracks ( $Z \rightarrow \text{hadrons}$ )
- this was the only trigger for the two photons physics

## ❑ Energy trigger (done here in Rome by our group).

Analog sum of ecal and hcal channels to form a trigger channel (for instance, in the BGO barrel 30 crystals summed in one trigger channel, digitised with a faster ADC, less precise)

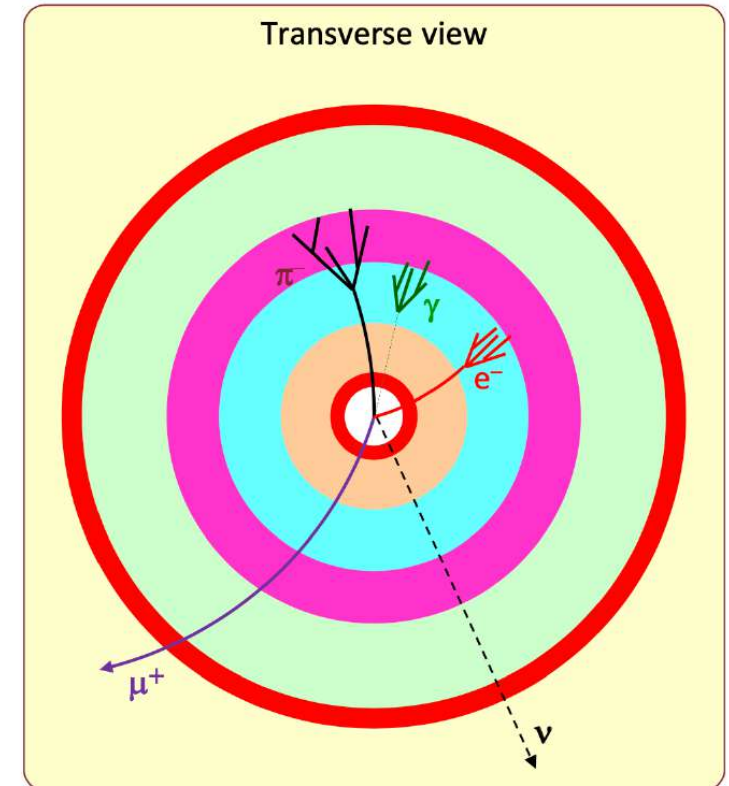
- ECAL cluster energy ( $> 5 \text{ GeV}$ ) ( $Z \rightarrow e^+e^-$ )
- ECAL total energy ( $> 30 \text{ GeV}$ ) ( $Z \rightarrow e^+e^-$ )
- ECAL single photon trigger ( $> 0.9 \text{ GeV}$ ) ( $Z \rightarrow \nu\bar{\nu}\gamma$ )
- ECAL + HCAL total energy ( $Z \rightarrow \text{hadrons}$ )
- Luminosity monitor cluster energy (Bhabha events for luminosity measurement)

## ❑ Scintillator trigger (resolution of 1 ns)

- at least n (5?) scintillator ( $Z \rightarrow \text{hadrons}$ )
- it was used in AND with the muon trigger

## ❑ Muon trigger

- two tracks back to back ( $Z \rightarrow \mu^+\mu^-$ )
- one muon track (B mesons decaying into muons)
- it was used in AND with the scintillator to get rid of the cosmic muons



Level-1 trigger was (and still is) a hardware trigger, based on custom electronics.  
**The trigger decision was taken within  $22.2 \mu\text{s}$**

## L3: second and third level trigger

- ❑ L1 potential background (no physics background, contrary to hadron colliders [no QCD background]):
  - beam gas, beam halo (very little, LEP was extremely clean), electronic noise, cosmic muons, ....
  
- ❑ second level trigger: it used also custom made electronics in the first stage (and then moved to transputers)
  - it used the same L1 trigger data, but it was able to make correlations among different detectors, for instance to match a BGO cluster with a TEC track.
  - The design L1 rate was about 100-500 Hz, with a L2 foreseen reduction by a factor of 10. But the achieved L1 rate was about 10 Hz, so the L2 rejection was not needed to reduce the event rate to a value sustainable by the L3 trigger (10-50 Hz).
  
- ❑ The third level trigger used the “offline” data, namely data with full granularity and resolution.
  - However, given the timing constraint (10 Hz = 100 ms; 50 Hz = 20 ms), we can not “simply” use the offline reconstruction program, but instead a fast code (written in fortran) with ad hoc algorithms needed to be developed.
  - L3 third level trigger used IBM emulators in 1989-92, then transputers in 1993 and then alpha-vax computers.
  - L1 multi-triggers and luminosity events were accepted without any rejections
  - All other events were processed and selected. No inefficiencies were introduced by the third level trigger analysis.
  
- ❑ Total trigger inefficiencies (including L1) less than  $10^{-3}$  for  $Z \rightarrow e^+e^-, \mu^+\mu^-, hadrons$
  
- ❑ Dead time about 5% were introduced by L2, L3 and DAQ chain on the events accepted by the L1 trigger.
  
- ❑ Other LEP detectors had a similar trigger structure.

# A first look at the events

# LEP events

Slide from  
P. Bagnaia

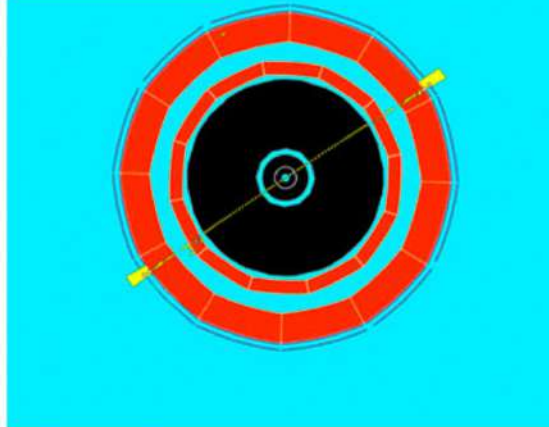
The  $e^+e^-$  initial state produces very clean events (parton system = CM system = laboratory, no spectators).

In these four LEP events the beams are perpendicular to the page.

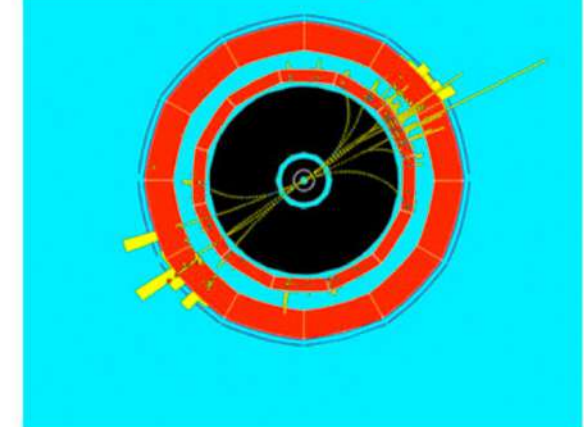
The recognition of the events is really simple, also for non-experts.

Great machines for high precision physics ...

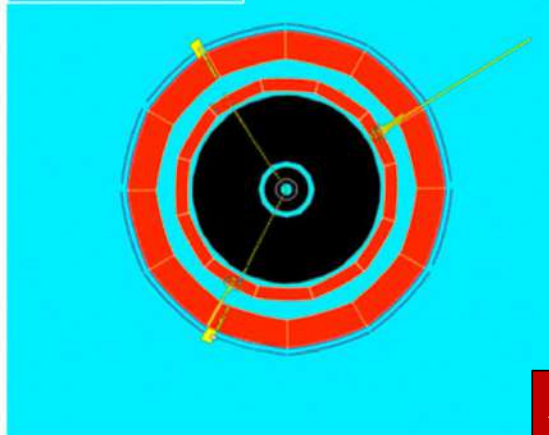
$e^+e^- \rightarrow e^+e^-$



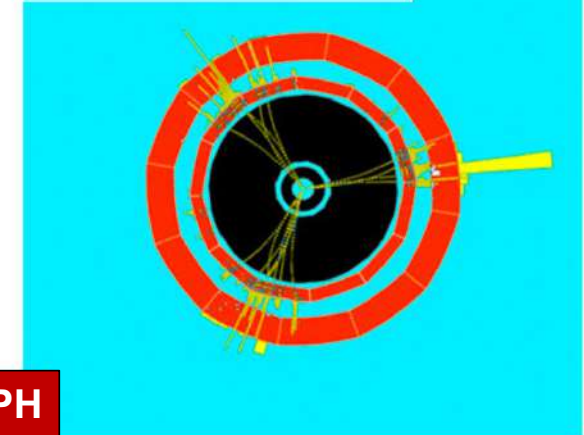
$e^+e^- \rightarrow q\bar{q}$  [two jets]



$e^+e^- \rightarrow e^+e^-\gamma$



$e^+e^- \rightarrow q\bar{q}g$  [three jets]

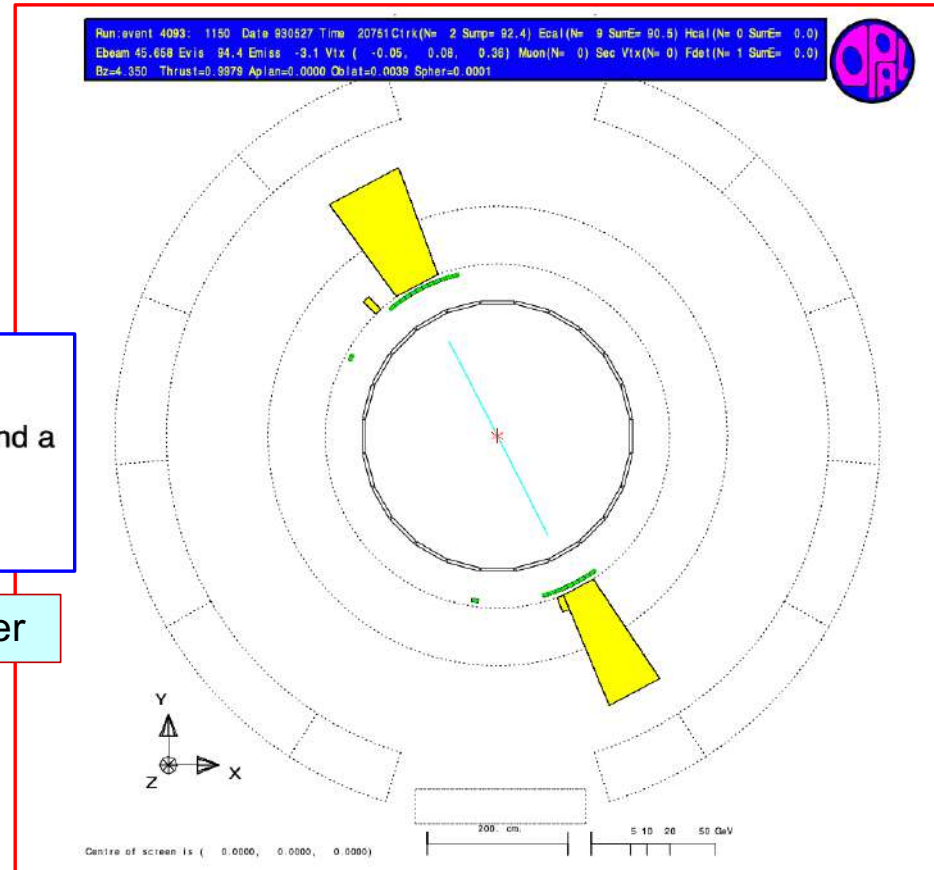


**ALEPH**

# LEP events: $e^+e^-$

- Lepton pair events have low multiplicity
- Electrons are identified by a track in the central detector, and a large energy deposit in the electromagnetic calorimeter,  $E/p = 1$ .

and “nothing” in the hcal behind the ecal cluster

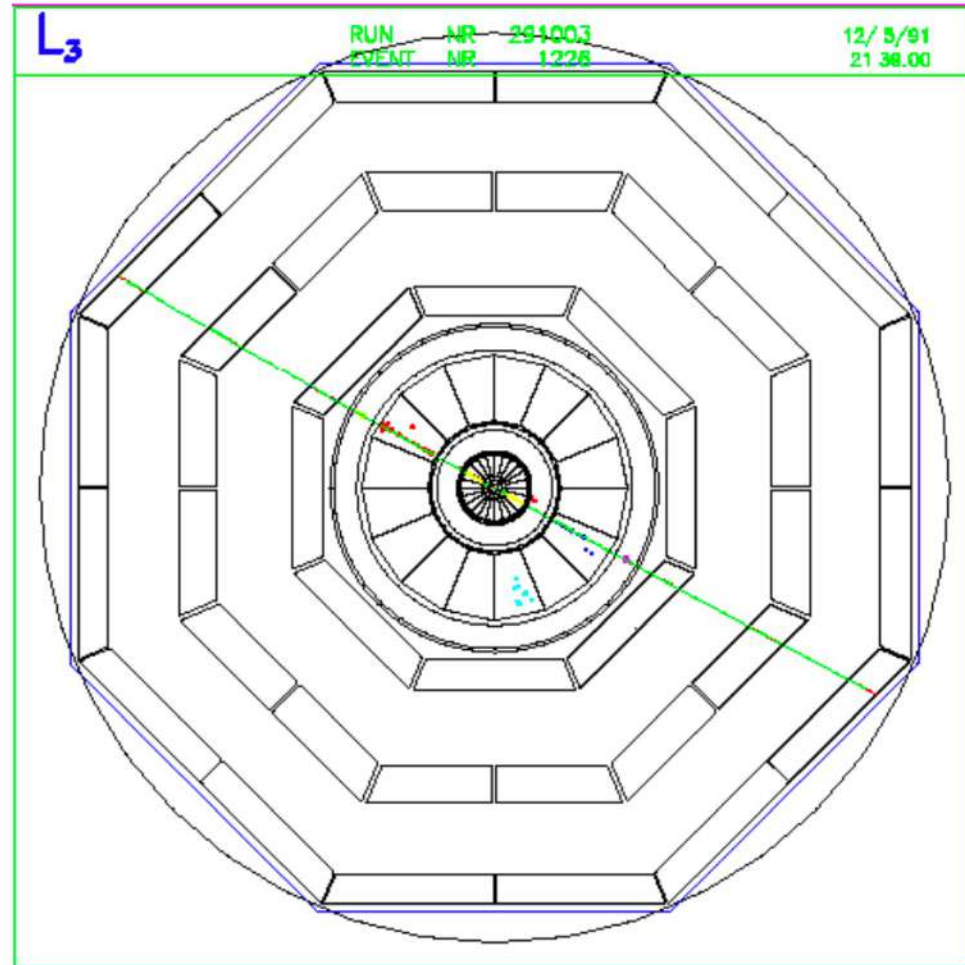


# LEP events: $\mu^+\mu^-$

Slide from  
P. Bagnaia

$$e^+ e^- \rightarrow \mu^+ \mu^-$$

- + signals in SMD
- + track in TEC (  $\rightarrow$  momentum and charge)
- + mip in calos
- + signals in  $\mu$  chambers (  $\rightarrow$  momentum and charge)
- = identified and measured  $\mu^\pm$ .



# LEP events: $e^+e^- \gamma$

Slide from  
P. Bagnaia

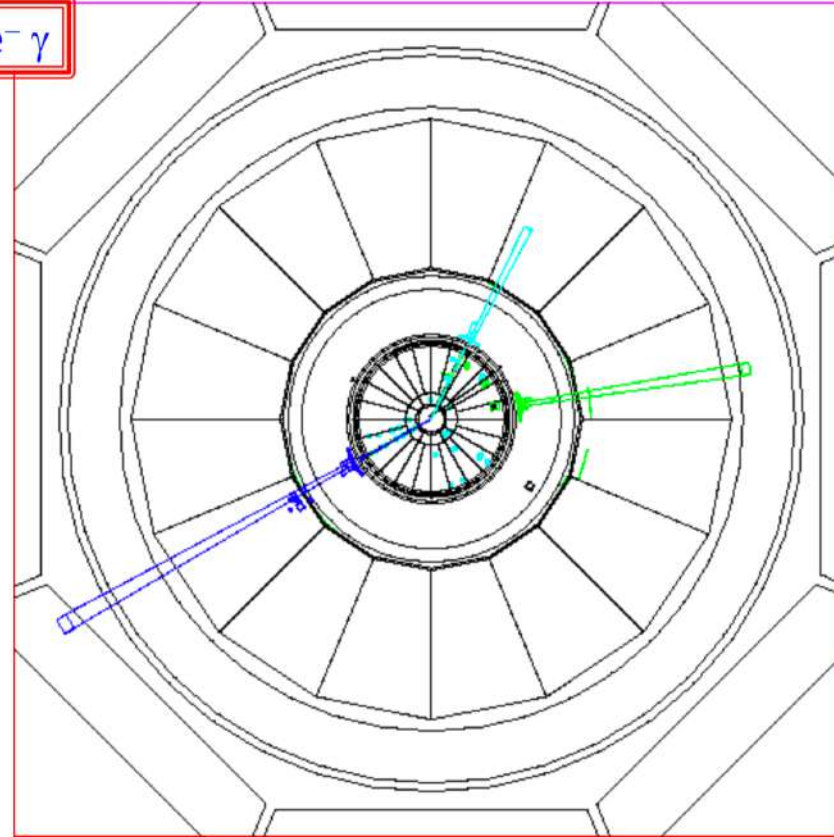
$$e^+ e^- \rightarrow e^+ e^- \gamma$$

- + signals in SMD
- + track in TEC ( $\rightarrow$  momentum and charge)
- + e.m. shower in e.m. calo
- + (almost) nothing in had calo
- + absolutely nothing in  $\mu$  chambers

= identified and measured  $e^\pm$ .

- + no signal in SMD
- + no signal in TEC
- + e.m. shower in e.m. calo
- + (almost) nothing in had calo
- + absolutely nothing in  $\mu$  chambers

= identified and measured  $\gamma$ .



# LEP events: $\tau^+\tau^-$

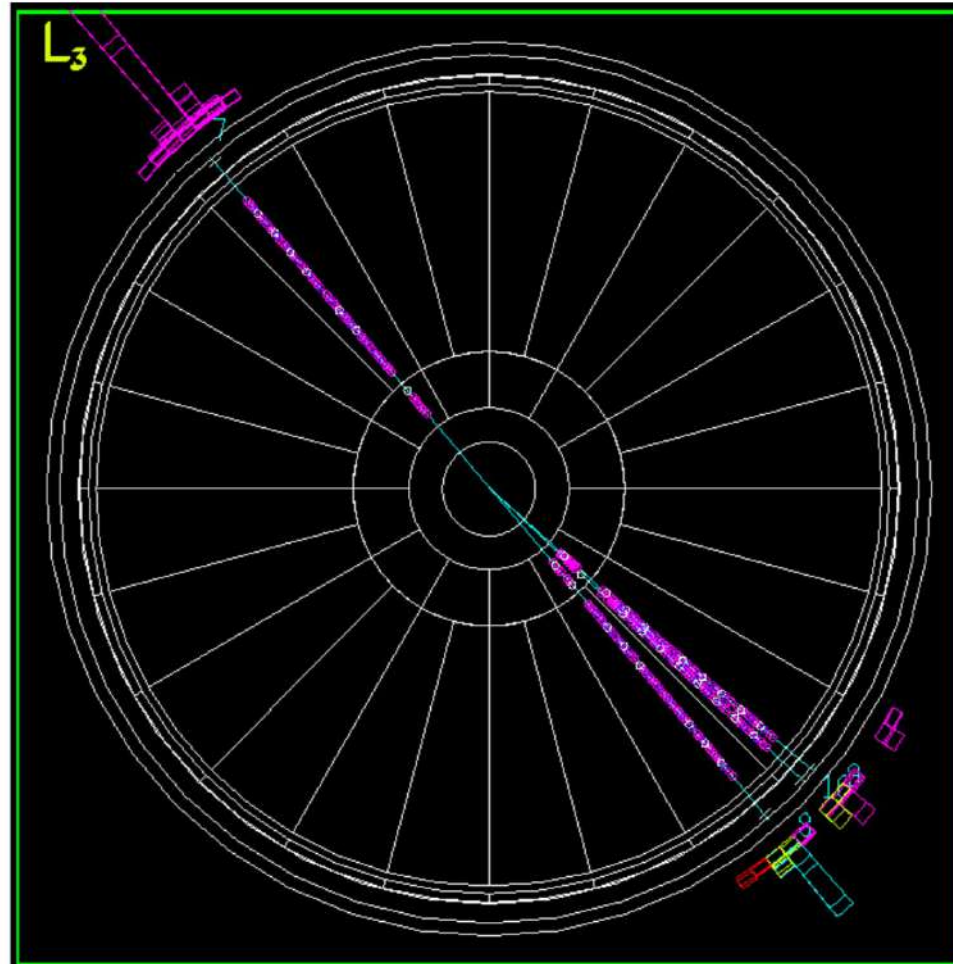
Slide from  
P. Bagnaia

$$e^+ e^- \rightarrow \tau^+ \tau^-$$

$\tau^\pm$  id. does depend on decay:

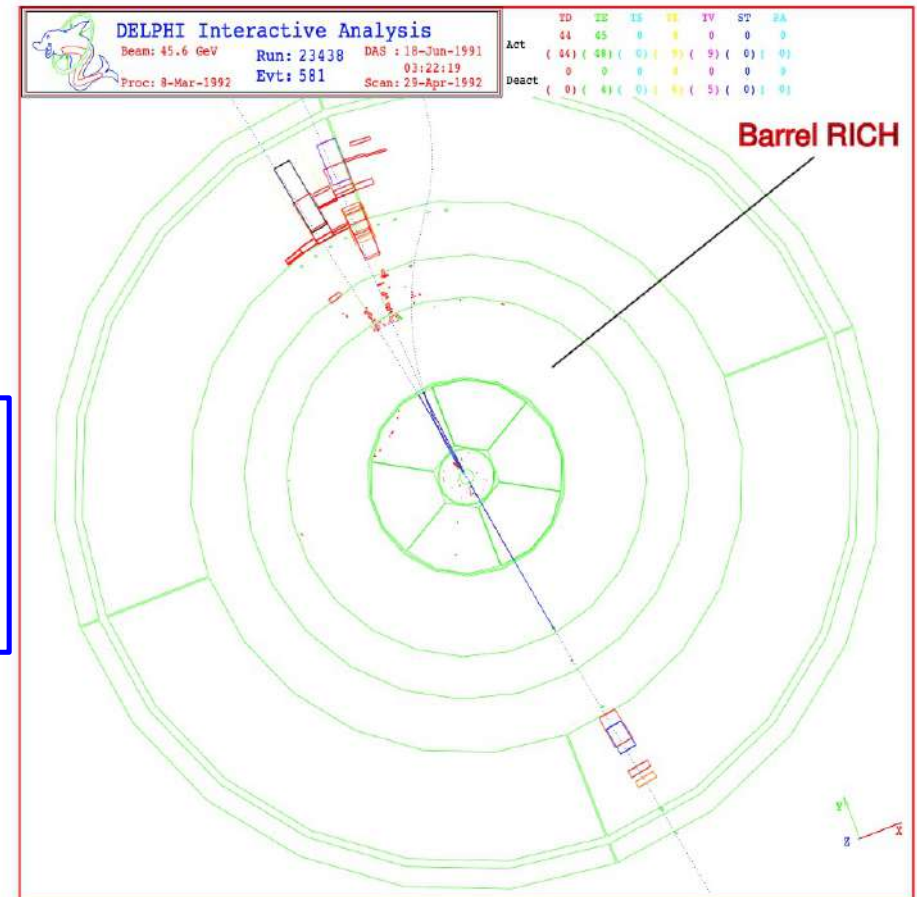
- 1/3/5 had tracks;
- [ or identified single  $\ell^\pm$ ;]

+  $\cancel{E}$  (i.e. a  $\nu_\tau/\bar{\nu}_\tau$ )  
(the evidence comes from the combination of the two decays in the opposite hemispheres).



# LEP events: $\tau^+\tau^-$

- Tau lepton decays dominated by 1 and 3 charged tracks, with or without neutrals, missing neutrino(s), back-to-back very narrow “jets”.
- DELPHI has extra particle ID detectors, RICH.

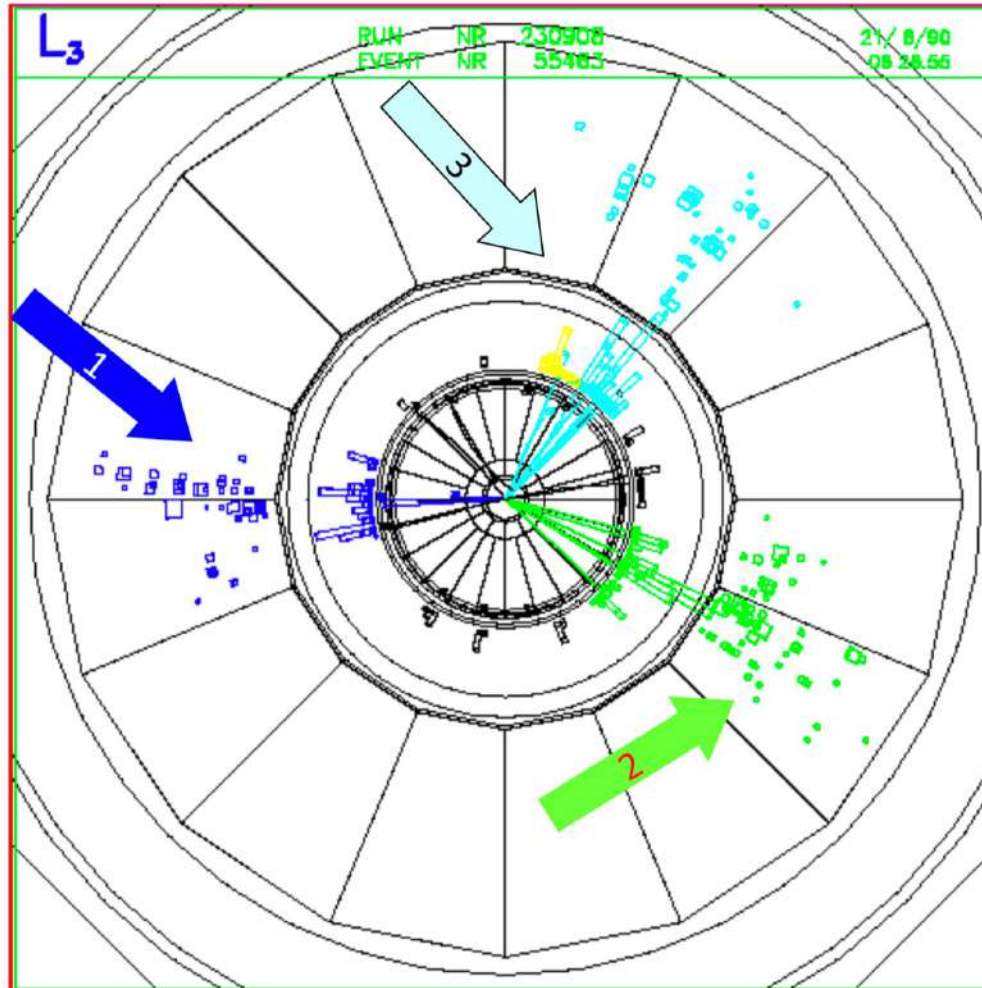


# LEP events: 3 jets

Slide from  
P. Bagnaia

$$e^+ e^- \rightarrow q \bar{q} g$$

a (anti-)quark or a gluon  
gives a hadronic jet:  
+ many collimated tracks  
+ large splashes in e.m. and  
had calos  
+ (possibly) low momentum  
associated  $e^\pm/\mu^\pm$



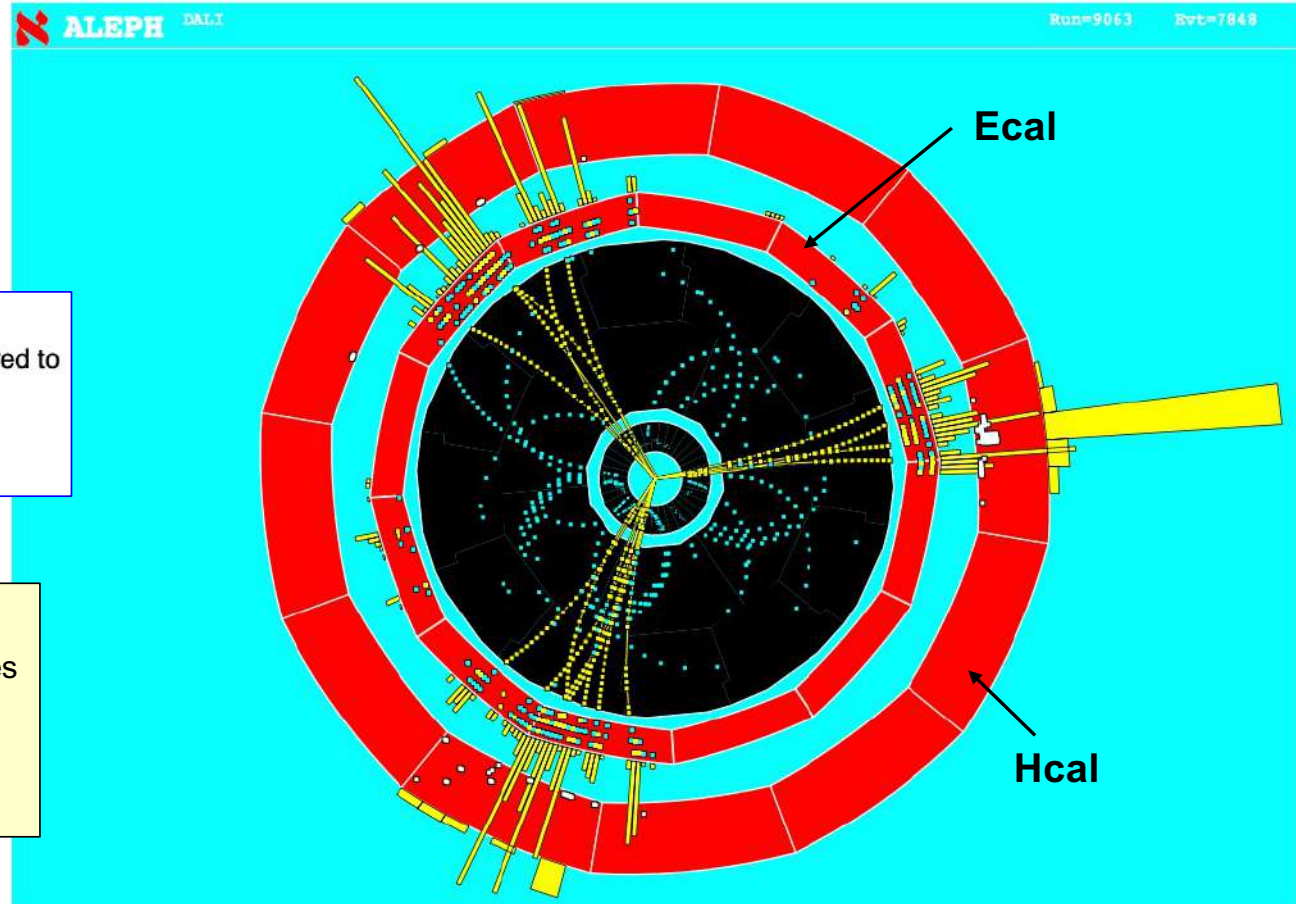
# Lep events: 3 jets

$$e^+ e^- \rightarrow q \bar{q} g$$

- Curved tracks in B field (ALEPH and DELPHI have superconducting solenoids - B field about 1.5 T compared to about 0.5 T in OPAL and L3)
- Many tracks and clusters in calorimeters

## Energy flow

- Momentum measured in the tracking devices
- Energy measured in the calorimeters
- They are combined together in a proper way to give the energy flow of the jet.



# LEP events: $b\bar{b}$ , $b \rightarrow e^+$

$$e^+ e^- \rightarrow b \bar{b}$$

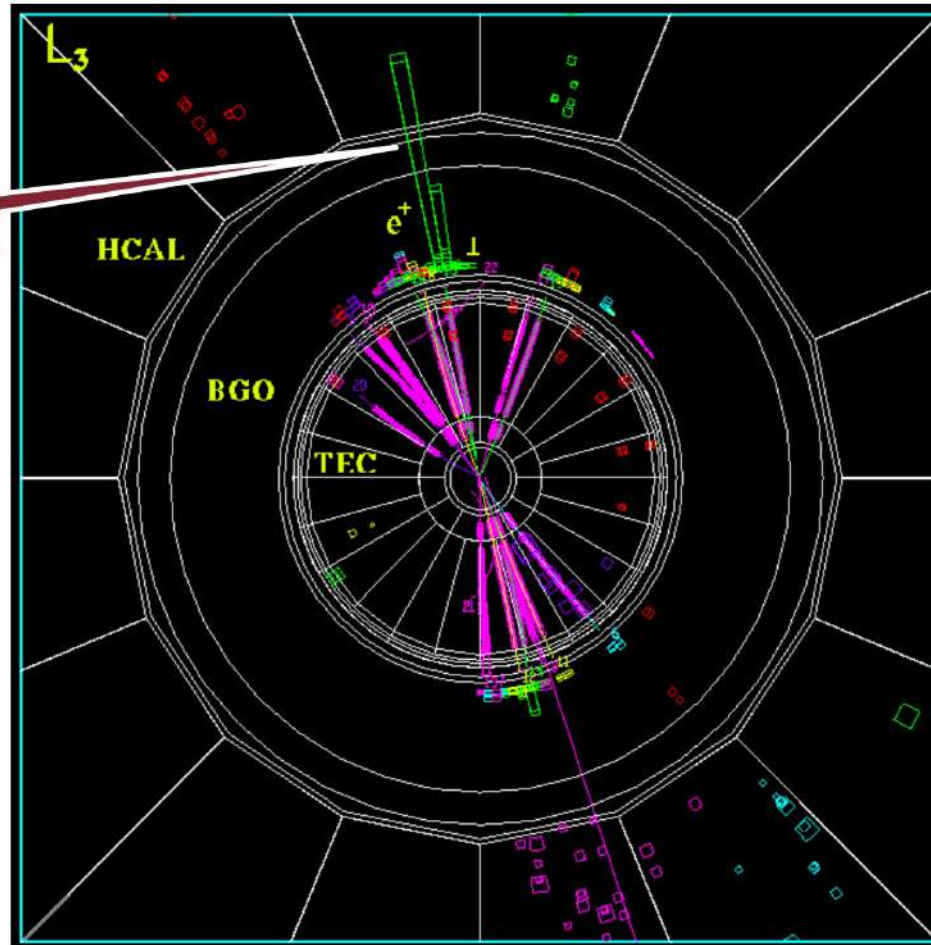
LEP Detectors had the capabilities to identify the b quarks and, to a lesser extent, also the c quark

a heavy flavor quark is a quark (i.e. a jet) with:

- + displaced secondary vertices (SMD)
- + high momentum leptons from quark semileptonic decays

[not all h.f. have one or both characteristics  $\rightarrow$  h.f. id. efficiency not complete (see next)]

identified  $e^+$

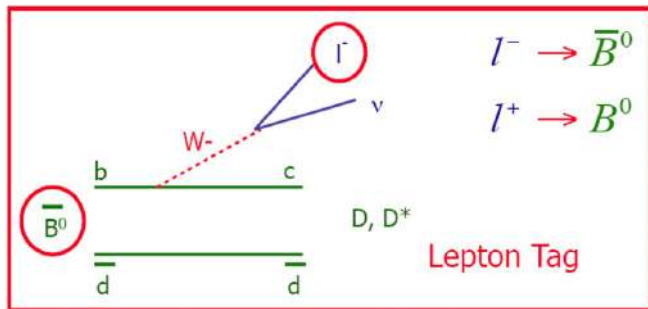


Slide from  
P. Bagnaia

# LEP events: $b\bar{b}, b \rightarrow \mu^+$

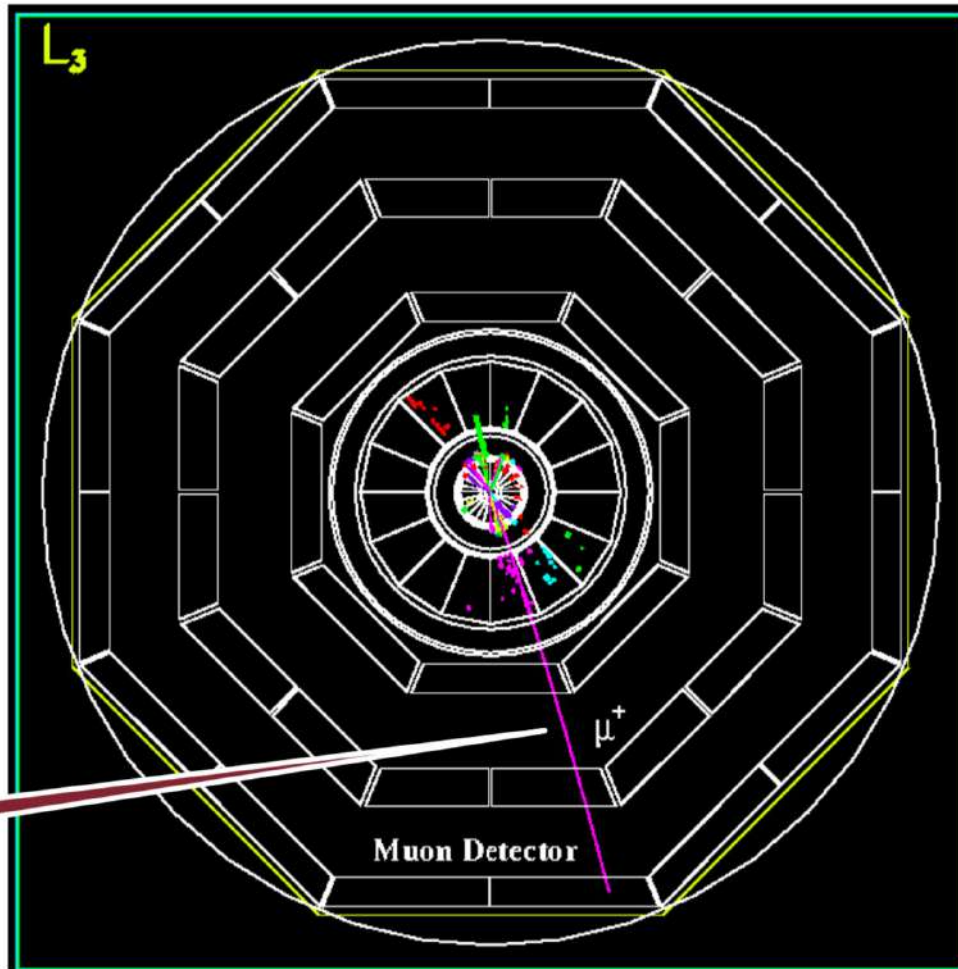
Slide from P. Bagnaia

$$e^+ e^- \rightarrow b \bar{b}$$



D mesons decay preferentially into K mesons, so if one can distinguish pions from K, one could tell if it is a c quark or not.

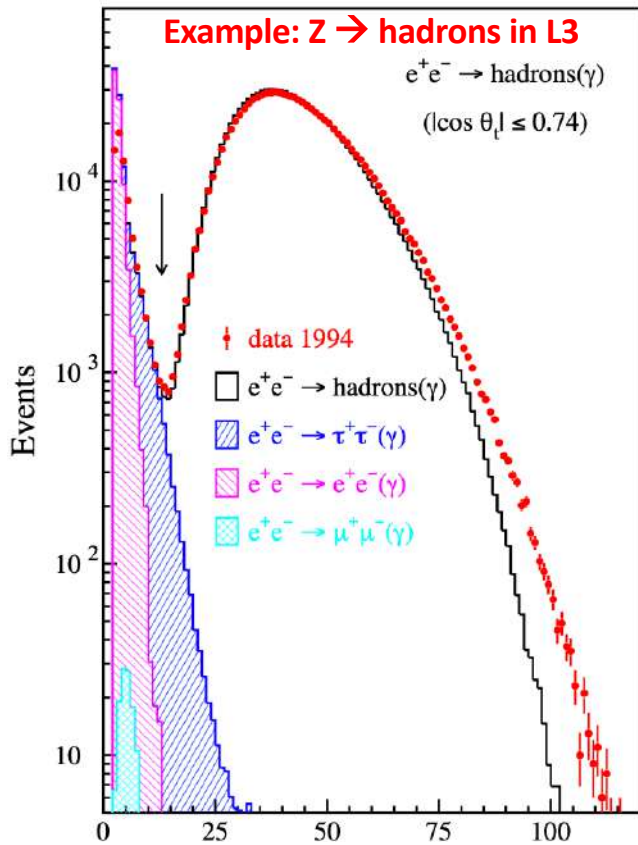
identified  $\mu^+$



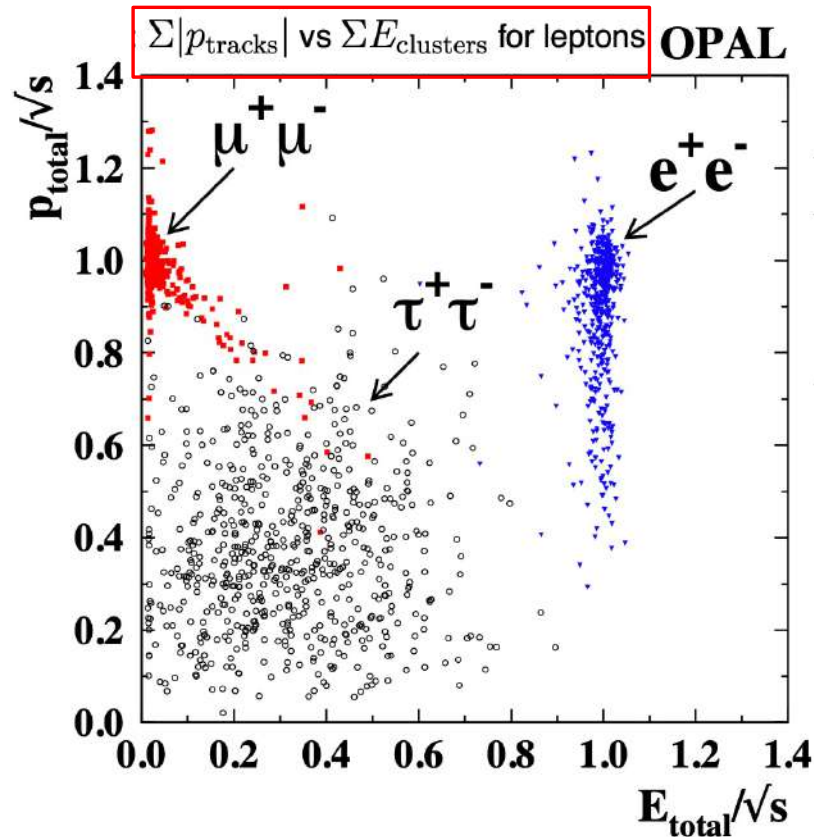
# Experimental methods: event selections, efficiency, purity and contaminations

# First step of the analysis: event selection

- ❑ A very few simple cuts could distinguish hadronic,  $e^+e^-$ ,  $\mu^+\mu^-$  and  $\tau^+\tau^-$  from background due to  $\gamma\gamma$ , cosmic rays, etc...
- ❑ The difficult task was to control systematic errors – how good is the Montecarlo description of the data?



$N_c$  = Number of clusters in the calorimeters



Representative values  
(they changed slightly from experiment to experiment)

Channel	hadron	$e^+e^-$	$\mu^+\mu^-$	$\tau^+\tau^-$
Efficiency %	99	98	98	80
Background %	0.5	1	1	2
Syst error %	0.07	0.2	0.1	0.4

- In other analysis where signal and background have a significant overlap we have to make a compromise between signal efficiency and background contributions
- Today (i.e. LHC but not only) we do not have any longer analysis cut based due to large overlap between signal and background or to a tiny signal but we use other techniques based on neural network tools.

# Efficiency, purity and contamination: definition

- No selection method is fully “pure” and “efficient”, i.e. in a selected sample of events of type “signal”, there are some events of type “background”, while some events “signal” have been rejected.

$N^{sel}$  is the total number of events in the sample; we define:

- **Efficiency** :  $\varepsilon = N^{sel, signal} / N^{signal} < 1$  [ideally  $\varepsilon = 1$ ]
- **Purity** :  $p = N^{sel, signal} / N^{sel} < 1$  [ideally  $p = 1$ ]
- **Contamination** :  $k = N^{sel, bkg} / N^{sel} = 1 - p$

$N^{sel}$  : total number of selected events (the ones inside the red box)

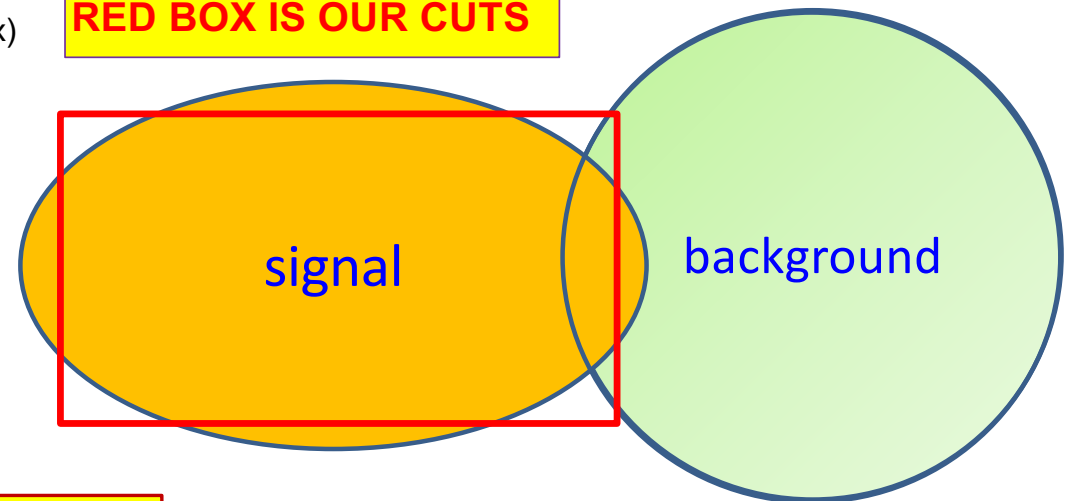
$N^{sel, signal}$  : number of selected signal events (inside the red box)

$N^{signal}$  : total number of signal events (inside the orange shape)

$N^{sel, bkg}$  : number of selected background events  
(the ones inside the red box)

$$N^{sel, signal} + N^{sel, bkg} = N^{sel}$$

RED BOX IS OUR CUTS

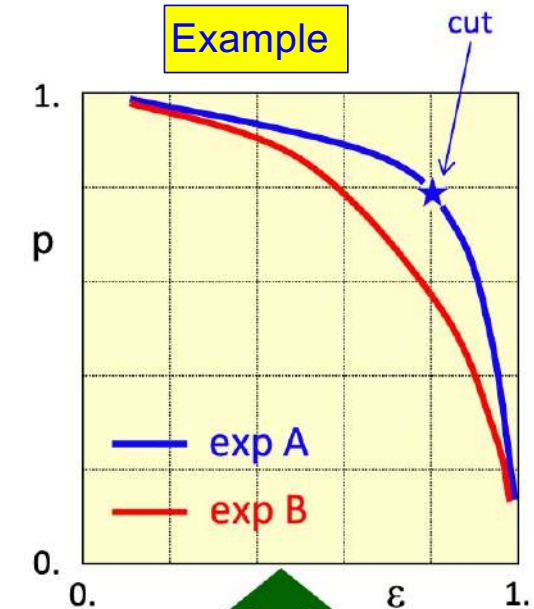
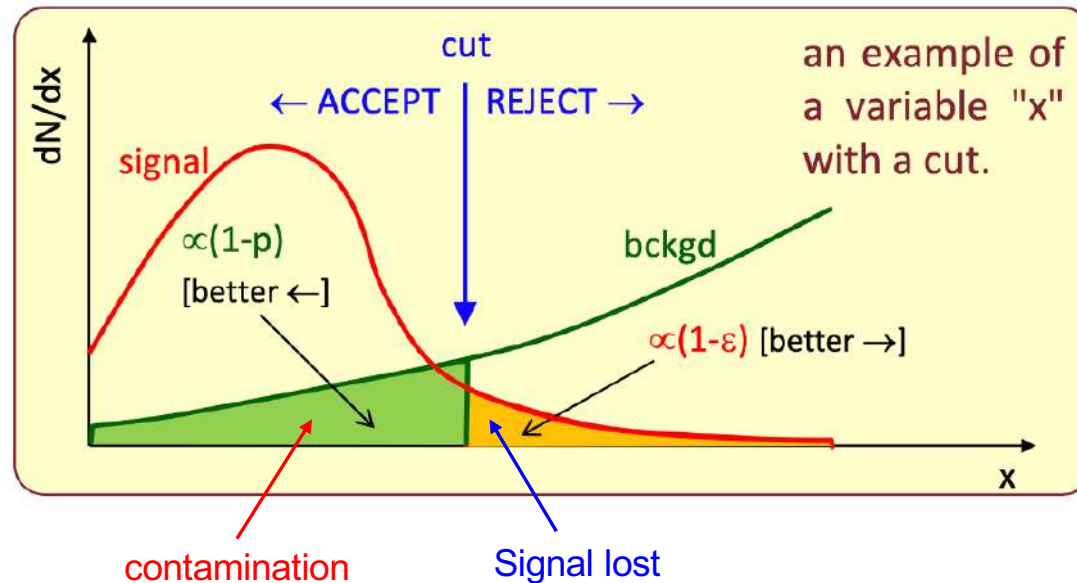


Problem: we only know  $N^{sel}$ , we don't know  $N^{signal}$  and  $N^{sel, bkg}$

# Efficiency versus purity

- **Efficiency** :  $\epsilon = N^{sel, signal} / N^{signal} < 1$
- **Purity** :  $p = N^{sel, signal} / N^{sel} < 1$

- ❑ In general,  $\epsilon$  and  $p$  are anti-correlated.
- ❑ An algorithm (for instance a cut in a kin. variable) produces  $\epsilon$  and  $p$ .
- ❑ The “optimal” choice depends on the analysis and on  $\mathcal{L}_{int}$ .



- Two cases of  $p$  versus  $\epsilon$  when the cut varies.
- Exp. A “is better” than B, because for the same efficiency has a better purity, or for the same purity has a better efficiency.
- The “star” shows a possible choice for  $(p, \epsilon)$  for exp. A

# How to determine efficiency and background

- ❑ When we apply cuts in our selection, we can not determine  $N^{\text{signal}}$  and  $N^{\text{sel, bkg}}$ , so we need to find some methods to evaluate the efficiency and the background of the signal in our selected sample.
- ❑ Usually we rely on simulated data (Montecarlo events). It is done in three steps:
  - physics [event generator: 4-momentum] +
  - detector [tracking of the particle inside the detector [with Geant], simulating all effects, for instance including also detector noise and pile-up] +
  - analysis [exactly the same as in real data]
  - pros: large statistics, flexible, easy ; cons: (some) systematics can not be studied
- ❑ Test beam, in particular to study efficiency and contamination to identify a given particle.
  - intrinsic purity plus large statistics;
  - Pros: less systematics ; cons: not flexible, difficult, expensive.
- ❑ “data themselves” (for instance :  $\mu$  from  $Z \rightarrow \mu\mu$  to study  $b \rightarrow \mu X$ ):
  - “tag and probe” ; ABCD method, sideband method, ...
  - it is generally ok for the systematics
  - It is difficult to reproduce exactly the required case, for instance in the example above, muon from the Z has 45 GeV, while the one of the b decay is inside a jet and it has much lower energy
- ❑ Usually it is a combination of all these methods, need iterations and new ideas. Most of the time and effort spent in a analysis it just goes to measure the efficiency and to evaluate the background (and possibly to reduce it).

# Efficiency: tag and probe method

- For instance it can be used to measure the trigger efficiency, that can not be really evaluated with Monte Carlo events.

- Example: let's try to evaluate the efficiency of the L1 muon trigger; it is defined as:

$$\epsilon = \frac{N_{trigger}}{N_{total}}$$

$$N_{total} = N_{trigger} + N_{not-triggered}$$

- $N_{trigger}$  are the triggered events, hence they are in our sample, while  $N_{not-triggered}$  are not in the sample by definition.

- Therefore we need to find a way to include the  $N_{not-triggered}$  events in our sample.

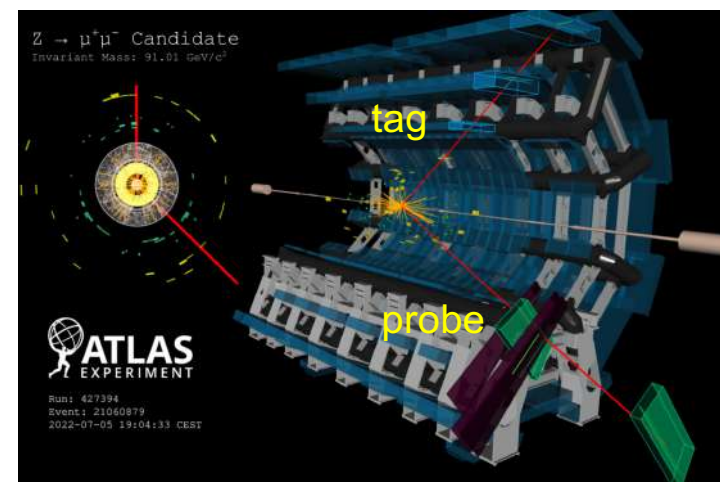
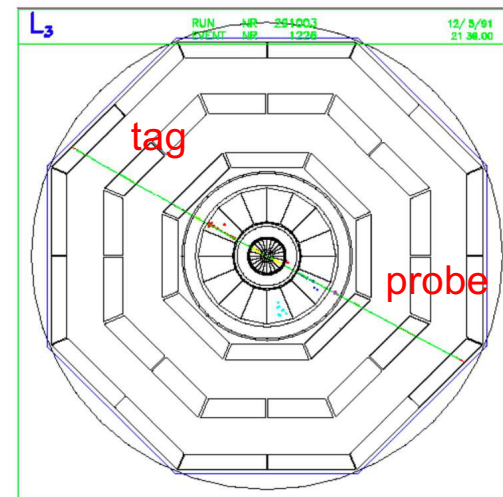
- In L3 we used the muons triggered by the TEC trigger, providing  $N_{total}$ , and among those we checked how many of them were triggered also by the muon trigger.

- Tag and probe method: for instance let's take  $Z \rightarrow \mu^+ \mu^-$ ; in L3 or in ATLAS

- one of the two muons is taken as the tag (it doesn't matter which one); the tag must have been triggered by the muon trigger, then we look at other muon, the probe, and we check if it has been also triggered by the muon trigger. The muon trigger efficiency is defined as:

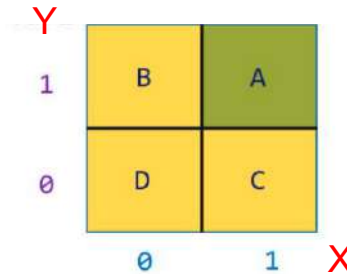
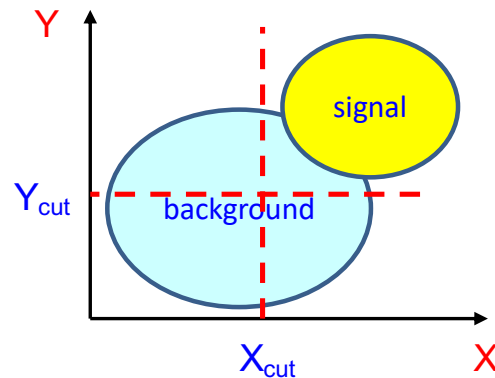
$$\epsilon = \frac{N_{trigger-probe}}{N_{tag}}$$

Of course, it is implicit in the definition that, in order to accept the event, it is sufficient that only muon fulfill the trigger requirements (single muon trigger)



# Background: ABCD method

- The **ABCD method** is commonly used to estimate the size of the **background** contribution from real data. It takes its name from the fact that it uses four regions, which are labelled A, B, C, D. One of the regions is the **signal region** for which one wishes to make the background estimate. The other three are obtained by reverting **two different cuts X and Y**, that are supposed to be not correlated



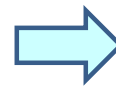
Region A: pass X and pass Y (this is the signal region)
Region B: fail X and pass Y
Region C: pass X and fail Y
Region D: fail X and fail Y

- It is essential that the criteria X and Y can be treated as **uncorrelated**. This is true if the probability to pass criterion X does not (significantly) depend on whether criterion Y passes, and vice versa. With this *assumption*, the following relation holds for the numbers of background events in the four regions:

$$\frac{N_A}{N_B} = \frac{N_C}{N_D}$$

or equivalently

$$\frac{N_A}{N_C} = \frac{N_B}{N_D}$$



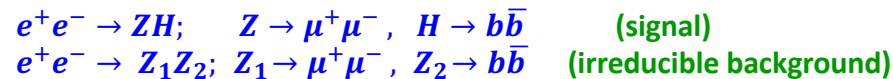
$$N_A = \frac{N_B N_C}{N_D}$$

- **Contributions other than the background of interest must be subtracted in the regions B, C, D.** This could be done using MC simulation. The method is usually most robust if the criteria X and Y can be chosen in such a way that the regions B, C, D are very much dominated by the background of interest. In particular, there should only be very little predicted signal leakage into those regions.

# Background: sideband method

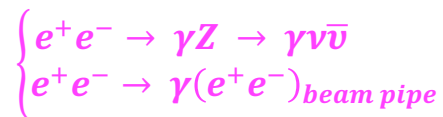
□ The background can be conceptually divided in two categories:

➤ **irreducible background:** other processes with the same final state, e.g.:



➤ **reducible background:**

- Badly measured events;
- Detector mistakes;
- Physics processes that appear identical in the detector because part of the event is not detected, like for instance in the single photon analysis:



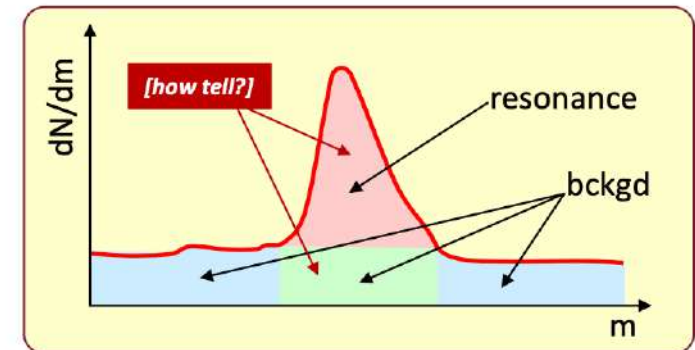
□ The meaning of the distinction is that the reducible background can be improved with a better detector, or with a more accurate selection (at the price to lose some efficiency), while the irreducible background is intrinsic and can only be subtracted statistically, by comparing:

- $N^{\text{exp}}$ : background only hypothesis
- $N^{\text{exp}}$ : background plus signal hypothesis

## Sideband method

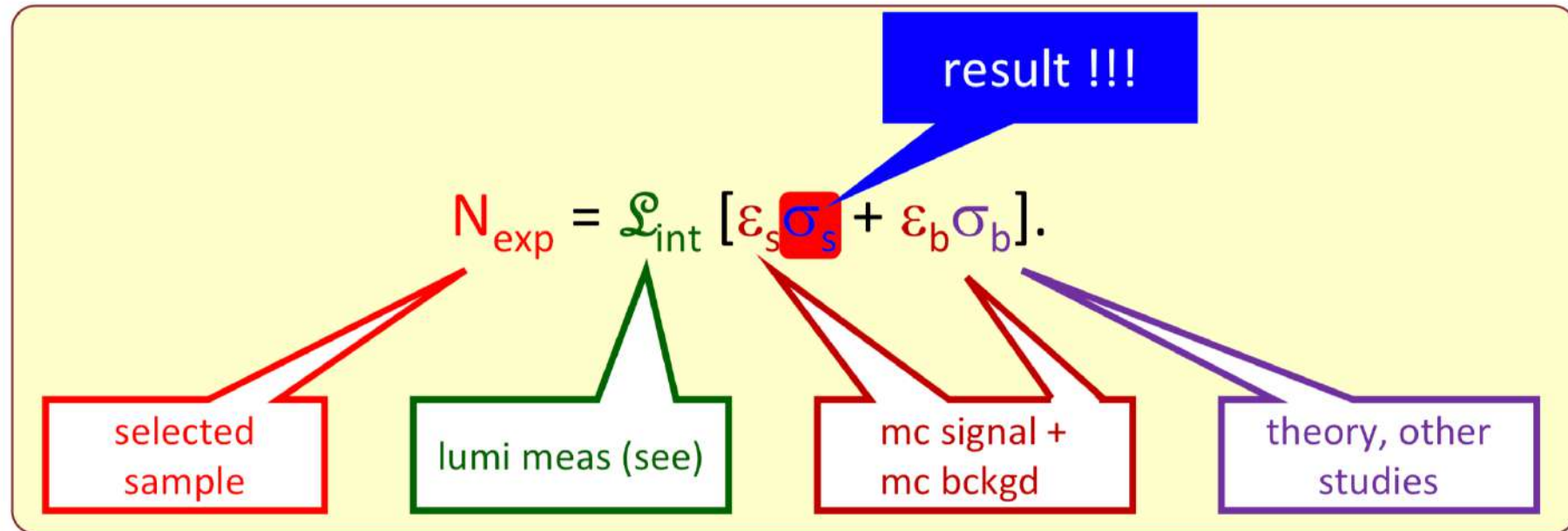
In a distribution we select two regions nearby the signal region where we are sure we have only background; then we extrapolate the background value into the signal region.

Similar to the "resonances" of the strong interactions, where a mass distribution exhibits peaks, interpreted as short-lived particles. However, it is impossible to assign single events to the resonating peak or to the non-resonant bckgd.



**You can not tell event by event which is which**

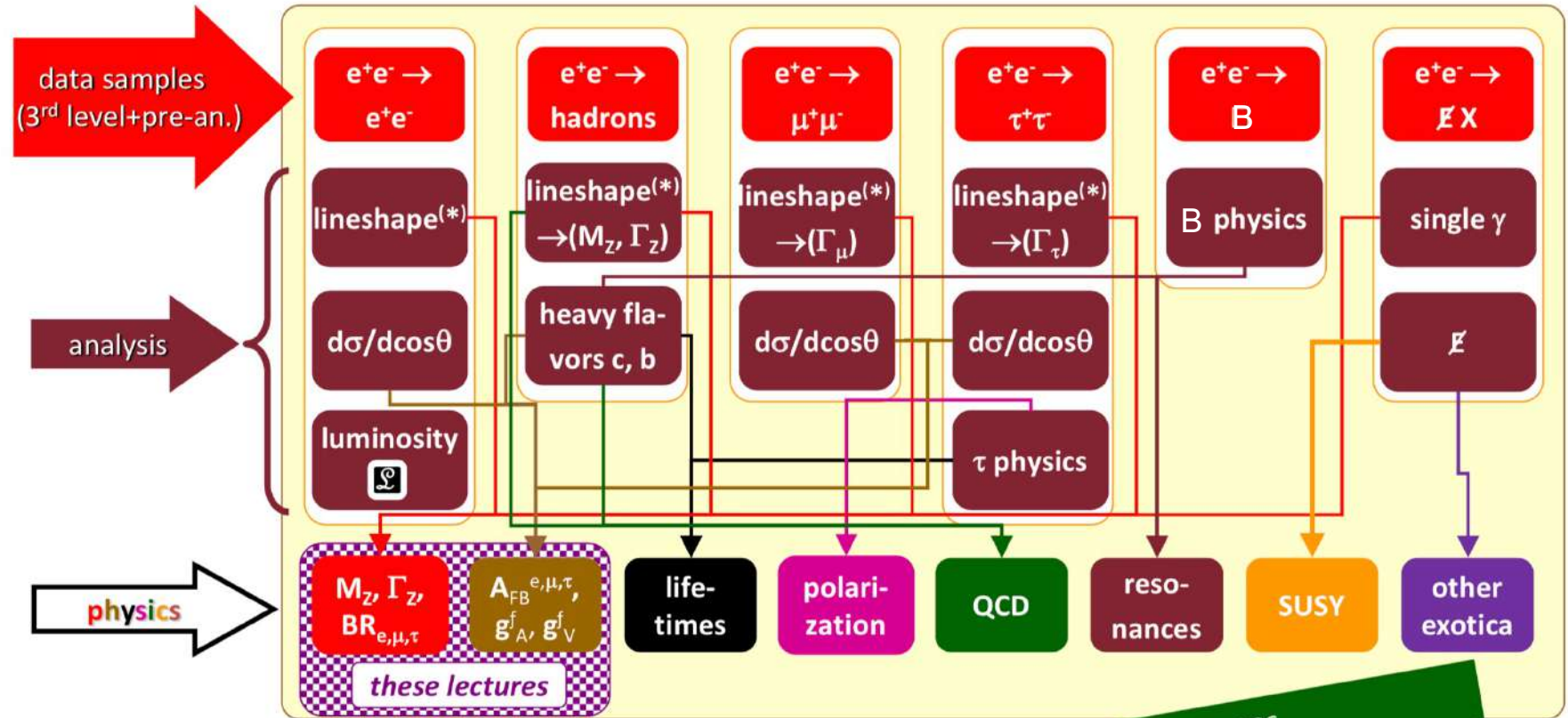
# Data analysis: events $\rightarrow \sigma$



- ❑ **Statistical error: depends on the number of events selected, usually negligible at LEP.**
- ❑ **systematic error: depends on the knowledge on the terms on the “right” part of the formula: luminosity, signal efficiency (selection and trigger efficiency) and background subtraction.**

# Data analysis: general scheme

Slide from P. Bagnaia



very simplified – just for the lectures

(\*) "lineshape" :  $\sigma = \sigma(\sqrt{s})$

# Luminosity measurement

For the exam, just the main ideas; the details are for your education

# Luminosity measurement

- We have the following relationship among Number of Event selected, Integrated Luminosity and cross-section of a given process (*for the time being we do not consider efficiency and background contamination, i.e.  $\epsilon=1$  and  $p=1$* )

$$N_{exp} = \mathcal{L}_{int} \cdot \sigma$$

- If we want to measure the cross section we use the following relationship:

$$\sigma = \frac{N_{exp}}{\mathcal{L}_{int}}$$

- ... but if we wanted to measure the Integrated Luminosity we could turn the formula around:

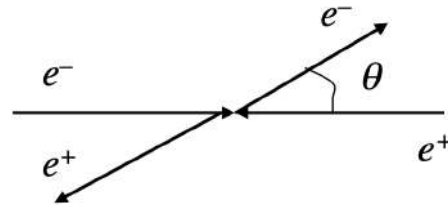
$$\mathcal{L}_{int} = \frac{N_{exp}}{\sigma}$$

- ... therefore we have to find a process for which we know how to calculate the cross section with great precision.

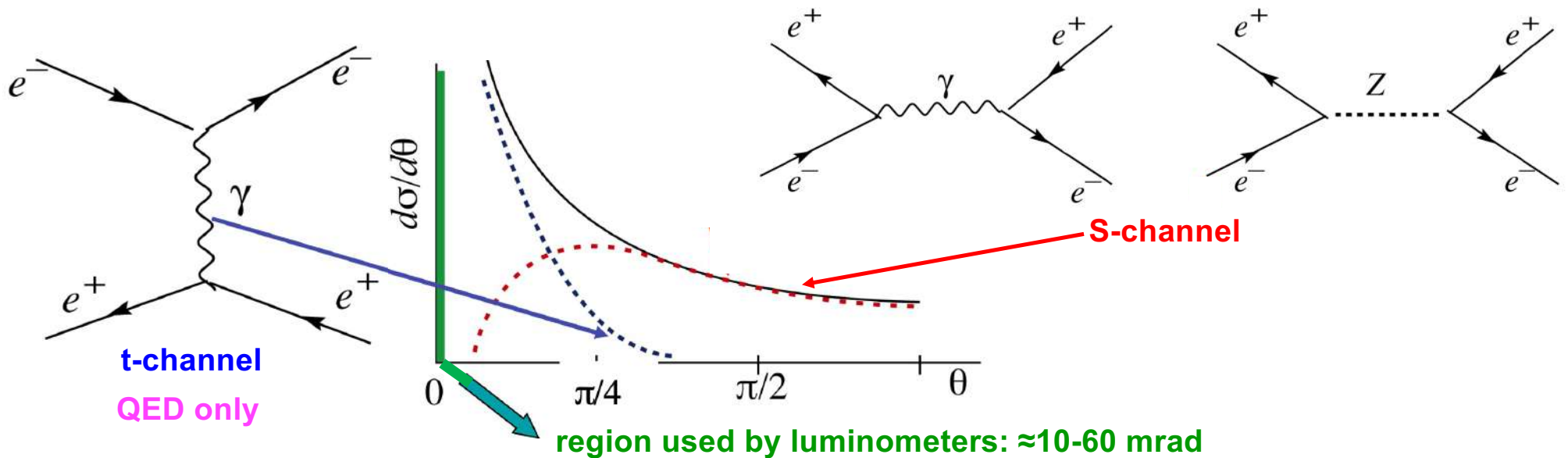
# Luminosity measurement: Bhabha scattering

- ... the process we are looking for is the Bhabha scattering at small angle:

$$e^+e^- \rightarrow e^+e^-$$



- The process is described at the tree level by the following Feynman diagrams, but at small angle is completely dominated by the exchange of a photon in the t channel (which is computable within the QED with great precision):



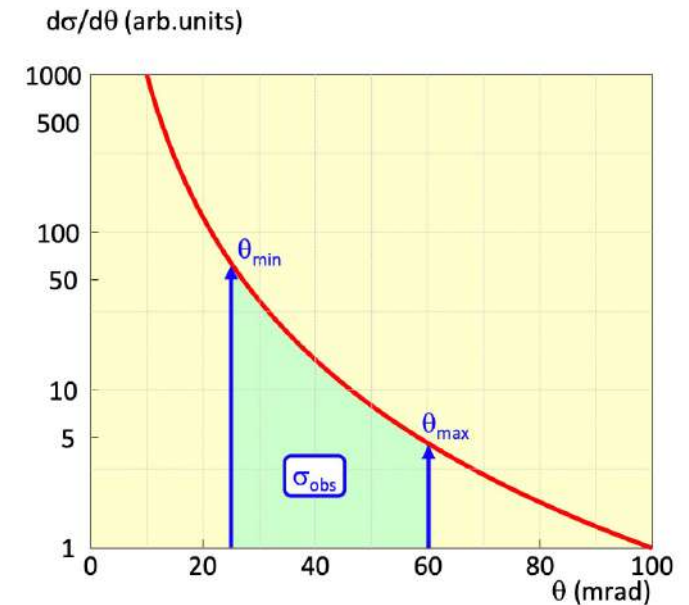
# Luminosity measurement: cross-section

- To lowest order, the small angle Bhabha cross section (integrated over the azimuthal angle  $\phi$ ) in a detector with a polar angle coverage from  $\theta_{\min}$  to  $\theta_{\max}$ , is given by:

$$\sigma = \frac{16\pi\alpha^2}{s} \left( \frac{1}{\theta_{\min}^2} - \frac{1}{\theta_{\max}^2} \right)$$

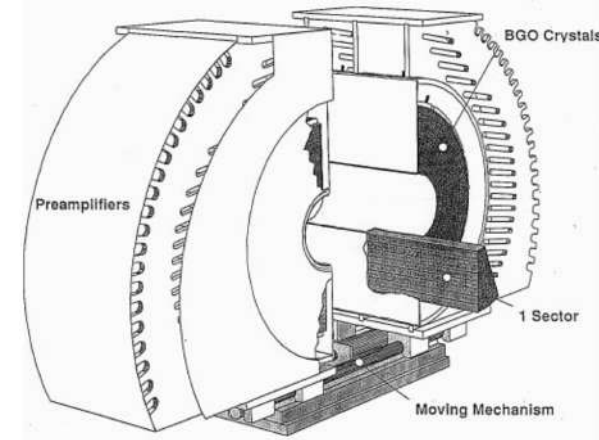
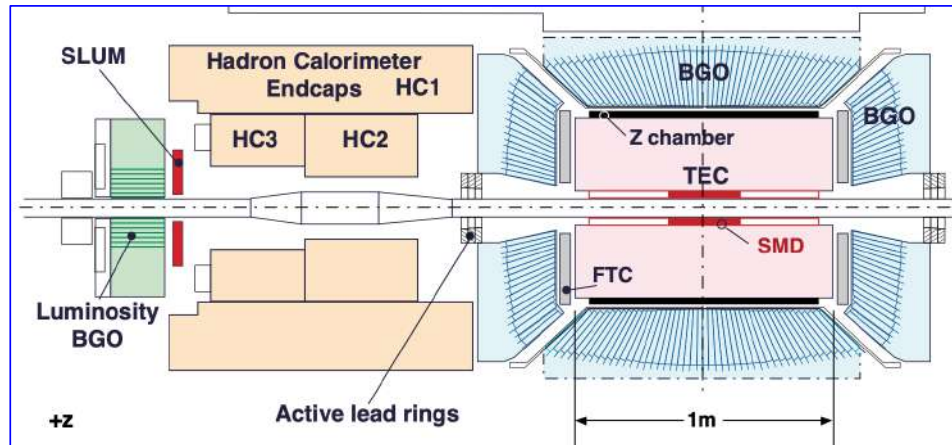
- To determine the visible cross section (inside the Luminometer acceptance) for Bhabha scattering  $e^+e^- \rightarrow e^+e^-(\gamma)$  events are generated at  $\sqrt{s} = 91.25$  GeV using the BHLUMI MonteCarlo program.
- The generated events (about 11 million) are passed through the L3 simulation program and fully reconstructed with the same software used for data. The systematic uncertainty in the visible cross section due to the Monte Carlo statistics is 0.06%.
- background contamination:  $e^+e^- \rightarrow \gamma\gamma(\gamma)$  is at the level of 0.02%
- The theoretical uncertainty due to the approximations used in the BHLUMI calculation is estimated to be 0.25%. A new version of the MC with better calculation brought this error down to 0.11%.

At  $\sqrt{s} = 91.25$  GeV the visible cross section is about 70 nb



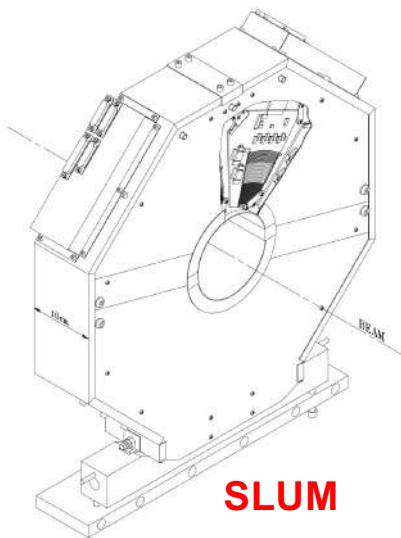
The critical part of the measurement is the determination of the integration volume. It can not be done analitically and must be done “numerically”, using Montecarlo events.

# Luminosity measurement: L3 luminosity monitor



During the injection and ramping phases, the detector was "opened". Only at the stable beam it was closed.

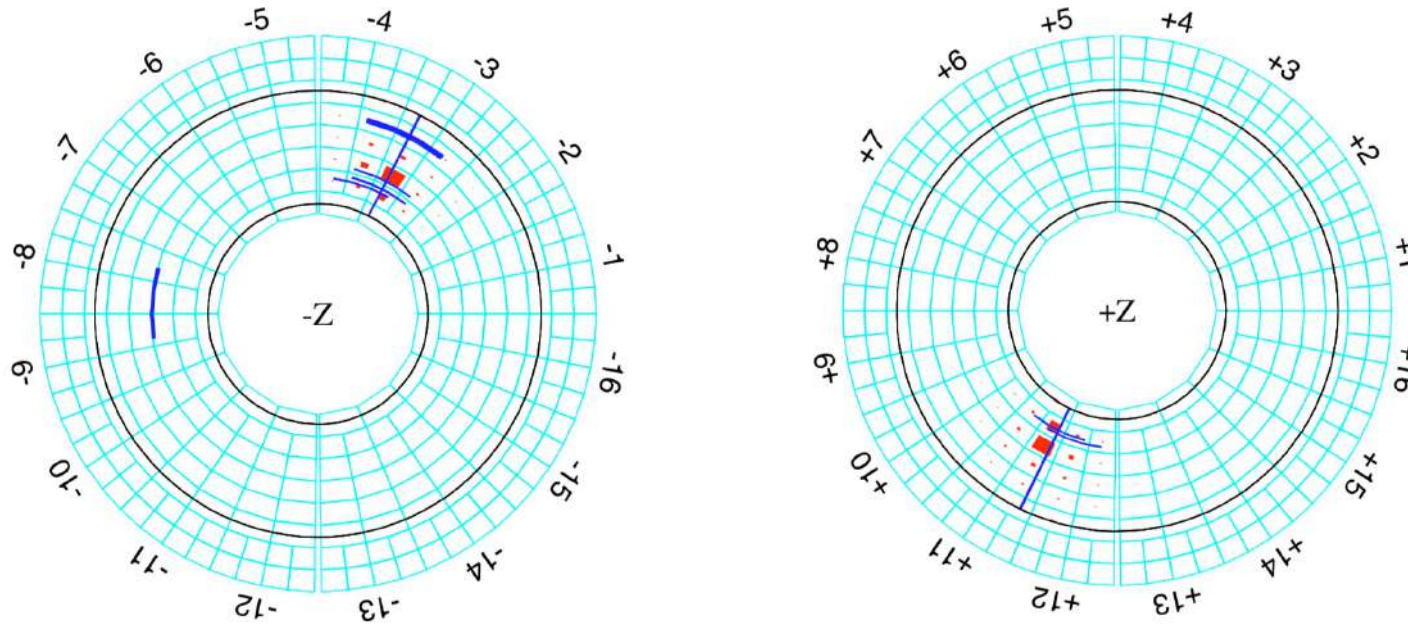
The movement was controlled remotely by a hydraulic device, with a position reproducibility of better than 10  $\mu\text{m}$ .



Distance of central layer from the I.P.	2650 mm
Minimum radius	76 mm
Maximum radius	154 mm
Wafer size in $\phi$	24°
$r$ wafer small strips	64 $\times$ 0.500 mm
$r$ wafer large strips	16 $\times$ 1.875 mm
$r$ wafer medium strips	16 $\times$ 1.000 mm
SiO <sub>2</sub> insulation between strips	0.1 mm
$\varphi$ wafer strip size	0.375°
Layer spacing	40 mm

Distance of the front from the I.P.	2730 mm
Minimum radius	68 mm
Maximum radius	192 mm
Crystal length	260 mm
Crystal length in radiation lengths	24
Number of crystals per sector	19
Angular coverage of a sector	22.4°
Number of sectors per side	16

# Bhabha events in the luminosity monitor



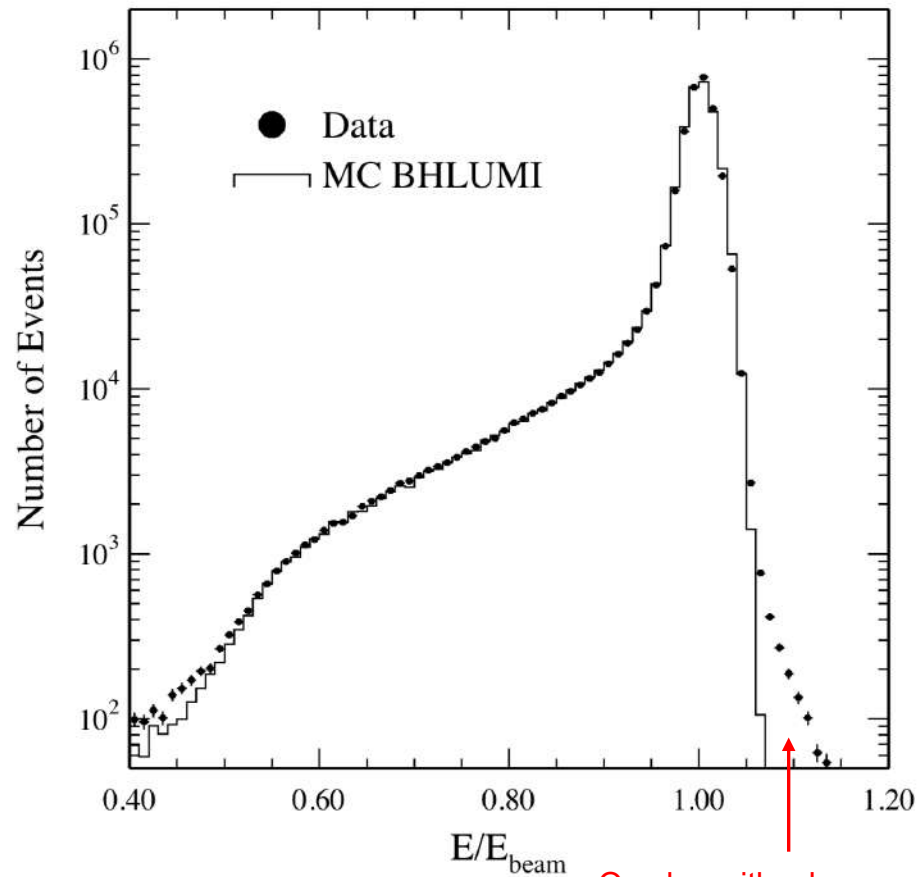
- The energy detected in the BGO is shown by squares, the areas of which are proportional to the amount of energy deposited;
- The hits in the silicon detector are shown by highlighted line segments.
- The goal is to determine the electron impact position as precisely as possible (this info enters in the cross-section integration volume)

- Tight selection:  $32 < \theta < 54$  mrad; azimuthal angle:  $|\phi - 90| > 11.25^\circ$  and  $|\phi - 270| > 11.25^\circ$
- Loose selection:  $27 < \theta < 65$  mrad; azimuthal angle:  $|\phi - 90| > 3.75^\circ$  and  $|\phi - 270| > 3.75^\circ$

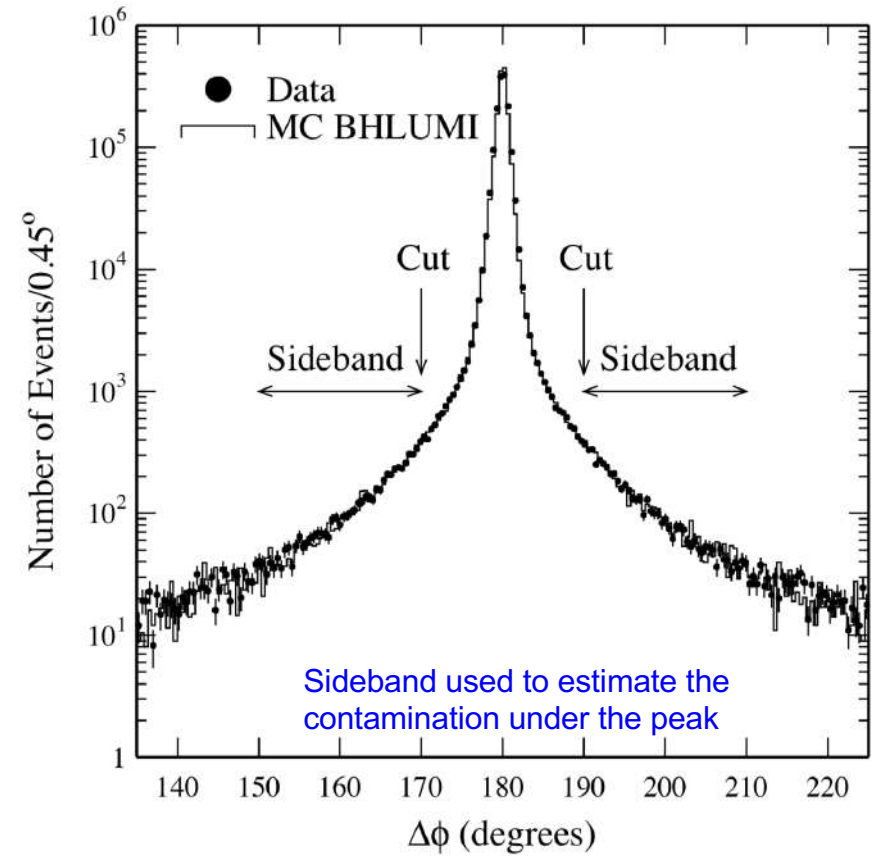
The cut in phi is needed to avoid the vertical "crack"

# Bhabha events: comparison data-MC

□ d



Overlap with a beam gas interaction



# Luminosity determination

- ❑ The integrated luminosity is calculated from:

$$\mathcal{L} = \frac{1}{\epsilon} \frac{N_{\text{acc}}}{\sigma^{\text{vis}}}$$

- ❑  $N_{\text{acc}}$ : number of events in the fiducial volume,  $\sigma$  is the cross-section in the same fiducial volume and  $\epsilon$  is the data selection and trigger efficiency not taken into account in the MC.
- ❑ The integrated luminosity is measured by doing a comparison between data and simulated MC events using the same cuts in order to reduce the systematic errors:

$$\mathcal{L} = \frac{1}{\epsilon} \frac{N^{\text{Data}}}{\sigma^{\text{vis}}} = \frac{1}{\epsilon} \frac{N^{\text{Data}}}{N^{\text{MC}}} \frac{N_{\text{gen}}^{\text{MC}}}{\sigma_{\text{gen}}^{\text{MC}}} f_{s_0/s}(s) f_{\gamma\gamma} f_{\gamma Z}(s).$$

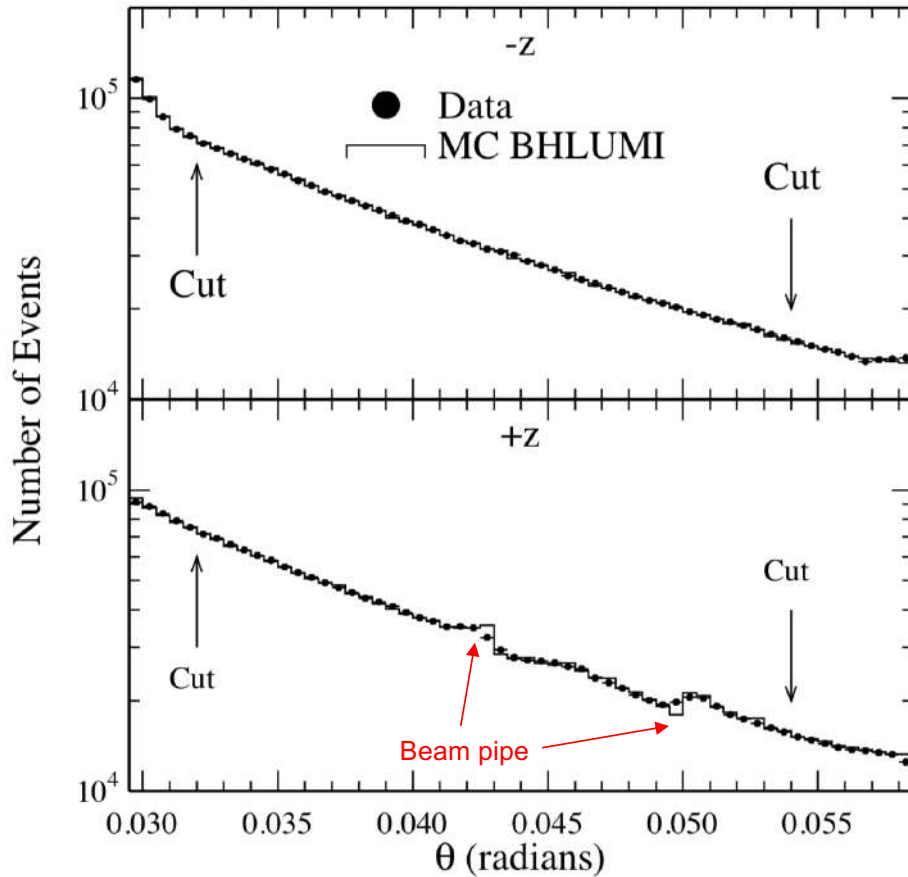
Number of generated events (points to  $N_{\text{gen}}^{\text{MC}}$ )  
 Correction for the  $\gamma Z$  interference (points to  $f_{\gamma Z}(s)$ )  
 Number of reconstructed MC events (points to  $N^{\text{MC}}$ )  
 Center of mass energy correction (points to  $f_{s_0/s}(s)$ )  
 Correction for the  $\gamma\gamma$  background (points to  $f_{\gamma\gamma}$ )

In the MC event generator, the events are generated flat in phi in the entire angle, and in theta according to the differential cross-section, in a region slightly exceeding the one covered by the luminosity monitor.

$\frac{N_{\text{gen}}^{\text{MC}}}{N^{\text{MC}}}$  takes care of the generated events that are not reconstructed, for instance because they go in a dead area of the luminosity monitor

$\mathcal{L}$  is proportional to  $N_{\text{lumi-events}} (N^{\text{Data}})$

# Luminosity measurement: final results



Source	Contribution to $\Delta\mathcal{L}/\mathcal{L}$ (%)		
	BGO Analysis	BGO+Silicon Analysis	
		1993	1994
Trigger	Negligible	Negligible	Negligible
Event Selection	0.3	0.04	0.05
Background	Negligible	Negligible	Negligible
Geometry	0.4	0.06	0.03
Total Experimental	0.5	0.08	0.05
Monte Carlo Statistics	0.06	0.06	
Theory	0.11	0.11	
Total	0.5	0.15	0.14

Systematic uncertainties on the luminosity measurement.

“design” luminosity uncertainty was 1%



SAPIENZA  
UNIVERSITÀ DI ROMA

End of chapter 6